AN ABSTRACT OF THE DISSERTATION OF

Christopher J. Sharp for the degree of Doctor of Philosophy in Mechanical Engineering presented on March 19, 2018.

Title: Wave Energy Converter Array Optimization: Algorithm Development and Investigation of Layout Design Influences

Abstract approved: ____

Bryony L. DuPont

Realizing the vast amount of energy available in ocean waves, an industry has emerged that is progressing towards the deployment of grid–connected wave energy converters. Likely to be deployed in arrays, a challenge to the wave energy industry is maximizing the energy production of such arrays. We have been developing a metaheuristic array optimization method specifically for the design of wave energy converter arrays. Over the last several years, we have progressed from an initial binary genetic algorithm to a real–coded genetic algorithm that has allowed us to better explore the characteristics of wave energy converter array design. We have tested the influence of minimum separation requirements, row spacing effects, passive damping for WECs, probabilistic sea states, and converter geometries. This work has been used to better understand the many influencers affecting array design and for considering the potential of wave energy to be used in emergency scenarios for coastal communities. Our work reveals the ability of our novel genetic algorithm to generate optimal layouts given a range of influencing factors.

Wave Energy Converter Array Optimization: Algorithm Development and Investigation of Layout Design Influences

by

Christopher J. Sharp

A DISSERTATION

submitted to

Oregon State University

in partial fulfillment of
the requirements for the
degree of

Doctor of Philosophy

Presented March 19, 2018
Commencement June 2018

Doctor of Philosophy dissertation of Christopher J. Sharp presented on March 19, 2018.

APPROVED:

Major Professor, representing Mechanical Engineering

Head of the School of Mechanical, Industrial, and Manufacturing Engineering

---

Dean of the Graduate School

I understand that my dissertation will become part of the permanent collection of Oregon State University libraries. My signature below authorizes release of my dissertation to any reader upon request.

Christopher J. Sharp, Author

ACKNOWLEDGEMENTS

I would first and foremost like to thank my advisor, Bryony DuPont. The passion and drive in your work and life is inspirational. Thank you for your encouragement and advocacy — it's been an honor to be your first PhD student. I would also like to thank the rest of my committee, Belinda Batten, Bob Paasch, Chris Hoyle and Ted Brekken for providing insight and support throughout this process. And Flaxen Conway, my minor advisor, thank you for challenging me to think beyond an engineering framework.

The Pacific Marine Energy Center provided funding for this research and has been influential in the promotion and advancement of wave energy in the U.S. I am grateful to have been a part of this organization and for the associated faculty within MIME who advocated for their students and created a place for me to thrive in my studies.

Chapters 6 and 7 are based upon work supported by the U.S. Department of Energy under Award Number DE-EE0006816. Neither the U.S. Government nor any agency thereof, nor any of their employees, makes any warranty, expressed or implied, or assumes any legal liability or responsibility for the accuracy, completeness, or usefulness of any information, apparatus, product, or process disclosed, or represents that its use would not infringe upon privately owned rights. Reference herein to any specific commercial product, process, or service by trade name, trademark, manufacturer, or otherwise does not necessarily constitute or imply its endorsement, recommendation, or favoring by the U.S. Government or any agency thereof. The views and opinions expressed herein do not necessarily state or reflect those of the U.S. Government or any agency thereof.

The National Science Foundation National Research Traineeship (NRT) in the quantification and communication of risk and uncertainty in marine science supplied funding for a year of my work as I investigated the broader potential and implications of marine renewable energy in a transdisciplinary group. I am grateful to my cohort for the many invigorating conversations and specifically to my team for a willingness to embrace the challenges associated with tackling our specific problem.

Additionally, I would like to acknowledge the International Network on Offshore Renewable Energy (INORE). INORE introduced me to the global considerations of marine renewable energy and has provided many great networking connections and friendships.

Thank you to my labmates here at OSU (Adam, Blake, Brad, Andrew, Caitlin, Caity, Aisha, and Annalise) for creating a space of friendship and support. I have thoroughly enjoyed working alongside individuals who are genuinely caring and considerate.

I would like to thank my family for their understanding, sacrificial support, and encouragement throughout my entire educational journey. Mom and Dad, your passion for education and learning, your pursuit of excellence and your faith has been such an example. Hannah and Heidi, thanks for being my faithful friends.

And finally, I would like to thank my fiancé, Laura, for being so understanding of my insane schedule and lack of availability over the past couple of years. Your care, encouragement, and willingness to join me on this adventure means the world and I'm excited to experience what's next for us.

TABLE OF CONTENTS

Page

1 Introduction 1
1.1 Motivation 1
1.2 Previous Work 4

I Algorithm Development 12

2 Binary Genetic Algorithm Overview 13
2.1 Binary GA Results 22

3 Algorithm Comparison Study 25
3.1 Introduction 25
3.1.1 Evolutionary Algorithm 26
3.1.2 Genetic Algorithm 27
3.1.3 Simulated Annealing 27
3.2 Methods 28
3.2.1 Evolutionary Algorithm 28
3.2.2 Genetic Algorithm 30
3.2.3 Simulated Annealing 30
3.3 Five–converter case results 32
3.3.1 Evolutionary Algorithm 32
3.3.2 Genetic Algorithm 33
3.3.3 Simulated Annealing 34
3.4 Five–converter array discussion 36
3.5 Exploration of increased number of converters 38
3.6 Conclusion 42

4 Real-Coded Genetic Algorithm 44
4.1 Introduction 44
4.2 Real–coded genetic algorithm overview 44
4.3 Objective Function Formulation 49
4.4 Problem Formulation 49

TABLE OF CONTENTS (Continued)

Page

4.5 Results and Discussion . . . 51
4.6 Conclusion . . . 56

II Investigation of Layout Design Influences 59

5 Binary Genetic Algorithm Row Spacing Study 60
5.1 Introduction . . . 60
5.2 Study Parameters . . . 61
5.3 Row Spacing Study . . . 63
5.4 Discussion . . . 67
5.5 Conclusion . . . 68

6 Array Optimization of Fixed Oscillating Water Columns for Active WEC Control 69
6.1 Introduction . . . 69
6.2 Project Overview . . . 70
6.3 Assumptions . . . 71
6.4 Current Optimization Scheme . . . 71
6.5 OWC Modeling . . . 72
6.6 Array Optimization . . . 76
6.7 Results . . . 78
6.7.1 Fixed Valve Angle - 44° . . . 78
6.7.2 Varied Valve Angles . . . 84
6.8 Discussion . . . 88
6.8.1 Wave Period . . . 88
6.8.2 Wave Type (Regular and Irregular Behavior) . . . 90
6.8.3 Valve Angle (Damping) . . . 91
6.9 Conclusion . . . 93

7 Array Design and WEC Damping Assignment of Fixed Oscillating Water Columns 95
7.1 Methodology . . . 96
7.1.1 OWC Damping Assignment . . . 97

7.1.2 Array Design 97

7.2 Results 99

7.2.1 Case 1: Fixed Layouts with Fixed Damping 100

7.2.2 Case 2: Fixed Layouts with Optimized Damping 100

7.2.3 Case 3: Optimized Layouts with Fixed Damping 102

7.3 Observations 105

7.3.1 Interaction Factor 105

7.3.2 Damping 106

7.3.3 Layout Design 106

7.4 Conclusions 107

8 WEC Arrays for Blackout Risk Mitigation: Influence of WEC Size and Location 108

8.1 Introduction 108

8.2 Motivation 109

8.3 Problem Formation 110

8.3.1 Geometries 110

8.3.2 Sea State 111

8.4 Results 114

8.5 Discussion 119

8.6 Conclusion 121

III Concluding Discussion 123

9 Conclusion 124

9.1 Contributions of the Work 124

9.2 Avenues for Continued Research 126

9.3 Final Thoughts 127

Bibliography 127

LIST OF FIGURES

Figure		Page
1.1	Effect of a single WEC on a wave field demonstrated by change in wave height	5
1.2	Example arrays achieved by previous research	9
2.1	Binary GA relationship between physical space and algorithm strings	16
2.2	Binary GA crossover method	17
2.3	Binary GA flowchart	19
2.4	Costs associated with arrays for differing numbers of WECs	21
2.5	Portion of modeled converter below the water surface	23
2.6	Optimal layouts generated by a binary GA	23
3.1	Best found layout for an array of five converters	33
3.2	Optimal layouts for arrays with 10 and 25 converters	39
3.3	Algorithm interaction factor comparison	41
4.1	Real GA crossover method	46
4.2	Real–coded GA flowchart	48
4.3	Best layout achieved for the first scenario	52
4.4	Best layout achieved for the second scenario	53
4.5	Second best layout achieved for the second scenario	54
5.1	Optimal arrangement found for 20 WECs	61
5.2	Starting point for the rows of WECs	62
5.3	Optimal separation spacing in a 60x60 meter space	63
5.4	Interaction factor as a function of distance between rows for a 60x60 meter space	64

LIST OF FIGURES (Continued)

Figure Page

5.5 Interaction factor as a function of distance between rows for a 60x700 meter space . . . 65

5.6 Alternative starting point for the rows of WECs . . . 65

5.7 Interaction factor as a function of distance between offset rows for a 60x700 meter space . . . 66

5.8 Smoothed interaction factor as separation distance increases . . . 66

6.1 Optimization process overview . . . 73

6.2 OWC Prototype . . . 74

6.3 RAO comparison between WAMIT results and tank data . . . 76

6.4 Optimal layouts with regular waves, a valve angle of 44° and H=0.136m . 81

6.5 Optimal layouts with irregular waves, a valve angle of 44°, and H_{mo}=0.136m 83

6.6 Optimal layouts with regular waves, a valve angle of 80° and H=0.136m . 85

6.7 Optimal layouts with regular waves, a valve angle of 0°, and H=0.136m . 86

6.8 Optimal layouts with irregular waves, a valve angle of 80° and H_{mo}=0.136m 87

6.9 Optimal layouts with irregular waves, a valve angle of 0° and H_{mo}=0.136m 87

6.10 Interaction factor sensitivity based on valve angle and wave period . . . 93

7.1 Overview of cases being considered. . . . 96

7.2 Predetermined Layouts for Cases 1/2 . . . 99

7.3 Optimized Layouts for Case 3 . . . 105

8.1 Buoy Locations . . . 112

8.2 Optimal layouts for OWCs from ALFA Project (Dia = 0.62m) . . . 115

8.3 Optimal layouts for OPT WEC (Dia = 2.7m) . . . 116

LIST OF FIGURES (Continued)

Figure Page

8.4 Optimal layouts for WEC from Child and Venugopal's research (Dia = 10m) 117

8.5 Comparing the WEC geometry against location specific sea states 118

LIST OF TABLES

Table | Page

2.1 Tunable GA parameters used in initial binary work 24

3.1 Evolutionary algorithm simulation results for five converters 34

3.2 Tunable GA parameters 34

3.3 Genetic algorithm simulation results for five converters 35

3.4 Simulated annealing algorithm simulation results for five converters 35

3.5 Objective function evaluation comparison 36

3.6 Interaction factor comparison 37

3.7 Comparison of function evaluations 37

3.8 Objective function evaluation comparison for 10 & 25 converter arrays . . 39

3.9 Interaction factor comparison for 10 & 25 converters arrays 40

4.1 Test scenario parameters 50

4.2 Tunable GA parameters 50

4.3 Objective function evaluations and interaction factors of presented results 55

4.4 Objective function evaluations and interaction factors of presented results compared against previous research 55

6.1 Tunable GA parameters 77

6.2 Wave scenarios 79

6.3 Interaction factors from different wave scenarios 89

7.1 Evaluated Sea States and Associated Single WEC Optimal Damping. . . . 97

7.2 Case 1 Results 101

7.3 Case 2 WEC Damping 103

LIST OF TABLES (Continued)

Table Page

7.4 Case 2 Results 104

7.5 Case 3 Results 105

8.1 WEC geometry dimensions 111

8.2 Representative Sea States by Location 113

Chapter 1: Introduction

1.1 Motivation

The United States (U.S.), in addition to countries around the world, is actively supporting avenues for expanding its energy portfolio to include sources that are renewable and locally accessible. The White House and U.S. Department of Energy (DOE) have set guidelines for reducing dependence on foreign oil and better implementing water power methods. More specifically, the U.S. is seeking to generate 80% of its energy using renewable sources by 2035 and to achieve an 80% reduction in carbon emissions by 2050 [1]. Currently the primary renewable energy sources used to supply electricity to the grid are hydropower, solar, and wind. However, energy provided by these sources is minimal in comparison the actual amount of energy used and as such other avenues for finding energy need exploring [2]. Relatively recently, research has turned to the ocean — with the vast amount of power contained in its waves, tides, and currents — in an attempt to satisfy energy needs while minimizing dependency on fossil fuels.

The estimated global amount of energy in ocean waves is between 16,000 TWh per year and 18,500 TWh per year [3]. Quantified, one terawatt–hour of generated electricity is roughly the amount of energy that 9,000 U.S. homes use over the course of a year [4]. The DOE has reported that in the U.S. the ocean waves, ocean tides and river currents have, theoretically, enough extractable power to supply one–third of the nation's energy requirements [5]. Furthermore, the recoverable ocean wave resource is estimated to be approximately 1,170 TWh per year [5] which could provide the electricity needed by over one million homes. In Hawaii, Alaska, and Oregon — states with prime wave resources — wave energy could potentially supply 100%, 100%, and 57% of these states' respective energy needs [1].

Additionally, in the United States, 50 percent of the population resides within 50 miles of a coastline [6]. Such proximity to the energy source would limit energy waste due to electricity transfer and potentially limit extended blackout scenarios caused by disparate power sources and an aging grid. For some specific cases where electricity is derived from fossil fuel often transported from far away, those living in remote coastal areas or on islands not connected to the grid, the use of wave energy as a source of electricity would greatly improve energy security.

Due to the number of individuals residing near an ocean, the push to develop and implement renewable energy sources, and the quantity of energy to be extracted from the ocean, wave energy is a promising source of electricity for which there are many wave energy converters (WECs) under development that are nearing the point of full–scale ocean deployment. Following ocean deployment of individual converters, developers are planning the implementation of arrays of WECs to provide grid–connected power to a large consumer base with many electrical needs. The process of developing WEC arrays involves comprehending and overcoming associated challenges such as volatile sea states and associated costs. As it is vital that the wave energy industry be well–informed regarding the potential deployment of arrays to ensure the industry's survival and future competitiveness, determining optimal array configurations at this stage in research is essential.

In light of the progression of the wind and solar industries, the wave energy industry will likely follow a similar trajectory and ultimately deploy WECs in array scenarios utilizing advanced WEC control techniques. By using optimization techniques to account for the many influencing factors that determine optimal layout configurations, developers will better understand layout designs that maximize the power produced and minimize cost before taking the risk of deploying WECs in the ocean. While at the current time, industry is primarily focusing their efforts on converter design and optimization, it is important that research be conducted to prepare for the potential of wave energy grid integration. Additionally, WEC behavior in array settings may influence a converter's design.

Array design can be an efficient solution to power maximization and cost reduction, as higher energy may be produced by WECs integrated into arrays than by the same number of isolated WECs. Based on studies of the wave fields created by converters in grouped scenarios, the possibility of attaining increased power due to positive WEC-WEC wave interaction has been theorized [7, 8, 9, 10]. Indeed, the radiated and scattered waves resulting from the interaction between incident waves and WECs has shown to amplify the interaction factor, q, expressed in Eq. 1.1 [9]

$$q = P_{array}/(N * P_{iso}). \tag{1.1}$$

In Eq. 1.1, P_{array}, P_{iso}, and N represent the power extracted from the array, the power extracted from an isolated WEC and the number of WECs [11]. Hence, the proximity of WECs to one another will affect the power production, as well as contribute to reducing array costs, which are functions of aspects such as the mooring and power cable length, space limitations and maintenance [12]. Therefore, it is critical to examine optimal array layouts and to evaluate the effect that the calculating algorithm has on finding such an optimal configuration.

Regarding WEC array design, most research has focused on empirical layouts – assumed layouts given a designers best understanding of how converters behave and interact in a wave field. However, the complexity of the ocean space excludes these solutions from being readily used by industry as they do not wholly account for many influences that will affect a configuration. As such, research has shifted towards leveraging automated optimization methods to generate potential layout designs by better exploring and exploiting the search space. This dissertation will present the problem–specific genetic algorithm (GA) we have developed and tested.

1.2 Previous Work

WECs in the ocean affect the wave field through radiated waves (waves that ripple out from a WEC) and diffracted waves (the bending of the incident wave around a converter). Figure 1.1 shows a single WEC's effect on a wave field, where yellow indicates an increase in wave height as compared to the incident wave height, and dark blue indicates a decrease in compared wave height. Essentially, Fig. 1.1 shows the effect of wave diffraction when an incident wave experiences a WEC in the ocean — the waves pile up and bend around the obstructing converter.

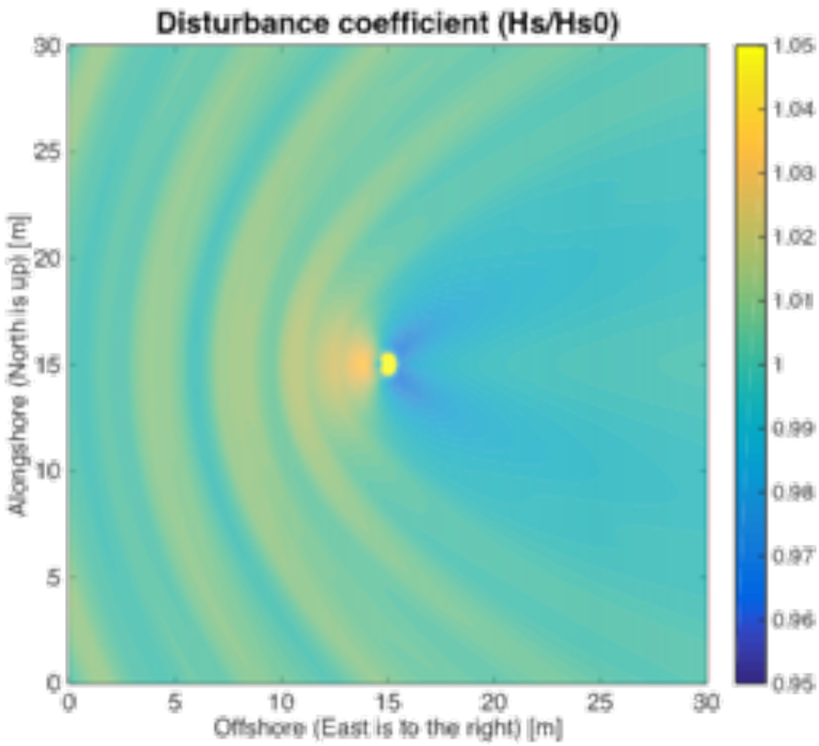

Figure 1.1: Effect of a single WEC on a wave field demonstrated by change in wave height

Unlike wind energy farms — where placing turbines too close to one another results in negative interactions between turbines and a decrease in power production — WECs have the potential to generate more power when placed in an array than the combined power that the same number of WECs would produce acting in isolation [9]. This concept is described using the interaction factor, q, shown in Eq. 1.1. Having focused on finding arrays where this interaction factor is greater than one, previous research has noted that there are many elements which influence the power produced by an array, including sea state, wave directionality, and array configuration [12]. An understanding of these elements is necessary for the design of WEC layouts [13]. However, the impact that these factors have on an array's power production is yet to be well quantified.

Research in array configuration design has primarily focused on pre–determined layouts and their resulting q factors. Examples of layout shapes that have been considered include lines (both parallel and orthogonal to the oncoming wave), triangles, squares, and various grid designs [14, 15, 16, 17, 18, 19, 20].

Additional research has observed that beyond layout configuration, individual WEC and global control schemes would greatly improve power production [21, 22, 23]. Ricci et al. suggested that the benefit a converter can experience from a neighboring WEC degrades as distance between converters increases. From a configuration study where heaving point absorbers are theoretically placed off the coast of Portugal, the distance proposed at which interaction effects become negligible is four times the WEC radius [24]. The required minimum spacing between WECs in an array is currently not known definitively as converter designs have yet to converge. For example, depending on if converters are fixed or floating; on where WECs exist in the water column; or on WEC specific watch circles, the required minimum spacing distance will differ. Consequently, minimum separation distances in research and industry depend on problem specific parameters.

The main approach in WEC array optimization research has been to focus on maximizing the power production. It has been shown that controlling the spacing of converters in an array can increase the interaction factor q (through wave radiating and scattering effects), resulting in an augmentation of power generation [25]. In addition, general approaches address the control strategies of the array and individual WECs, as well as power take off (PTO) characteristics for maximizing the overall array power extraction in waves with linear, regular and fixed incident direction parameters for specific deployment locations. Consideration of more realistic conditions has been applied to model predictive and PTO control optimization uniquely [26], but, prior to our research, the effect of array layout optimization on power output maximization in realistic scenarios has not been fully studied.

Several researchers have utilized optimization methods for determining layouts that maximize the interaction factor. Using a point approximation to determine WEC array power production, Fitzgerald and Thomas implement a sequential quadratic algorithm based on a selected starting point [27]. Considering two variations of a GA and a greedy algorithm, Mao determines that the GA performs better since the optimal configurations differ depending on the number of WECs being utilized [28]. Snyder & Moarefdoost used a two-phase heuristic algorithm that assumes a unidirectional wave in combination with a convex optimization solver and is dependent on an assumption of symmetry [29, 30]. They present two optimization methods, a max–min model and a maximization expected value model, to account for variability in incident wave direction [31]. They determine that an increase in uncertainty yields a decrease in optimal spacing between two converters. Moarefdoost et al. later presents a heuristic algorithm that exploits solutions believed to be near optimal [30]. More recently, McGuinness Thomas developed an analytical method for determining optimal spacing between converters when placed in a single row parallel to the oncoming wave; in this work, arrays are optimized based on a maximization of the mean of the interaction factor rather than just maximizing the interaction factor itself [32].

Using a unidirectional, regular sea state and a set number of point absorber type converters constrained in the vertical or heave direction, Child & Venugopal implement two methodologies to generate layout configurations: Parabolic Intersection and MATLAB's GA toolbox [33, 34, 35]. Parabolic Intersection assumes that the diffracted waves around a WEC take the shape of a parabola and so, once the first WEC is placed, following WECs are then placed to benefit from the higher wave heights in the parabolic shaped diffracted waves generated by the first WEC. For both the PI method and the MATLAB GA method, the achieved layouts have the shape of a *"W"* with the two bottom points of the *"W"* pointing towards the oncoming wave. The GA method returned the highest interaction factor of the two methodologies. Figure 1.2(a) and 1.2(b) show examples of generated arrays for these two methods. These figures were created based on results shown in [34].

The private company DNV–GL has also worked on the creation of an optimization tool, WaveFarmer [36]. In available DNV–GL research, an array consisting of four converters is placed in a square formation such that the WEC positions are constrained and the individual WEC's power take–off systems are controlled [23]. A ten–converter array is also

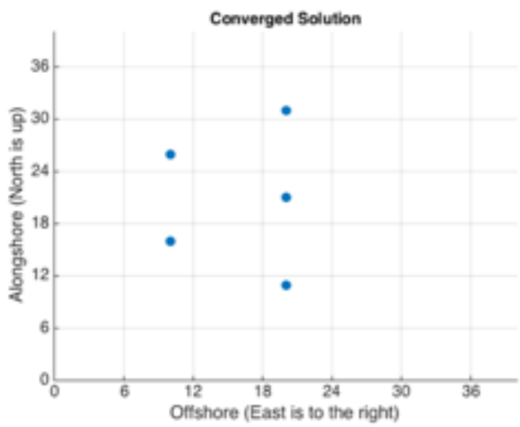

(a) Child and Venugopal – Parabolic Intersection

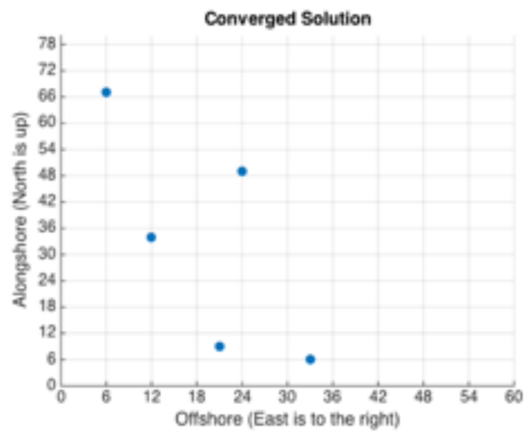

(b) Child and Venugopal – MATLAB's Genetic Algorithm Toolbox

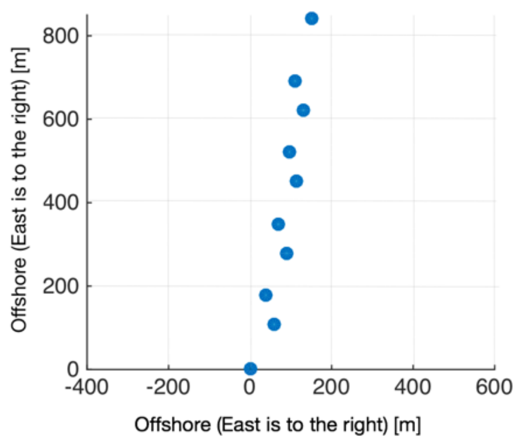

(c) DNV-GL – MATLAB's Genetic Algorithm Toolbox

Figure 1.2: Example arrays achieved by previous research

considered, using a Brettschneider spectrum wave field input, and optimal WEC layout is determined using MATLAB'S GA toolbox. The ten–converter array is arranged in two offset parallel lines that are generally perpendicular to the oncoming incident waves with five WECs in each row as shown in Fig. 1.2(c). For each of the evaluated cases an interaction factor greater than one was reported [23]. The layout shown in Fig. 1.2(c) was created based on a result shown in [23].

The potential for determining a layout that would provide an interaction factor greater than one is promising; however, developers are ultimately interested in reducing the cost of energy, which helps drive down barriers of new, renewable energy source implementation. Consequently, economics must be considered during the computational WEC array design process. Vicente et al. and Balitsky et al. both note that array costs will affect the configuration of WEC arrays [17, 21]. However, we have found no reported work, excluding our own previous work [25], that incorporates cost as an objective or into the objective function.

More recently, a WEC–specific machine learning approach has been applied to the WEC array optimization problem by Sarkar et al. [37]. Evaluating a bottom mounted flap type WEC, it is determined that, for submerged, surge–type converters, clustering should be avoided. Wu et al. also examines a submerged type WEC and implements two evolutionary type algorithms, a (1+1)–EA algorithm and a Covariance Matrix Adaptation based Evolutionary Strategy (CMA–ES) [38]. Optimizing an array of mid–water column, floating spheres, the methods do not perform well independently. However, when the (1+1)–EA is used to get close to converging on a solution, the CMA–ES is able to fine–tune that solution.

McGuinness and Thomas have created an analytical method of optimizing the spacing between WECs that are placed in a row [32]. Observing that in certain scenarios WECs tend to cluster, they postulate that these WECs could be replaced with a larger WECs to minimize physical WEC interaction while still achieving increased power production. The optimal spacings also differ due to incident wave direction.

As the wave energy industry advances towards full scale deployment, research has continued to explore how to achieve maximum array power generation and interaction factor (defined in Eq. (1.1)) [39]. While is not well known what most influences power development, both array optimization and active WEC control have theoretically shown substantial increases [40, 41, 42, 26]. This thesis will provide an overview of how our work has contributed to this field.

Part I

Algorithm Development

Chapter 2: Binary Genetic Algorithm Overview

Our work in the realm of WEC array optimization began with the development of a binary genetic algorithm specific to the design of array design [11]. We used a GA approach because of its ability to efficiently converge on optimal solutions while considering continuous and discrete factors. Recognizing the need to eventually consider more than just power as a design influence, we conducted initial research with an objective function that included a rough cost estimate [43]. As a part of our previous work, we investigated existing models of WEC array economics and found at the current stage of the industry that there is not enough known or available information for WEC arrays. Consequently, we created an initial cost model using what information was available from Sandia National Laboratory's Reference Model 6 [44]. Continuing this research, this chapter will introduce the concept of our specific GA in detail and will discuss the workings of a discretized version.

To achieve optimal layouts, we first model a single WEC using the boundary element software, WAMIT [45]. This informs how a WEC behaves in a given wave field for a range of wave directions – specifically, we obtain the WEC's added mass, hydrodynamic damping, hydrodynamic restoring force, and excitation force. The developed GA will then create generations of potential layouts based on the process of survival of the fittest in combination with how chromosomes are shared between generations as children are produced by combinations of parents' chromosomes.

Within our optimization process there are several sets of code that must be linked together.

- ***WAMIT***: A boundary element software used to determine how waves interact with offshore WECs. For our project, the outputs required of WAMIT are the added mass, hydrodynamic damping, hydrodynamic restoring force, and excitation force of a single WEC (for a single water depth and a range of wave periods/directions).

- ***mwave***: A MATLAB computational package for evaluating WEC(s) and ocean waves. We are using *mwave* both as a pre– and post–processor for WAMIT and for determining an array's power output such that converter–to–converter wave interactions are included.

- ***optimization algorithm***: The problem specific algorithm we are developing for the purpose of determining optimal WEC layout designs. This algorithm is being written in MATLAB specifically to interface with the other programs.

As an evolutionary optimization algorithm, a GA mimics the passing of traits from parents to children, with mutations diminishing local optima convergence. Utilizing stochastic attributes — such as generating a random parent population – improves the GA's performance. In our GA, several tunable parameters exist — elitism, crossover, and mutation. An individual parent represents a unique array solution.

As part of initializing the genetic algorithm, the first step is to generate an initial population of parents, p. p is the number of initial parents, which is also the number of solutions in each generation. A discrete number, N, of WECs are placed in an $x * y$ grid with discrete cells that represent all the possible locations for WECs offshore (x

cells along x–axis) and alongshore (y cells along y–axis), and whose x–axis and y–axis represent the distance of array footprint offshore and alongshore respectively. Consequently, the maximum distance offshore and alongshore must be defined, as well as the minimum allowable distance between WECs. This initial array of dimension $p * (x * y)$ is converted to a row vector (depicted in Fig. 2.1) with dimension $1{*}x * y$. x and y are the number of grid cells along the x–axis and y–axis respectively. At each of these randomly generated locations, the cell is assigned a value of "1," while every other cell is assigned a value of "0." Hence, the initial parent grid of $p * (x * y)$ cells with each row containing N WECs is created, and is defined as the first generation.

With the initial parents generated, evaluated, and sorted, children are created using elitism, crossover, mutation, and random layout generation. Each of these facets is a tunable parameter that can be adjusted in order to help the GA converge upon a solution.

For the GA, elitism involves cloning the best solutions from the parent set into the children set. This means that a set amount of the children set will be identical to the best of the parents. Additionally, the same percentage of parents that are cloned are killed off and that percentage of the children set is populated with random solutions to ensure that the GA can fully explore the solution space and avoid getting stuck in local minima.

After elitism is complete, crossover is performed on a set upper percentage of the parent population. The parents that were cloned are included in this crossover population to allow the current best solutions more influence on the propagated solutions. The crossover is performed by randomly swapping a set fraction of WECs between parents being mated. For example, if the fourth WEC from parent one is chosen to be moved,

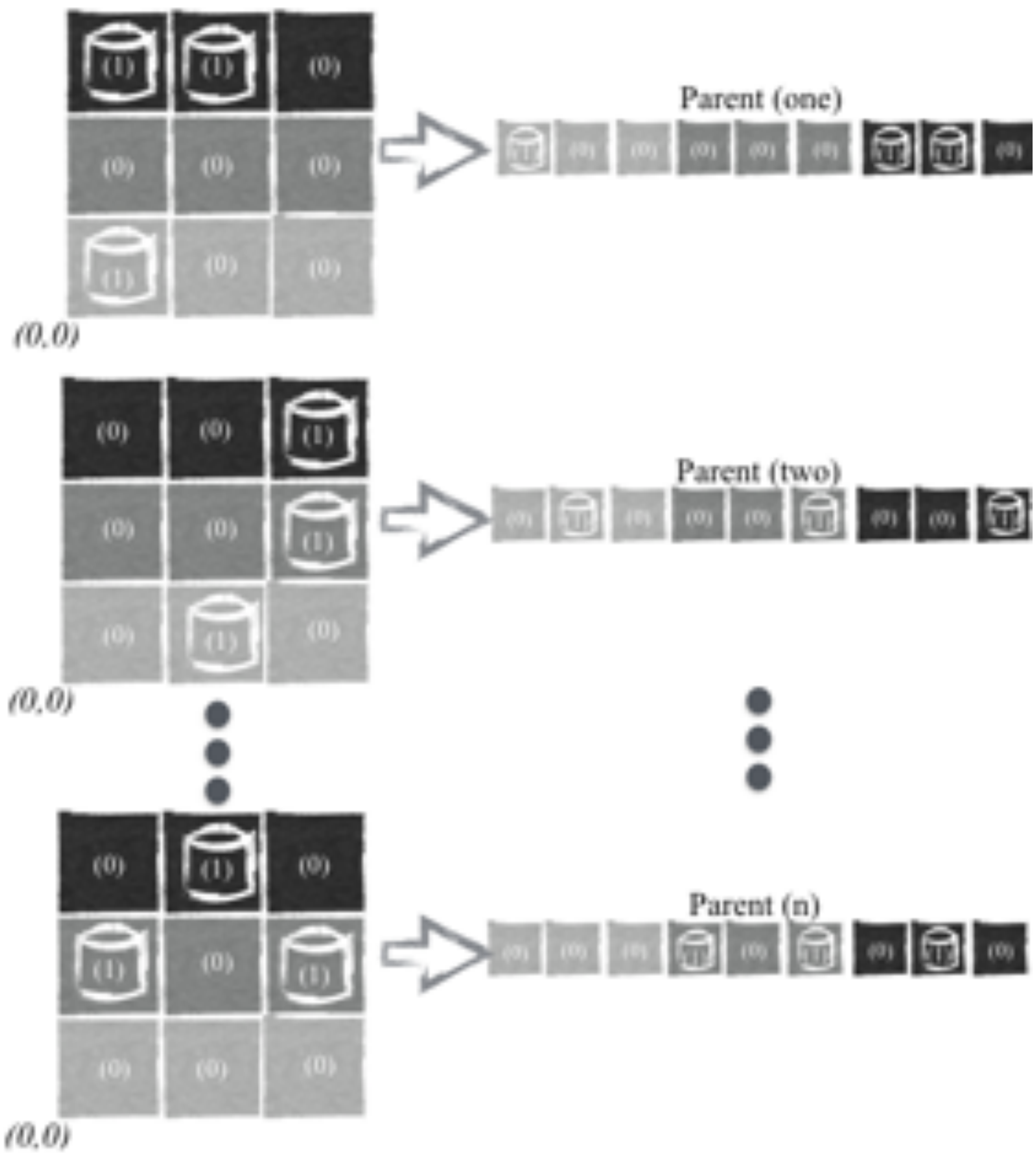

Figure 2.1: Binary GA relationship between physical space and algorithm strings

then it would be removed from parent one and a converter would be placed in parent two at the location from which it was moved in parent one. This new layout, comprised primarily of parent one, but with the variation introduced from parent two, constitutes one of the two children to be created. The second child solution is made by using the same process — by randomly choosing a WEC from parent two and moving it to parent one. To ensure that the defined number of converters is maintained, WECs from both parents are also removed. In short, moving a random WEC or WECs in each parent to a new location or locations that is acquired randomly from the other parent makes the children solutions. Figure 2.2 demonstrates this process.

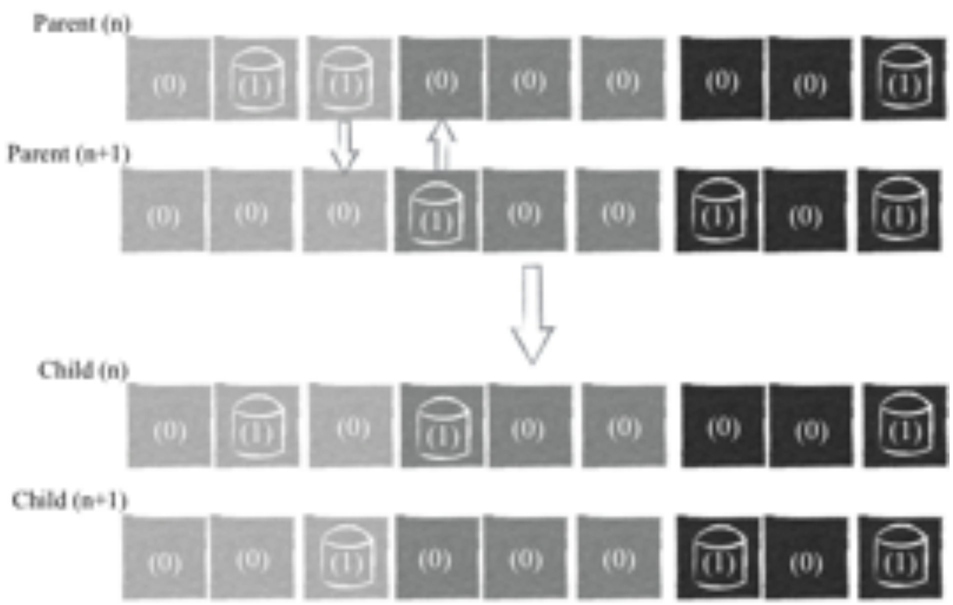

Figure 2.2: Binary GA crossover method

After the crossover procedure is complete then this portion of the children population is mutated. Mutation allows the method to explore the local solution space around a proposed layout with less randomness than through the introduction of new completely random solutions in elitism. Within our GA it is important to both explore the solution space well and exploit found solutions. The introduction of mutation allows for the exploitation of found solutions to potentially improve upon these solutions. The method involves randomly moving a WEC in a layout based on a set percentage. Like mutation is relatively rare in the physical world, mutation within our GA is a small percentage and an example mutation rate will be shown later.

With elitism, crossover, and mutation complete, the objective function of each new layout is computed. Then this newly generated children set is sorted and checked for convergence. If attained, the algorithm reports the converged solution, but if not, then the children set becomes the next parent set and the process is repeated. Convergence is defined as a prescribed upper percentage of the children set reporting the same layouts. Once convergence is attained the algorithm returns the converged solution as the reported optimal array layout. (If convergence is not attained the children population becomes the next parent population and the process continues.) Figure 2.3 shows the pseudocode for the binary version of our developed GA.

Through implementing this binary GA, our previous work in WEC array optimization introduced cost into the objective function in addition to generated power [25, 11]. To find the power generated by an array, the isolated WEC's hydrodynamic behavior, individual converter orientation, wave diffraction, and wave radiation are required. This information is used to calculate each WEC's excitation force as well as the total array's added mass and damping. The power for an individual WEC is then found using Eq. 2.1

Figure 2.3: Binary GA flowchart

$$P = \frac{1}{8}\mathbb{X}^{*}B^{-1}\mathbb{X} \tag{2.1}$$

where B^{-1} represents the damping and $\mathbb{X}$ represents the complex excitation force [46]. This process is described in detail in [20].

With the total power development for the array found, the next component of the objective function to determine is the cost associated with an array of WECs. As noted in [43], the particulars to be included in array economic calculations lack specificity due to limited deployment data. As such, models that exist for determining array costs need further development to provide realistic results. We chose to use Sandia National Laboratory's Reference Model Project 6 (RMP) as it is the most comprehensive model found, and because it provides information for arrays with differing numbers of WECs [44].

In general, array economics are separated into capital costs (CAPEX) and operations and maintenance costs (OM) as shown in Fig. 2.4. The information provided by the RMP was used to generate an equation for estimating array cost based on the number of converters in the array, N, with an assumed lifetime of 20 years,

$$Cost = 3(10)^{7} * N^{0.6735}. \tag{2.2}$$

Equation 2.2 serves as a preliminary means of estimating WEC array costs and was derived by adding the capital and OM costs together from the information provided by the RMP and then fitting a curve to that data over the different sized arrays. It is understood that these costs depend on additional factors such as array location, distance to shore, location in the water column, mooring configuration, and electrical cabling. Though

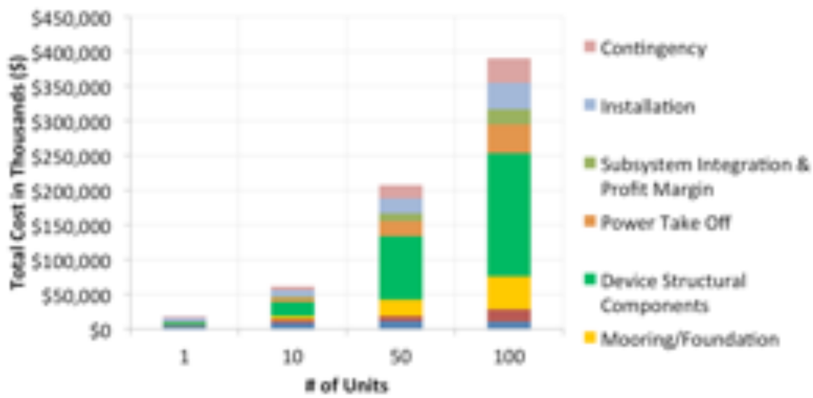

(a) Capital costs

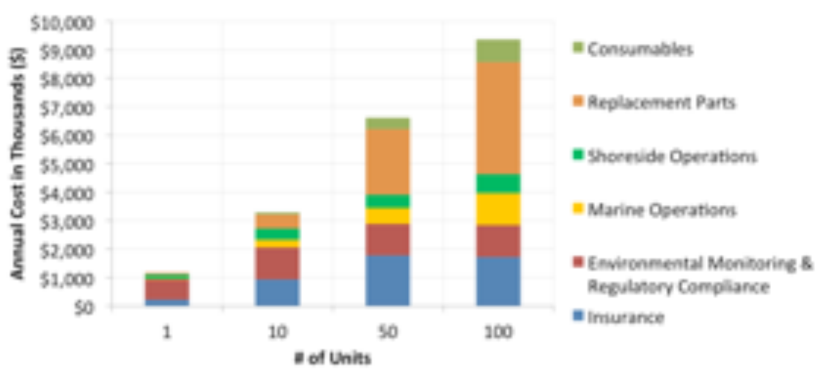

(b) Operations and maintenance costs

Figure 2.4: Costs associated with arrays for differing numbers of WECs

basic, an equation such as Eq. 2.2 is consistent with other energy system optimization scenarios in their early stages of development [47].To calculate power, the behavior of an isolated WEC is first considered using WAMIT [45]. The converter is subjected to incident waves from multiple directions in a sea–state with a limited water depth and a range of wave periods. With the hydrodynamic information of the single WEC obtained from WAMIT, the diffraction coefficient matrix, force transfer matrix, and radiated wave coefficients are found for the single WEC. The objective function used in our binary GA work includes cost in addition to power and is shown in Eq. 2.3

$$ObjFun = Cost/P_{20} \tag{2.3}$$

where P_{20} represents an array's generated power over an assumed 20–year lifetime and Cost represents the cost of the array over 20 years.

2.1 Binary GA Results

This initial work examined the effects of converter spacing on the optimal layout of one–meter radius truncated cylindrical point absorbers constrained in heave (similar to those used in [34] and shown in Fig. 2.5), and found that a defined minimum separation distance dictated whether radiated waves or diffracted waves improved the interaction factor. Figure 2.5 shows the portion of the truncated cylinder below the water surface. Figure 2.6(a) shows the result for a fixed three—meter minimum separation distance, which essentially means that the WECs are allowed to get within one meter edge–to–edge. With this proximity, the converters take advantage of neighboring converters' radiated waves.

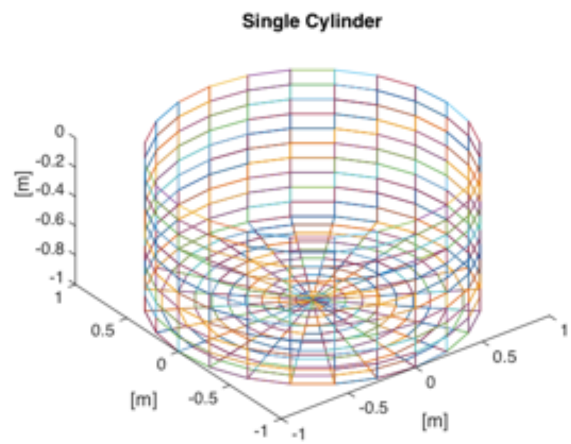

Figure 2.5: Portion of modeled converter below the water surface

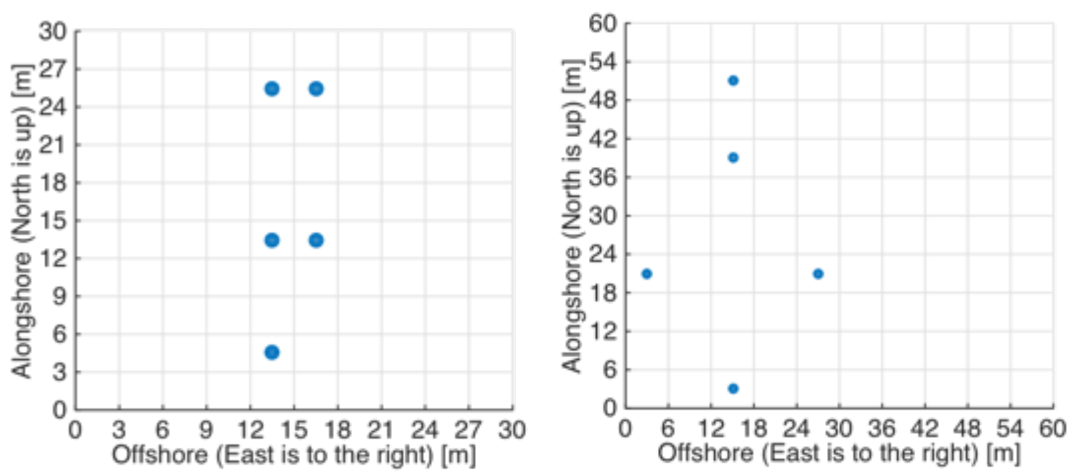

(a) Minimum separation distance of 3–meters

(b) Minimum separation distance of 6–meters

Figure 2.6: Optimal layouts generated by a binary GA

When a further minimum separation distance of six–meters (four meters edge–to–edge) is required, the interaction factor is found to improve through taking advantage of diffracted waves. The best–found layout given this minimum separation distance is shown in Fig. 2.6(b). The GA input parameters are shown in Table 2.1. The GA must be tuned in order avoid converging too quickly or never converging. This work demonstrates the potential ability of WECs to benefit from being deliberately placed in relative close proximity.

Table 2.1: Tunable GA parameters used in initial binary work

# of parents	100	100
Elitism rate	10%	8%
Crossover rate	80%	84%
Mutation rate	0.02%	0.2%
Convergence requirement	50%	50%

The layouts shown in Fig. 2.6 differ based on the type of altered waves the WECs are able to experience. For the three–meter minimum separation distance the converters can get close enough to each other to benefit from the radiated waves of neighboring WECs. However, these radiated waves dissipate quickly as a they move away from the converter and consequently, when a six–meter minimum separation distance is enforced, the WECs instead take advantage of the diffracted waves from neighboring converters. These configurations also have lone converters that are not a part of the patterns created by the remaining four converters. Likely, if the number of WECs and the physical space was increased these lone WECs become a part of these patterns. Or new patterns would emerge that include these new WECs.

Chapter 3: Algorithm Comparison Study

3.1 Introduction

Regarding the various parameters involved with optimizing arrays, different methods and even different runs in the same method, may converge to varying solutions given the same inputs. In this chapter, we will investigate the optimization of a WEC array's power production utilizing three types of optimization methods. The optimization methods to be implemented and compared are an evolutionary algorithm, a genetic algorithm, and a simulated annealing algorithm. Comparing the final generated solutions from these three algorithms will aid in determining which approach is better for optimizing WEC arrays containing different number of WECs and will provide the wave energy research community with information to aid in reducing overall array cost.

This chapter will first introduce previous WEC array design research and this will be followed by a discussion of the three selected algorithms: genetic, evolutionary and simulated annealing. The evolutionary algorithm (EA) and simulated annealing algorithm (SA) were chosen for comparison against our previously utilized GA to better understand the importance of exploring the solution space and exploiting potential solutions respectively. General approaches to the problem and related work will be presented, array modeling addressed, the three algorithms' performance compared, and resulting array layouts noted. The performance will be examined through consideration of obtained interaction factors, objective function evaluations, and number of function evaluations.

3.1.1 Evolutionary Algorithm

EAs are a class of search algorithms that are often used as function optimizers for static objective functions [48]. EAs are principally a stochastic search and optimization method based on the principles of natural biological evolution. Compared to traditional optimization methods such as calculus–based and enumerative strategies, EAs are robust and may be applied generally without recourse to domain–specific heuristics [49]. Genetic qualities influence the chance of a potential solution's survival in that the struggle to survive throughout generations leads to a natural selection or survival of the fittest, and genetic variants that have proven to be well adapted to the environmental conditions appear preferably in subsequent generations [50].

Two main concepts of evolutionary based optimization strategies are discussed in the literature: GAs [51] and EAs [52]. There are many similarities between these two methods, but they have some key differences as well. The most important difference comes from the crossover process that occurs in a GA. Both the EA and the GA include mutation d the mutation plays an important role in the implementation of an EA. The mutation operator randomly alters part of solutions within a generation to produce a new generation that is mostly like the original generation, but with a small amount of variation [53]. EAs operate on a population of potential solutions, applying the principle of survival of the fittest to produce successively better approximations to a solution [48]. Each generation seeks to improve the solutions in the way that eliminates the weak solutions according to their level of fitness and keeps the stronger answers for mutation in the next generation.

3.1.2 Genetic Algorithm

Related to the EA, the genetic algorithm (GA) is a method based on the evolutionary process in which traits are acquired through the implementation of mutation. However, unlike EAs, GAs also mimic the way that chromosomes are passed down from parent generations to child generations. This process was described in detail in Chapter 2.

3.1.3 Simulated Annealing

Simulated Annealing (SA) is a powerful optimization technique, proposed in 1983 by Kirkpatrick et al. [54], because of its ability to converge upon very good solutions for difficult combinatorial optimization problems, while easily dealing with complex non-linear constraints [55]. Simulated annealing takes advantage of the analogy between the minimization of an optimization problem's cost function and the slow procedure of gradually cooling a metal until it reaches its "freezing" point [54, 56, 57]. Based on the iterative method proposed by Metropolis et al., this system simulates the performance of atoms in equilibrium at different temperatures while cooling [58].

Less optimal solutions are more likely to be accepted in the early irritations of the algorithm, because of the high temperature; however, by cooling down the temperature, the successors move towards selection of only better solutions. One of the critical parameters used in simulated annealing algorithm is the temperature and the rate at which it decreases.

3.2 Methods

Each of the presented approaches has potential for determining optimally arranged WEC arrays given the many influencing factors involved in array design and the large solution space. This section will discuss the specific implementation of these algorithms for use with a binary WEC array optimization scenario. For all the methods, WECs with predefined bodies and known hydrokinetic properties are used as inputs. Additionaly, the solution space is discretized. The same objective function is used for all the algorithms and is the same as what was presented in Chapter 2. Assuming a 20–year lifetime, the cost value in this objective function is derived from information provided in Sandia National Laboratory's Reference Model Project (RMP) and is shown in Eq. 2.2 [44].

3.2.1 Evolutionary Algorithm

The first proposed method to create and optimize the layout of a WEC array is an EA. As part of initializing the EA, the first step is to generate an initial population of parents, p. A row vector, as demonstrated in Fig. 2.2, represents each parent. An initial array of dimension $p * (x * y)$ is generated in which N WECs are inserted in each parent's vector based on randomly generated values ranging from 1 to $x * y$. At each of these randomly generated locations, the cell is assigned a value of "1," while every other cell is assigned a value of "0." Hence, the initial parents grid of $p * (x * y)$ cells with each row containing N WECs is created, and is defined as the first generation. This is demonstrated in Fig. 2.1.

Once generated, this parent generation is evaluated based on the objective function presented in Eq. 2.3. Mutation is then applied to the parent array – a defined number of random cells are selected for mutation in each row (parent) of the sorted population. If a "1" cell is subject to mutation, it is swapped with a randomly selected "0" cell in the same vector to maintain the number of WECs. Similarly, if a "0" cell is subject to mutation in a vector, it is then swapped with a randomly selected "1" cell in the same vector in order to maintain the number of WECs. Once all the parent solutions have been mutated, the newly obtained children array is evaluated with the objective function. After evaluation, the children population is combined with the parent population and this combined pool is then sorted according to the objective function evaluations of each potential solution. The new parent generation is obtained by selecting the p best individuals from the combined solution array - this keeps the size of the population consistent between generations. Since the objective function in this project is defined by the ratio of cost to power, the goal is to minimize the objective function, thus minimizing the cost while maximizing the power. Therefore, as long as the objective function of the newly obtained generation is superior to the objective function of the best parents' generation on record, the process continues to search through mutated generations to find an optimum objective function and layout until a set number of generations has elapsed without improvement. On the other hand, whenever a generation obtains a solution with a lower objective function it is recorded as the overall best layout. The process continues as long as better solutions are being found or until a number of generations has elapsed without finding a better solution.

3.2.2 Genetic Algorithm

The binary GA methodology is described in depth in Chapter 2.

3.2.3 Simulated Annealing

The final method applied to the WEC array optimization problem is a SA approach. To implement the SA method, the initialization of the space for WEC placement is very similar to that described in the EA and GA sections prior, except that for the SA, the grid is not converted to row vector format. In the SA method, bad solutions may be accepted at the beginning of the process. The probability of accepting a worse solution in the algorithm is based on the difference between power generated in the previous and current solutions, and the iteration number. The objective function is found in the same manner as the EA and the GA using Eq. 2.3.

Implementation of this procedure depends on the temperature and its reduction or cooling rate parameters, which must be tuned based on the nature of the specific problem. The probability of accepting a worse solution is calculated at each epoch using on these numbers.

To implement the SA method, a single randomly generated layout is created by inserting a set number of WECs into discretized locations in a grid. At each iteration a converter is randomly chosen for repositioning to one of the eight potential surrounding cells – assuming that the potential cell is in the allowable space and that no converter already exists there. The new location of the chosen WEC is randomly selected from the potential eight locations. The objective function for the proposed new layout is calculated and compared against the objective function of the current layout. If the proposed position is better than the current position, the proposed position is accepted. However, if the proposed position is not better than the current position, it may still be accepted based on a determined probability,

$$P_{accept} = e^{(-(|\triangle E|/T))}, \tag{3.1}$$

where P_{accept} is the probability of acceptance, $\triangle E$ is the difference between the objective function evaluation of the proposed solution and the overall best solution, and T is the temperature value. The basic algorithm for simulated annealing is the following:

1. Generate a random solution;
2. Set initial temperature $T = T1$;
3. Calculate its cost using a defined objective function;
4. Generate a random neighboring solution;
5. Calculate the new solution's objective function;
6. Compare the new solution with the previous solution:
   - If $c_{new} < c_{old}$: move to the new solution;
   - If $c_{new} > c_{old}$: maybe move to the new solution with the probability of $P = e^{-(\triangle C/T)}$;
7. Update the temperature, T;

8. Repeat steps 3–7 above until an acceptable solution is found or you reach some maximum number of iterations.

Over the duration of the algorithm the best result is recorded and updated.

3.3 Five–converter case results

For the first portion of this work, five WECs are placed in a 60-meter by 60-meter space with a grid resolution of 10x10. This resolution equates to 100 different cells in which a WEC can exist. Each algorithm uses a heave–constrained truncated cylinder with a radius of one meter and a draft (distance below the water surface) of one meter.

Given the discretized space, the minimum separation distance allowed between WECs must be defined. For the work presented here the minimum separation is deliberately set at six meters based on previous research's defined minimal distance of three times the body's diameter [23]. The wave climate is drawn from a Bretschneider spectrum with a significant wave height of 2–meters and a modal frequency of 0.2 Hertz. The water depth is set at 8–meters with unidirectional waves coming directly from the west. Each algorithm is run a total of ten times and the objective function, interaction factor, and number of function evaluations recorded for the result of each run.

3.3.1 Evolutionary Algorithm

In the EA, an initial parent population of 100 individuals is generated. Two random locations in each solution vector are selected for mutation. A limit of 100 generations without improvement is set and once satisfied, the layout with the best objective function is reported and the search process is terminated. From the ten different runs, the EA obtained two different WEC configurations. Figure 3.1 shows the WEC configuration of the layout with the best objective function.

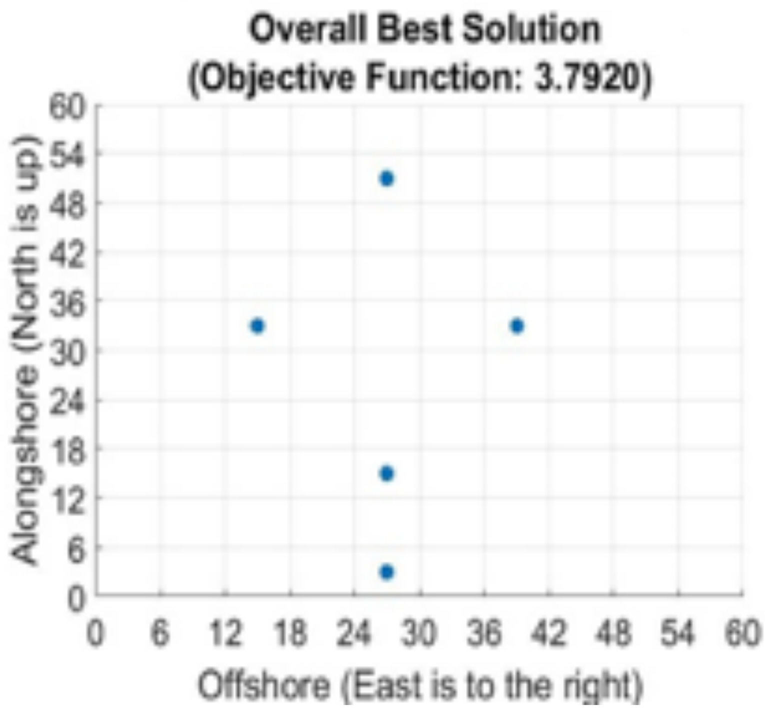

Figure 3.1: Best found layout for an array of five converters

The second configuration obtained involved the WECs lining themselves up perpendicular to the oncoming waves. Table 3.1 summarizes the objective functions, number of function evaluations and interaction factors, q, obtained for each of the ten trials.

3.3.2 Genetic Algorithm

As with the EA, an initial parent population of 100 individuals is randomly generated where each potential layout is comprised of five converters. For each of the ten GA runs,

Table 3.1: Evolutionary algorithm simulation results for five converters

	Run 1	Run 2	Run 3	Run 4	Run 5
Objective Function	*3.7920*	*3.7960*	*3.7920*	*3.7920*	*3.7960*
# of Evaluations	*22500*	*12800*	*16200*	*12500*	*18700*
Interaction Factor, q	*1.01899*	*1.01790*	*1.01899*	*1.01899*	*1.01790*
	Run 6	Run 7	Run 8	Run 9	Run 10
Objective Function	*3.7920*	*3.7920*	*3.7960*	*3.7920*	*3.7920*
# of Evaluations	*12800*	*31600*	*12000*	*18600*	*16200*
Interaction Factor, q	*1.01899*	*1.01899*	*1.01790*	*1.01899*	*1.01899*

Table 3.2: Tunable GA parameters

# of parents	100
Elitism rate	10%
Crossover rate	80%
Mutation rate	0.02%
Convergence requirement	50%

the parameters for elitism, crossover, mutation, and convergence are shown in Table 3.2. All the conducted trials utilize the same input parameters. The two overall best layouts found by the GA are the same as those found by the EA (previously shown in Fig. 3.1). The results for all ten runs with the GA are presented in Table 3.3.

3.3.3 Simulated Annealing

Unlike the EA and the GA, the simulated annealing algorithm only involves the random generation of one potential layout that then goes through the simulated annealing process. The temperature reduction results in high exploration of the search space at

Table 3.3: Genetic algorithm simulation results for five converters

	Run 1	Run 2	Run 3	Run 4	Run 5
Objective Function	*3.8080*	*3.7960*	*3.7920*	*3.8025*	*3.8087*
# of Evaluations	*6687*	*14524*	*8850*	*5776*	*3288*
Interaction Factor, *q*	*1.01471*	*1.01790*	*1.01899*	*1.01618*	*1.01452*
	Run 6	Run 7	Run 8	Run 9	Run 10
Objective Function	*3.8035*	*3.7960*	*3.7920*	*3.8012*	*3.7960*
# of Evaluations	*9555*	*6658*	*6432*	*7553*	*5487*
Interaction Factor, *q*	*1.01591*	*1.01790*	*1.01899*	*1.01653*	*1.01790*

the beginning of the process and exploitation of layouts later in the process. The best configuration achieved has the same layout as that attained by the EA and the GA with the objective function evaluation of 3.7920 and the interaction factor of 1.01899. As with the GA, the SA achieves the best result, as shown in Fig. 3.1, two out of ten runs. Additionally, the SA found the same second best solution one out of the ten runs. Table 3.4 compiles the results for all the SA runs.

Table 3.4: Simulated annealing algorithm simulation results for five converters

	Run 1	Run 2	Run 3	Run 4	Run 5
Objective Function	*3.8053*	*3.8064*	*3.7920*	*3.8083*	*3.7960*
# of Evaluations	*8805*	*7277*	*5983*	*6186*	*8856*
Interaction Factor, *q*	*1.01543*	*1.01426*	*1.01899*	*1.01464*	*1.01790*
	Run 6	Run 7	Run 8	Run 9	Run 10
Objective Function	*3.8049*	*3.7960*	*3.8046*	*3.7920*	*3.8068*
# of Evaluations	*4790*	*7207*	*1072*	*7486*	*6839*
Interaction Factor, *q*	*1.01553*	*1.01790*	*1.01561*	*1.01899*	*1.01501*

3.4 Five–converter array discussion

The performance of the three algorithms for the five–converter case is compared through analysis of the objective function evaluations, interaction factors and number of evaluations. It is important to remember that a minimized objective function is desired, which correlates to a maximized interaction factor. The optimal layout shown in Fig. 3.1, with the objective function of 3.7920 and interaction factor of 1.01899, was found by each of the three algorithms. This WEC array configuration provides a 1.9% increase in power when compared to the combined power of five WECs acting in isolation.

However, taking into account the frequency of finding the optimal solution over the ten runs, the EA shows a higher performance compared to the GA and SA. Attaining this solution seven out of the ten runs, the EA has the lowest mean objective function evaluation and although the GA and SA both found the same best result two out of ten runs, the GA performed slightly better than the SA. Additionally, as shown in Table 3.5, the GA was able to find the second best objective function (3.7960) three times in ten runs compared to two times for the SA.

Table 3.5: Objective function evaluation comparison

	Objective Function Evaluation			
	Mean	Algorithm Best	Overall Best	Frequency of Overall Best
Evolutionary Algorithm	3.7932	3.7920		7/10
Genetic Algorithm	3.7999	3.7920	3.7920	2/10
Simulated Annealing Algorithm	3.8012	3.7920		2/10

Similarly, the standard deviation analysis of the algorithm's interaction factors, displayed in Table 6, reveals that the EA is more consistent than the GA and SA. The mean and standard deviation of solutions' interaction factors, generated by the EA, GA and SA, confirm that the EA is better at finding maximized interaction factors than GA and SA when five converters are involved, while the GA is slightly more successful than the SA.

Table 3.6: Interaction factor comparison

	Interaction factor, q			
	Mean	Standard Deviation	Algorithm Best	Overall Best
Evolutionary Algorithm	1.01866	0.0005	1.01899	
Genetic Algorithm	1.01695	0.0016	1.01899	1.01899
Simulated Annealing Algorithm	1.01643	0.0018	1.01899	

Regarding the number of evaluations per run required to generate an optimal solution, the EA presents a significantly higher mean than the GA and SA. As shown in Table 3.7, while the EA requires an average of 18390 function evaluations to find a solution, the GA and SA only need 7481 and 6450 iterations respectively, on average, to generate a solution.

Table 3.7: Comparison of function evaluations

	Number of Function Evaluations Per Run		
	Mean	Minimum	Maximum
Evolutionary Algorithm	18390	12000	31600
Genetic Algorithm	7481	3288	14524
Simulated Annealing Algorithm	6450	1072	8856

Examining the results of all three algorithms, for the five–converter experiment, the EA yields better solutions than the GA and SA due to the EA's ability to thoroughly explore the solution space. The SA performs the worst of the implemented algorithms — though not by much when compared to the GA. Limiting the number of WECs, in a 10x10 discretized space, to only five creates a solution space with just over $9x(10^9)$ possible configurations. If the number of converters is increased, then the number of potential configuration also increases. The next section explores the obtained results of each algorithm if the number of WECs is increased in the same discretized space.

3.5 Exploration of increased number of converters

In order to better understand the difference in results from implementation of an EA, GA or SA in a WEC array optimization problem, five runs with 10 and 25 WECs are conducted for each algorithm. Other than the number of converters placed in the space, the parameters are the same as those discussed in Section 3. Similar to the five converter case, the performance of the three algorithms with an increased number of converters is compared through analysis of the objective function, and interaction factor. As previously noted, none of the algorithms converged to the same layout or had the same objective function. The best layouts are obtained using the GA and have objective function evaluations of 3.018 and 2.2741 with corresponding interaction factors of 1.02100 and 1.00462. Table 3.8 reports the objective function evaluation information from the different algorithms when 10 and 25 WECs are involved.

All of the layouts generated are unique between the three algorithms. Figures 3.2(a) and 3.2(b) show the configurations which yield the best objective function value between the three algorithms. Again, these layouts were generated by the GA. Table 3.9 confirms the performance of the GA, in that in addition to obtaining the best mean and overall

Table 3.8: Objective function evaluation comparison for 10 & 25 converter arrays

	10 Converters — Objective Function		
	Mean	Algorithm Best	Overall Best
Evolutionary Algorithm	3.0321	3.0287	
Genetic Algorithm	3.0222	3.0180	3.0180
Simulated Annealing Algorithm	3.0330	3.0237	
	25 Converters — Objective Function		
	Mean	Algorithm Best	Overall Best
Evolutionary Algorithm	2.3162	2.3042	
Genetic Algorithm	2.2794	2.2741	2.2741
Simulated Annealing Algorithm	2.3388	2.3315	

configuration, the GA also has the smallest standard deviation. As the number of WECs increases, the GA gives significantly greater interaction factors on average than the EA and SA, as indicated by the mean analysis results.

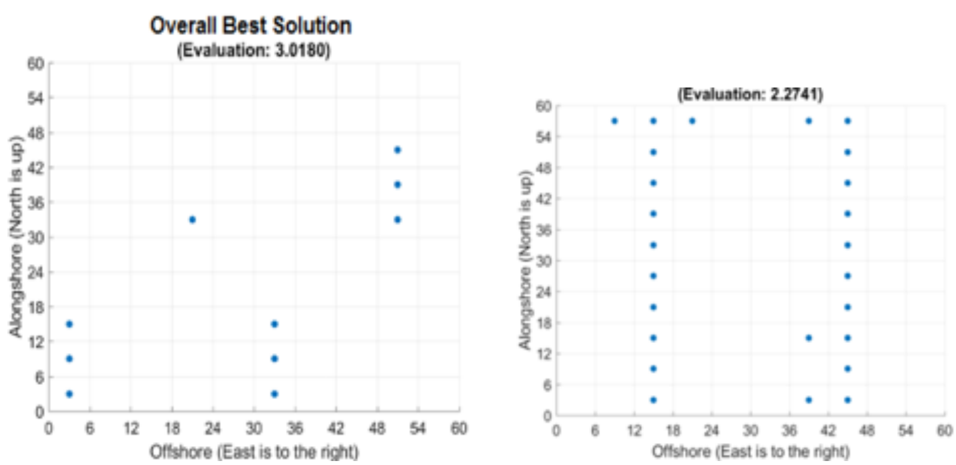

(a) 10 converters (b) 25 converters

Figure 3.2: Optimal layouts for arrays with 10 and 25 converters

Table 3.9: Interaction factor comparison for 10 & 25 converters arrays

	10 Converters — Interaction Factors			
	Mean	Standard Deviation	Algorithm Best	Overall Best
Evolutionary Algorithm	1.01625	0.0011	1.01714	
Genetic Algorithm	1.01958	0.0010	1.02100	1.02100
Simulated Annealing Algorithm	1.01599	0.0028	1.01907	
	25 Converters — Interaction Factors			
	Mean	Standard Deviation	Algorithm Best	Overall Best
Evolutionary Algorithm	0.98638	0.0045	0.99152	
Genetic Algorithm	1.00232	0.0017	1.00462	1.00462
Simulated Annealing Algorithm	0.97684	0.0030	0.97991	

These interaction factors indicate that the formation of WECs shown in Fig. 3.2 produce 2.1% more power with 10 converters and 0.46% more power with 25 converters than the combined power that would be produced by equivalent number of WECs acting in isolation. The results from the mean analysis of the objective functions obtained with the three algorithms show that the GA is also more robust at finding a minimized objective function evaluation, while the SA has the worst average result. Furthermore, while the percent yields indicated by the 25 converter are minuscule, this is likely because the physical space is constrained. The take away of this percent increase should not be it's numerical value, but rather that the algorithm was able to find a configuration, even in a constrained space, which yielded in interaction factor greater than one.

This further exploration demonstrates that the GA is more efficient when used in an increased search space. In fact, it shows that the GA is globally the best performing algorithm among the three compared, while SA has the worst performance for all numbers of WECs considered. Figure 3.3 portrays the interaction factor results of the different algorithms.

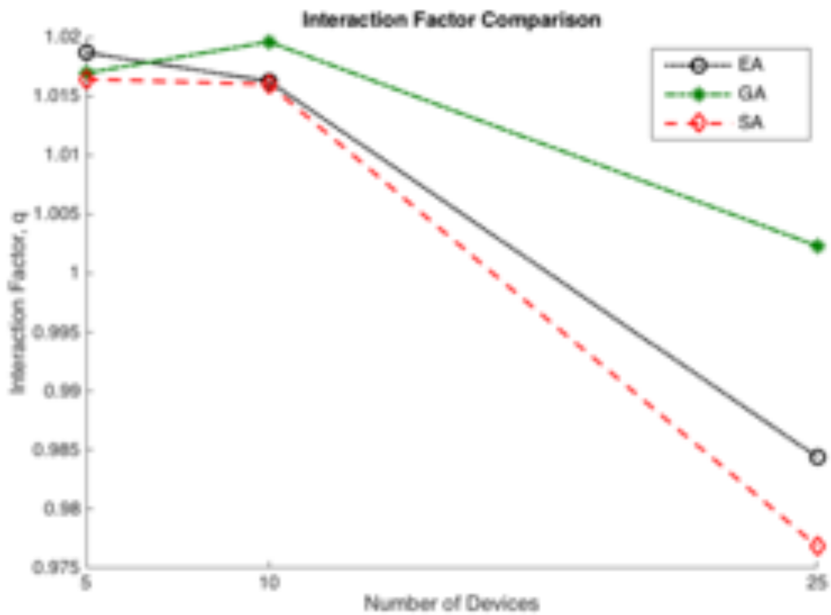

Figure 3.3: Algorithm interaction factor comparison

The figure indicates that for a given space with 100 discrete potential locations for WEC placement, the EA will perform better with fewer converters and consequently a smaller number of potential configurations; however, when the number of WECs and associated number of potential configurations is increased, the GA's performance becomes comparatively better. Specifically, for the case with 25 converters, the EA and SA both return layouts with interaction factors less than one indicating negative interaction, but the GA is able to still return layouts with interaction factors greater than one.

3.6 Conclusion

This chapter proposed three possible methods, an EA, GA, and SA, for determining the best configuration of a defined number of WECs in a discretized space.

The first case, using five truncated cylinders, was designed to compare again previous work in array optimization. It is found that the EA performs better than the GA and the SA and is able to find the best result seven out of its ten runs; however, the EA does average a higher number of function evaluations per run. The GA and the SA both also found the optimal arrangement, but only twice apiece out of their respective ten runs. Additionally, the EA has a smaller standard deviation when compared to the other algorithms. The SA performed the worst, but was relatively close in performance to the GA. The best result found for five WECs had in interaction factor of 1.01899 which correlates to a power increase of 1.9% when compared to five WECs acting in isolation.

To investigate what effect that the number of converters had on the different algorithms' performance, a continuation study was conducted where 10 and 25 devises are considered. For this case each algorithm was run five times. Of the fourteen total runs, none of the converged layouts are equivalent or have the same objective function. Unlike the case with five WECs, this case has the GA performing the best with the lowest mean and standard deviation values of objective function evaluations and interaction factors. In addition, the GA returns the best overall results with an interaction factor of 1.02100 and 1.00462 respectively. The SA once again performs the worst of the three algorithms.

Considering all the different WEC cases, it is determined that the EA performs better than the GA and the SA when the search space is relatively small due to its ability to explore the space. However, when the search space grows, the GA becomes the better option for finding an optimal configuration of WECs. This information demonstrates the importance of an optimization algorithm's need to both explore the solution space and exploit specific potential solutions. The wave energy industry has many hurdles to overcome as it moves towards WEC deployment and grid integration. Consequently, research regarding array deployment needs to consider the many influencing factors and needs to utilize algorithms well suited for the problem.

Chapter 4: Real-Coded Genetic Algorithm

4.1 Introduction

The results from the binary GA demonstrate the need for further investigation regarding the optimal placement of WECs in an array since potential power development may have been restricted by the discrete converter placement of our Binary GA. Accordingly, this chapter describes the process of a real–coded (also referred to as continuous) GA and the results we found using this method. This method is called real–coded because the converters are placed at coordinates based on any real value within the solution space. We created this real–coded genetic algorithm (GA) approach to determine optimal WEC array designs that incorporate cost information in addition to generated power. In our prior work (using a discretized GA method), we preliminarily explored the effects of WEC spacing. In continuation, this chapter will present a previously unexplored, real–coded approach that allows for the optimization of WEC spacing in a continuous solution space.

4.2 Real–coded genetic algorithm overview

A real–coded GA generates potentially optimal solutions via a representation of the biological reproduction process, wherein children solutions are comprised of components of the parent solutions and are potentially subject to prescribed mutation. The methodology of the real-coded GA is similar to that of the binary GA with several key differences.

The initial parent population, generation zero, is created by randomly scattering a defined number of converters into the solution space. To facilitate comparison to previous work, the space is defined as a 60x60 meter square and the number of WECs is limited to five. Each WEC location is specified by a random X and Y coordinate that is confined within the space; a critical difference between the continuous GA and the binary GA is that in the continuous algorithm, locations can take any value on a continuous scale (abiding by spatial constraints). That is, WEC locations are not limited to discrete coordinates. Throughout the entire execution of the algorithm, converter placement is only accepted when no physical overlap exists with any converters already in the space. Once the initial parents are generated, their objective function evaluations are found and sorted from lowest (best) to highest (worst). At this point the reproduction phase begins.

In our presented continuous GA, the children set is built over several stages — elitism, mutation of the elite, crossover and mutation, and random solution generation. Elitism occurs by cloning a set number of the best parent solutions directly into the children solution set. Doing so ensures that the global best solution in the parent population will not be lost during the GA process. In addition to these cloned solutions, a mutated set of cloned solutions is also added to the children set; the mutation process is described later in this section.

With elitism complete, crossover and mutation is conducted on a defined upper percentage of the parent solution set. Since previous research (including our previous binary GA work presented in Chapter 2 and 3) includes a fixed number of WECs, crossover is performed such that the number of converters is defined and retained. To accomplish this, we find pairs of parents using rank roulette selection as described in [59]. Once the crossover and mutation pool has been filled with the selected parent pairs generated through the rank roulette process, children are created as follows. First, based on a set probability, child solutions are made by combining WEC locations from two selected parents. In other words, the two children solutions created by a parent solution pair contain locations of WECs from each of the parents. To avoid a converter being placed in physical contact with another pre-existing converter, only non-overlapping converters are eligible for crossover.

Figure 4.1 demonstrates the utilized method of crossover. In this scenario all points in both parent solutions are available for crossover and two points will be swapped — the second and fourth points from the first parent and the first and second points from the second parent. Thus, the first child is comprised of points one, three and five from the first parent as well as points one and two from the second parent. Conversely, the second child contains points three, four and five from the second parent and points two and four from the first parent.

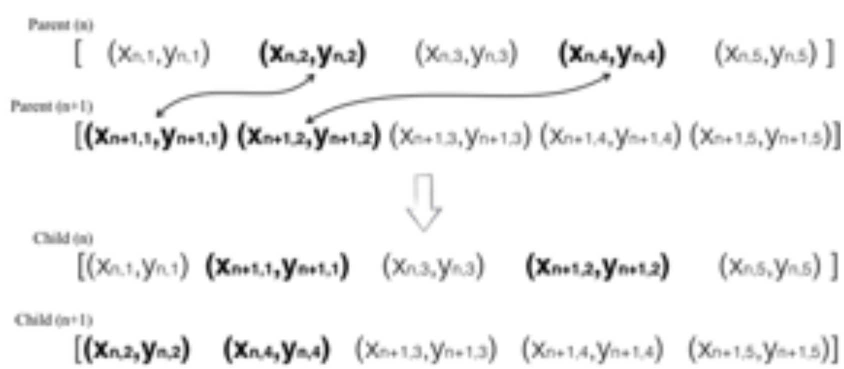

Figure 4.1: Real GA crossover method

Once the crossover children are created, they are potentially subject to mutation. If selected for mutation, based on a defined probability, a number of WECs in a child solution (up to a defined fractional amount of the total number of converters) are moved to new random locations in the solution space. Implementation of prescribed mutation, combined with crossover, allows for better exploration of the solution space to avoid being stuck in local minima.

The children set is now comprised of the elite group, the mutated elite group, and the solutions generated from crossover and mutation. In the final stage of the reproduction phase random solutions are introduced. These solutions are created in the same manner as the initial parent population and are incorporated into the children population to again allow the algorithm further exploration of the solution space.

Throughout the execution of the algorithm, new solutions (unique to a generation) are tracked so that only their objective functions need evaluation. In this manner, the number of function evaluations is reduced by only evaluating solutions that are different from the previous generation. With a children solution set created, the objective function is evaluated for each solution and a check for convergence is conducted. Convergence is determined by the number of elapsed generations without improvement in the evaluation of the best layouts. Once this criterion is satisfied, the best solution will be reported; however, prior to convergence, the children set becomes the parent set and the process repeats. An overview of the algorithm is represented in Fig. 4.2. This flow is the same as Fig. 2.3 with one particular update. In the reproduction phase we implemented an additional mutation component to the elitism component.

Figure 4.2: Real–coded GA flowchart

4.3 Objective Function Formulation

To calculate power, the behavior of an isolated WEC is first considered using the linear wave–body software WAMIT [45]. The WEC is subjected to incident waves from multiple directions in a sea–state with a limited water depth and a range of wave periods. With the hydrodynamic information of the single converter obtained from WAMIT, the diffraction coefficient matrix, force transfer matrix, and radiated wave coefficients are found for the single WEC. The process is explained more fully in Chapter 2. To best compare against our previous binary GA work we used the objective function, power calculation, and cost equation shown in Eq. 2.1, 2.2, and 2.3 respectively.

4.4 Problem Formulation

The WEC used in this research is the same converter as is modeled in [11, 25], and is consistent with the WEC modeled in previous work and in the preceding chapters [34]. This WEC is a truncated cylinder constrained in the vertical direction (heave) with a radius of one meter and a draft of one meter. Placed in water with a depth of eight meters, these parameters are a scaled representation of an array of 10–meter diameter converters in a water depth of 40 meters [34].

When placed in an array, the WECs experience unidirectional, irregular waves defined by a Bretschneider spectrum. This spectrum is generated with a significant wave height of two meters, a modal frequency of 0.2 Hertz, and periods in half–second increments distributed between 4 and 8 seconds. Two different test scenarios, each with 5 converters, are conducted. The first allows the WECs to be placed anywhere in the solution space with the only requirement being that no physical overlap occurs. Additionally, since WECs deployed in the ocean will most likely need to be separated from neighboring WECs to allow OM access and to minimize harmful physical interaction, the second scenario imposes a minimum separation distance of three times the diameter (six meters center–to–center) as is proposed in [23]. Tables 4.1 and 4.2 show the tunable parameters for both scenarios.

Table 4.1: Test scenario parameters

Scenario	# of WECs	Solution Space [m]	Minimum Separation Distance
1	5	60 x 60	– –
2	5	60 x 60	6 [m]

Table 4.2: Tunable GA parameters

	Scenario 1	Scenario 2
# of Parents	100	100
Elitism Rate	3%	5%
Crossover & Mutation Rate	81%	75%
Probability of Mutation	35%	35%
Max Percentage of WECs to Mutate	40%	40%
Convergence Requirement (Generations Without Improvement)	75	75

For the problem presented here, with a small and constant number of WECs in a relatively large space, the main parameters that were tuned to achieve the presented results are the elitism rate (and consequently the crossover and mutation rate), the probability of mutation, and, to a small extent, the probability of crossover. The convergence requirement was empirically determined, and set at 75 generations without improvement.

Using five converters allows for results which can be readily compared against previous work that use the same number of converters [34, 25]. The size of the solution space is defined to match the maximum sized space from the binary GA work, 60 x 60 meters.

4.5 Results and Discussion

As GAs are inherently stochastic and the number of potential array arrangements infinite, each scenario was conducted multiple times and the best results, based on the objective function evaluation, are reported here.

The overall best result between the two scenarios is shown in Fig. 4.3(a). For all the following layout images in this chapter, the unidirectional incident waves are traveling due East (from left to right). With no minimum separation distance imposed, the best layout is achieved when the WECs line themselves up in pairs, parallel to the oncoming incident wave. This layout is similar to the best layout found by the three-meter minimum separation distance case of the binary GA (Fig. 2.6(a)). The effect of this layout on the wave field is portrayed in Fig. 4.3(b).

With the incident waves approaching from the left, the center–to–center distance between paired WECs in the offshore direction is approximately three meters and the center–to–center distance between up–wave WECs in the alongshore direction is about eight and one–half meters. While this scenario allows the converters to be closer than three meters (unlike in the binary case) the optimal result is found when the WECs are separated from each other by a small amount in the offshore direction in order to take

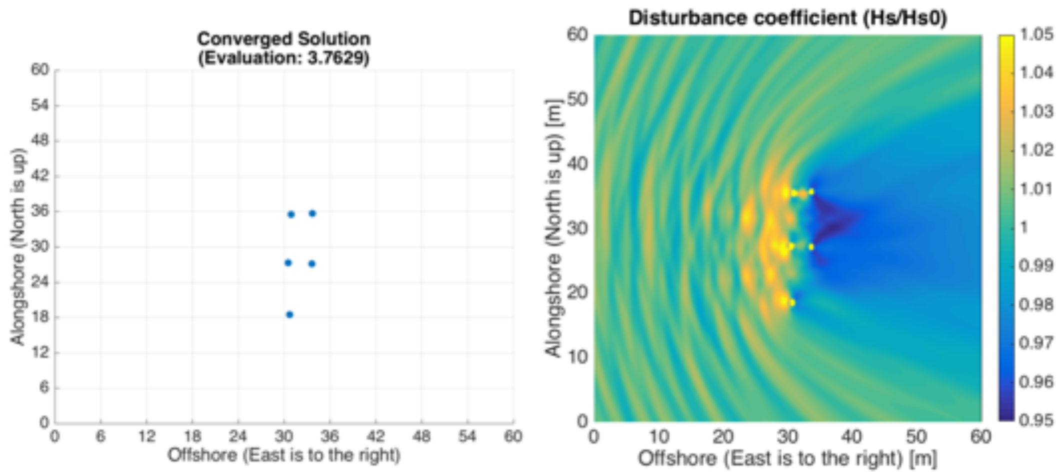

(a) Layout (b) Effect on the wave field

Figure 4.3: Best layout achieved for the first scenario

advantage of the radiated waves, and far enough apart in the alongshore direction to benefit from the diffracted waves.

The next scenario considered includes a minimum separation distance in order to model realistic array deployment and to compare against the results from the scenario with no spacing constraint. For this scenario, the two layouts with the best function evaluations will be examined. As with the binary GA, when the WECs are required to stay a certain distance apart, the resulting WEC placement transitions away from capitalizing on radiated waves to solely taking advantage of the diffracted waves since the radiated waves dissipate quickly with distance from a converter. Figure 4.4(a) shows the layout with the best objective function evaluation given the spacing constraint. Figure 4.4(b) demonstrates the effect that this layout has on the wave field.

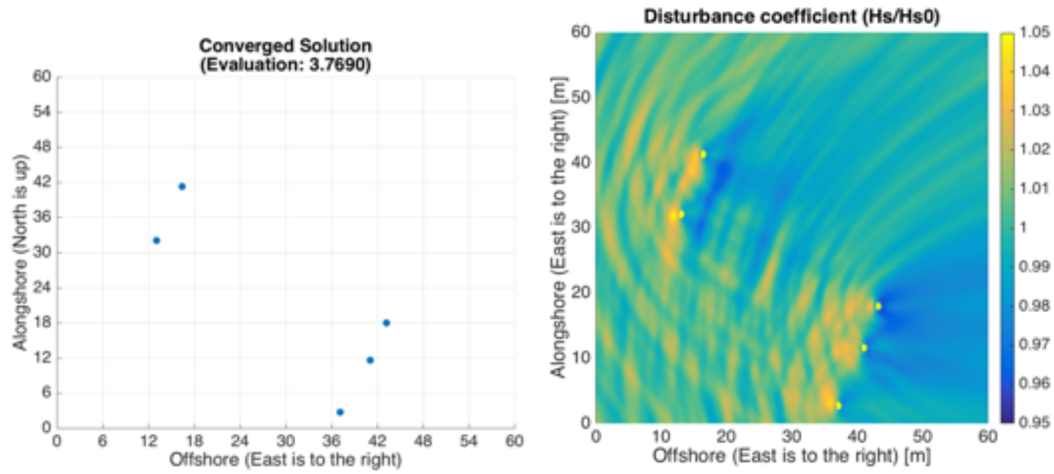

(a) Layout

(b) Effect on the wave field

Figure 4.4: Best layout achieved for the second scenario

Examining the wave field effect, it is observed that within the two clusters, WECs benefit from each other's diffracted waves and that, in addition, the group of converters further down–wave also benefit from the up-wave pair of WECs. It is worth noting that the layout that achieves the second best objective function evaluation, with the spacing constraint imposed, demonstrates the general shape of a layout that occurs relatively often between both scenarios.

The grouping of four WECs, close to equally spaced, at an angle slightly offset from the perpendicular to the incident wave occurs often in the results of this study. Of this type of result, the best, and the second overall best for the second scenario, has a 0.09 percentage difference in objective function evaluation when compared to the second scenario's best overall result. Comparatively, the worst of this type of layout has only a 0.48 percent difference when compared to the function evaluation of the second scenario's overall best. Because these values are small we can see that, though the layouts may

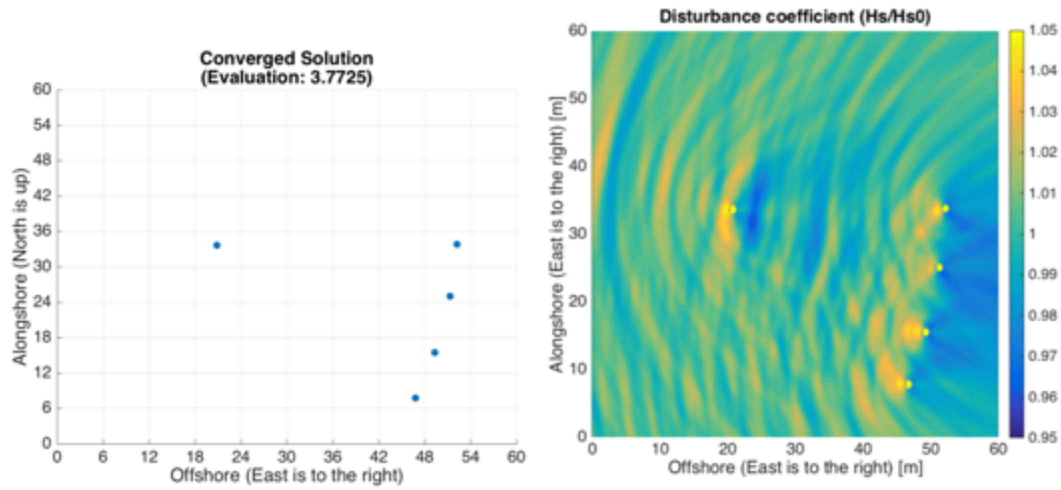

(a) Layout (b) Effect on the wave field

Figure 4.5: Second best layout achieved for the second scenario

differ in shape, they are generating a similar amount of power. The angled alignment of the grouped converters is allowing an improved cascading interaction effect due to diffracted waves. Since the potential locations for WECs is infinite, if the WECs line up exactly perpendicular to the incident wave, they would need precise placement in order to benefit from the diffracted waves of neighboring WECs. However, with the angled placement shown, the converters further down-wave can capture the diffracted waves of more up–wave WECs. This offset angle is also observed in the results of Child and Venugopal and DNV–GL [23, 34].

The isolated fifth converter seems to be deemed unnecessary by the algorithm in regards to array design. Variation in function evaluation between similar layouts is primarily affected by the grouped WECs and less by the isolated WEC. Table 4.3 shows the objective function evaluations and the interaction factors for the results of both scenarios.

Table 4.3: Objective function evaluations and interaction factors of presented results

	Scenario 1	Scenario 2a	Scenario 2b
Objective Function Evaluation	3.7629	3.7690	3.7725
Interaction Factor (q)	1.0269	1.0252	1.0243

If the WEC spacing is left unconstrained, then the algorithm finds a layout that has a power improvement of 2.7% when compared to the power produced by five WECs acting in isolation. Once a spacing constraint is put in place, then the algorithm returns a layout with a 2.5% power increase. Table 4.4 compares the results presented here with the interaction factors of previous work. For the results shown from the parabolic intersection method and MATLAB's GA, the layouts obtained from [34] (shown in Fig. 1.2(a) and 1.2(b) respectively) were calculated using the method presented in this chapter for a more accurate comparison.

Table 4.4: Objective function evaluations and interaction factors of presented results compared against previous research

	Objective Function Evaluation	Interaction Factor (q)	Power Increase
MATLAB's GA	3.8864	0.9942	-0.6%
Parabolic Intersection	3.8793	0.9961	-0.4%
Binary GA (6m minimum spacing)	3.7920	1.0190	1.9%
Binary GA (3m minimum spacing)	3.7737	1.0239	2.4%
Scenario 2 (6m minimum spacing)	3.7690	1.0252	2.5%
Scenario 1 (no spacing constraint)	3.7629	1.0269	2.7%

The table shows clear improvement with the introduction of the real–coded GA. The results of the two scenarios found layouts that obtain a better increase in power production when compared to the best performing binary GA result. In fact, across all the runs conducted, both scenarios consistently achieved layouts with better results than their counterparts using the binary GA.

4.6 Conclusion

Research in array configuration design has solely focused on maximizing power production and only mentions the need for incorporating cost. Additionally, implemented methods have primarily been based on user-decided layouts which are dependent on many assumptions that are yet to be well understood or quantified. Our previous work, discussed in Chapter 2 presents the use of a binary genetic algorithm that includes array cost in the objective function. These preliminary results indicate that converters need the opportunity to be placed anywhere in the solution space.

Consequently, the real–coded GA presented here demonstrates the advantage of implementing non–discretized space. Allowing WECs to select any location in the stipulated space, the best overall layout achieves a 2.7% increase in power over the power that would have been produced if the five WECs were acting alone. This is a 12.5% increase over the best result found using the binary GA method. Even when a six–meter spacing constraint is set in place around the WECs, the real–coded GA obtains an array that performs 4.2% better than the best result from the Binary GA.

Similar to the binary GA, when the minimum separation distance is small or nonexistent, the WECs take advantage of neighboring converters' radiated waves, but transition to capitalizing on diffracted waves when imposed with minimum spacing requirements. Since developers will not want their WECs physically interacting with each other, layouts will not likely be deployed to take advantage of the radiated waves unless the WECs can be fixed to the ocean floor. As another alternative, if a WEC was created with multiple components that acted interdependently to generate power, those individual generators could benefit from the radiated waves and positioning would be important. When the objective function evaluations and interaction factors are compared to other research in array design, the real–coded GA outperforms in both the unconstrained and constrained scenarios.

The layout configurations from the algorithm vary due to a highly multi–modal solution space. Due to seemingly minor differences in WEC positioning, results from two different runs can have similar looking layouts, but different objective function evaluations. However, for the layouts from the second scenario with groupings of four, the results have a low percentage difference from the global best solution. This points towards a more robust design than the global best layout.

In the second scenario's second best layout (shown in Fig. 4.5), with the minimum spacing constraint in place, the fifth converter does not find a manner of incorporating itself into the array. GAs do not guarantee global optimality and it is possible that this fifth converter does not follow a similar trend to the other WECs because the algorithm was unable to find a better layout before reaching convergence. However, given the convergence criteria and the consistency of the generated layouts over the many trials, the potential for improvement is not likely. Also, this indicates the need for allowing a variable number of WECs in order to find the optimal number for a defined space. Additionally, constraining the number of WECs to a set value loses relational WEC information in the implemented crossover method, but allowing for a variable number of converters and implementing multi–point crossover would help alleviate this issue.

Finally, with the constant number of converters, cost is unable to influence the layout configuration with the current objective function equation. Through better inclusion and investigation of influencing elements, the application of a continuous algorithm is advantageous for determining the optimal spacing of WEC arrays, through the ability of the algorithm to dictate the optimal WEC placement in the solution space.

Part II

Investigation of Layout Design Influences

Chapter 5: Binary Genetic Algorithm Row Spacing Study

5.1 Introduction

With the many potential factors impacting arrays, it is vital that tools are created that realistically inform developers about the deployment of optimal WEC farms. To best account for the factors involved, it is useful and necessary to utilize optimization techniques. However, at this stage in WEC array design research, most work assumes prescribed layouts based on basic assumptions. Little research has been conducted regarding the use of optimization methods for array configuration. As an extension of our optimization work discussed in prior chapters, this chapter investigates how generated power is influenced by the separation distance between two rows of parallel wave energy converters perpendicular to a unidirectional wave field.

A majority of research investigating the configuration of arrays use assumed layouts based on geometric shapes such as squares, triangles, diamonds, stars, single rows, and parallel offset rows [14, 15, 16, 17, 18]. Beyond the research involving assumed layouts, there is some work investigating the use of optimization methods for determining layouts.

In Chapter 2, we introduced a customized genetic algorithm method used for determining optimal arrangements of five WECs (similar to those converters used in [34]) in a discrete space. This work is novel in the implementation of a customized genetic algorithm, and the inclusion of cost in the objective function equation [11, 25]. Further investigation of varying numbers of WECs reveals the WECs arranging themselves in two parallel lines perpendicular to oncoming wave field with a consistent spacing between rows. Figure 5.1 shows an example of the spacing seen with 20 converters (unidirectional waves are coming from the the left). We created this layout based on results we saw from the introduction of multiple converters in Chapter 3. To better understand this spacing effect, a specific study with 20 WECs was performed.

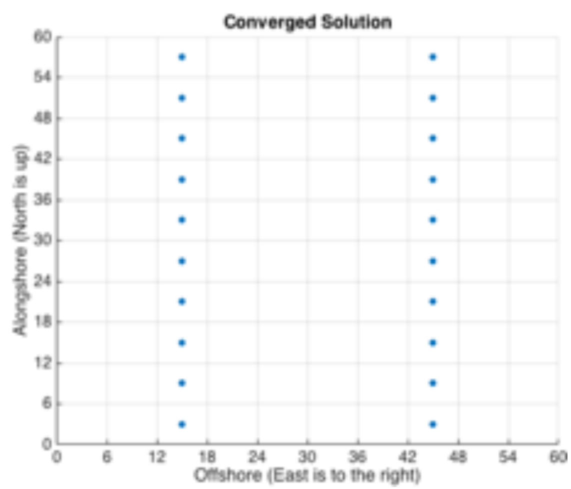

Figure 5.1: Optimal arrangement found for 20 WECs

5.2 Study Parameters

For this study, the scaled converter modeled is a truncated cylinder constrained in the heave direction. The radius is one meter and the draft (distance of the WEC below the free water surface) is one meter. As in Chapter 2, these WECs are placed in a water depth of eight meters and subject to a wave field derived from a Bretschneider spectrum that has a modal frequency of 0.2 Hertz and a significant wave height of two meters.

In this chapter, the interaction factor of configurations at different prescribed spacing are compared. The scaled converter modeled, the parameters (water depth and wave spectrum), and the objective function are the same as those used in Chapters 2, 3, and 4. The interaction factor, q, is determined using Eq. 1.1. The initial starting point of the study fixes the up–wave row of WECs at the front of the space with six meters between each converter in the alongshore or y direction. The secondary row is initially placed six meters down–wave from the fixed row and subsequently moved incrementally to the right.

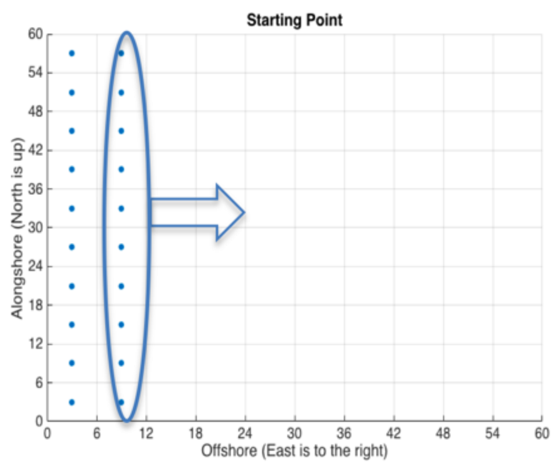

Figure 5.2: Starting point for the rows of WECs

Several different scenarios are considered. In the first, the space is constrained to 60 x 60 meters (shown in Figure 5.2) and the location with the maximum interaction factor is determined. In the second scenario we increase the space in the offshore direction to determine if a more optimal spacing exists beyond that which is found in the first scenario. The third scenario evaluates the trend of the interaction factor as the space changes. From these results a maximum interaction factor of 1.0334 is found at a spacing of 51 meters and is shown in Figure 5.3. The second best interaction factor of 1.0284 is located at a spacing of 30.75 meters. The interaction factors found are potentially limited by the defined nature of the layouts in the constrained space. It also appears that the rows of WECs are attempting to be placed at opposite ends of the space likely to minimize negative interactions between the rows.

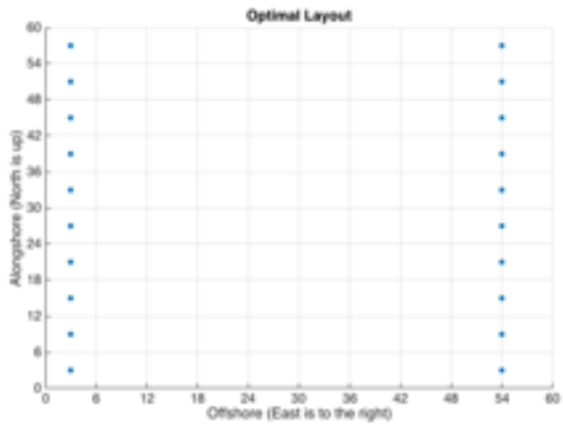

Figure 5.3: Optimal separation spacing in a 60x60 meter space

5.3 Row Spacing Study

For the first scenario, the optimal spacing is found in a 60x60 meter space. Figure 5.4 shows the interaction factor as a function of the distance, in meters, between the converter rows. The results are evaluated at quarter meter intervals. The interaction factor fluctuates greatly across the space and shows that specific placement of the converter rows is required to avoid destructive interaction. Also, since the array is experiencing irregular waves the larger increases in the interaction factor are like correlated to oncoming wave groups.

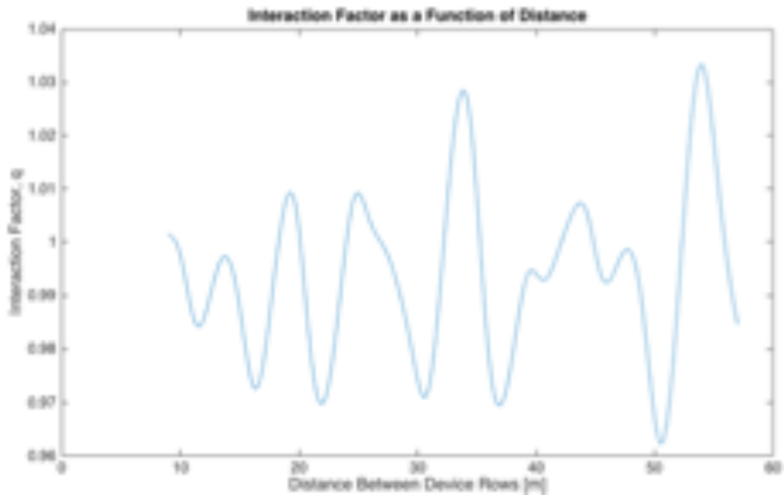

Figure 5.4: Interaction factor as a function of distance between rows for a 60x60 meter space

When the distance offshore is increased from 60 meters to 700 meters, the results obtained are shown in Figure 5.5. For these results the interaction factors are evaluated at one meter intervals. With the increased distance offshore, the maximum interaction factor of 1.0403 occurs at a separation distance of 270 meters. The 60x60 meter case shows that the row spacing is important and with the one meter intervals for the 60x700 case there is the possibility that some spacings were missed which could have resulted in an increased interaction factors. Again, the larger increases (and decreases) in interaction factor are likely connected with the incident wave groups.

As an alternative consideration, the row of WECs to be moved are offset in the alongshore direction - shown in Figure 5.6. Resulting behavior of the interaction factors for the 60 m x 700 m space is shown in Figure 5.7.

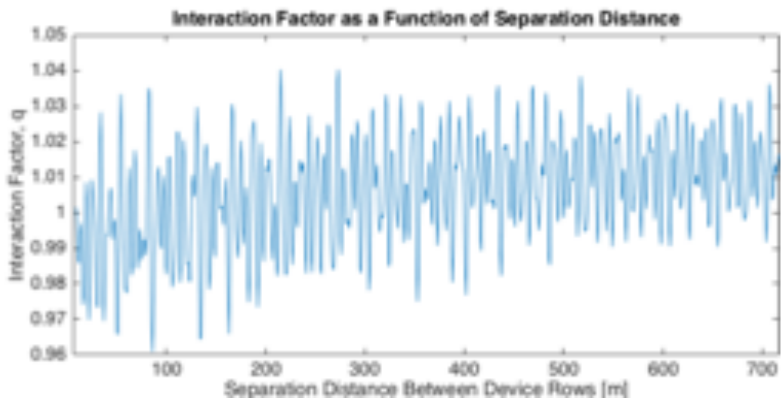

Figure 5.5: Interaction factor as a function of distance between rows for a 60x700 meter space

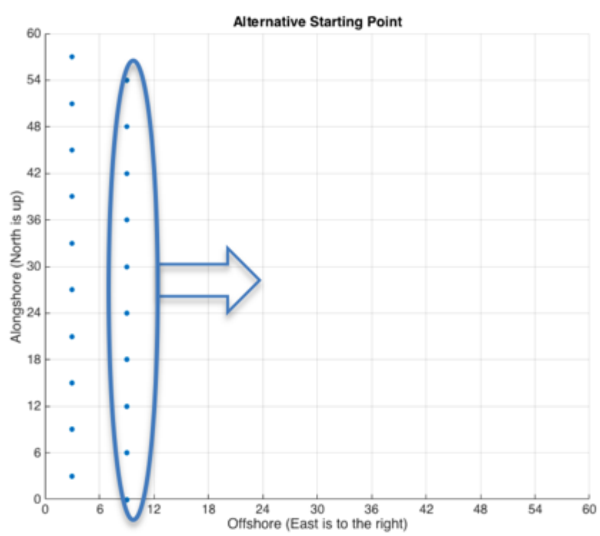

Figure 5.6: Alternative starting point for the rows of WECs

Figure 5.7: Interaction factor as a function of distance between offset rows for a 60x700 meter space

The offset lines yield a maximum interaction factor of 1.401 at a spacing of 212 meters and again at 270 meters. Lastly, the interaction factors every two meters are found for a 60 m x 1400 m space. The maximum interaction factor (and its location) is the same as the 60 m x 700 m case, but these results are generated to observe the overall behavior of the interaction factor as the separation distance increases. The smoothed data approaches an interaction factor of approximately 1.015.

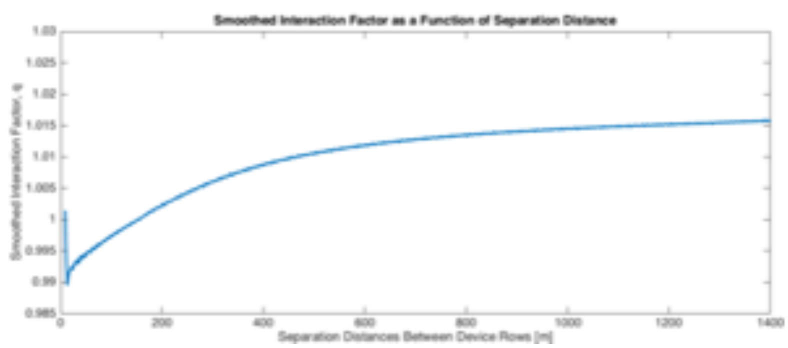

Figure 5.8: Smoothed interaction factor as separation distance increases

5.4 Discussion

Examining the results, beginning with the 60 x 60 meter case, a separation distance similar to that found using the binary GA (shown in Figure 1) is found at about 30 meters, but a better solution is found at 51 meters. The reason that the binary GA does not find the solution at 51 meters is because of its discretized nature. The arrangement shown in Figure 4, with an optimal distance of 51 meters, yields an increase in power of 3.34%. Once the distance offshore is increased to search for a more optimal separation distance, this maximum interaction factor is found to yield a 4.03% power increase (as seen in Figure 5). When the rows are set as offset the results are found to be a very similar to those of the inline rows. These results indicate that given two parallel lines of WECs in an array, the distance between these rows can yield up to a 4% increase in power, but that achieving such an increase is highly dependent on having optimal spacing between rows.

The interaction factor's trend demonstrates that, while the the optimal spacing distance occurs between 200 and 300 meters, placing the WECs even farther apart results in interaction factors that are more robust — having a consistently higher average interaction factor. (Shown in observed in Figure 5.5) This consistent higher interaction factor is likely due to the positive interactions within the the two separate lines of WECs, and not connected to interactions between the two lines. The WECs would likely perform better if placed in a single line of twenty WECs perpendicular to the incident wave.

5.5 Conclusion

Influencing developed power, configuration of WECs within an array is an important determination. We introduced a novel algorithm for determining optimal WEC layouts, and as an extension of this work, a pattern was observed where arrays of WECs are formed with two parallel lines perpendicular to the oncoming waves. Further investigating this observation reveals that there are specific separation distances where the interaction factor (defined in Eq. 1.1) is maximized. To achieve interaction factors that have a consistent average higher than one, the parallel lines must be adequately separated. The necessary separation distance indicates that the layout isn't optimal, but that the individual rows achieve increases in power. The fixed layouts and the constrained space limit the potential interaction factors and don't guarantee that the parallel lines are an optimal layout; however, these results do provide a preliminary understanding the influence of spacing on developed power. These solutions also reinforce our transition to a real-coded algorithm to allow the algorithm to determine the spacing.

Chapter 6: Array Optimization of Fixed Oscillating Water Columns for Active WEC Control

6.1 Introduction

It is expected that in addition to layout optimization, active control scenarios must be implemented to fully maximize power production of an array. Consequently, it is necessary that we consider optimal layouts in conjunction with active WEC control. As a part of the Advanced Laboratory and Field Arrays (ALFA) project (a U.S. DOE project), we have been determining optimal WEC layouts of an oscillating water column (OWC) array.

In this chapter we discuss an overview of our task within the project; prior optimization approaches to WEC array design; the tank–validated, boundary element method (BEM) model of our OWC; the optimal layouts generated by our problem specific genetic algorithm (GA); and our initial analysis of the power output sensitivity due to damping control and array design. The achieved layouts will indicate the influence of sea state on WEC layouts configuration and will show the need for active WEC control to enhance performance.

6.2 Project Overview

Of the ALFA project's many directives, we are specifically investigating the enhancement of WEC array performance. The goals of our task include generating optimal configurations of a WEC array, developing control strategies for the WECs within these arrays, and validating the use of these control strategies on an optimized array through tank testing.

Because the WECs being constructed are only intended for tank testing and the number of converters is fixed at five, cost has been excluded from consideration in this study and instead we are focusing on power development and the interaction factor. We will validate the array optimization and control results against tank test data later this year. More information can be found on the modeling and physical testing of our chosen WEC in [2].

An objective of our work is to better understand the integration of active control and array optimization. With the stochasticity of sea conditions, actively controlling converters within an array is believed to likely have greater influence on increasing power production than what can be achieved through array optimization of non–controlled converters [21, 22]. Active WEC control has been shown to effectively increase power production [26]; consequently, future array design should include such control to accurately determine layouts that maximize power. Unfortunately a model does not currently exist that includes both between–WEC wave interaction and active control. Our work will serve as a basis for the future inclusion of active control into an optimization scheme.

6.3 Assumptions

Research has only recently begun intentionally considering optimization methods for WEC layout design and the work presented in this chapter furthers our novel approach of utilizing a custom genetic algorithm [11, 40]. We are not looking at designing for a specific type of WEC or a specific location, but are creating a framework that allows for a high level of adjustment specific to the problem of WEC layout configuration.

For the project discussed in this chapter we are utilizing OWCs that have intentionally been designed to be simple – allowing us to inexpensively build five WECs and their associated hardware. These WECs are not designed to be scaled for commercial implementation at any point in the future. To enhance our ability at observing the connection between array design and WEC control, the OWCs will be fixed to the tank floor.

6.4 Current Optimization Scheme

The complexity of the array optimization problem is not limited to determining the power produced by an array, but should also include alternative factors which might alter an array's design. Some of these, such as cost and active WEC control, will likely have significant influence on a layout. We have developed a genetic algorithm (GA) specific to the problem of WEC array design that furthers the work of existing research. Our GA currently allows for the inclusion of array cost in addition to power [11, 40]; however, since the number of converters being tested in this study is fixed and the converters are solely intended for tank testing, we have simplified the objective function to only consider generated power. This will aid in moving towards including WEC control in the objective function through variable WEC damping. With a fixed number of WECs intended for tank testing, our optimization centers around the maximization of power. As such the objective function we are seeking to minimize is

$$ObjFun = -P_{20} \tag{6.1}$$

where P_{20} is the power generated by an array over a 20 year lifespan. The algorithm is visually shown in Fig. 6.1.

6.5 OWC Modeling

We have previously produced layouts of scaled heaving point absorbers in both the discrete and continuous spaces [11, 40]. For this project, five physical oscillating water columns (OWCs) have been constructed for layout optimization and control. Figure 6.2 shows one of these WECs and its dimensions. The remaining four converters are built in the same manner. We chose to construct and utilize these converters because of their inexpensive nature and consequently our ability to build five WECs for better array evaluation. Additionally, the design of these converters allows for more manageable controllability because the electronic hardware is out of water.

Our OWC operates by having a hollow cylinder extend both above and below the water surface. As the water rises and falls, air is forced in and out of the hollow interior through the cylinder's narrower, above–water component. If this WEC were to be used as an energy producer, the flow of air would likely turn a bidirectional turbine which would then generate electricity. For our work, a butterfly valve is used in place of a tur-

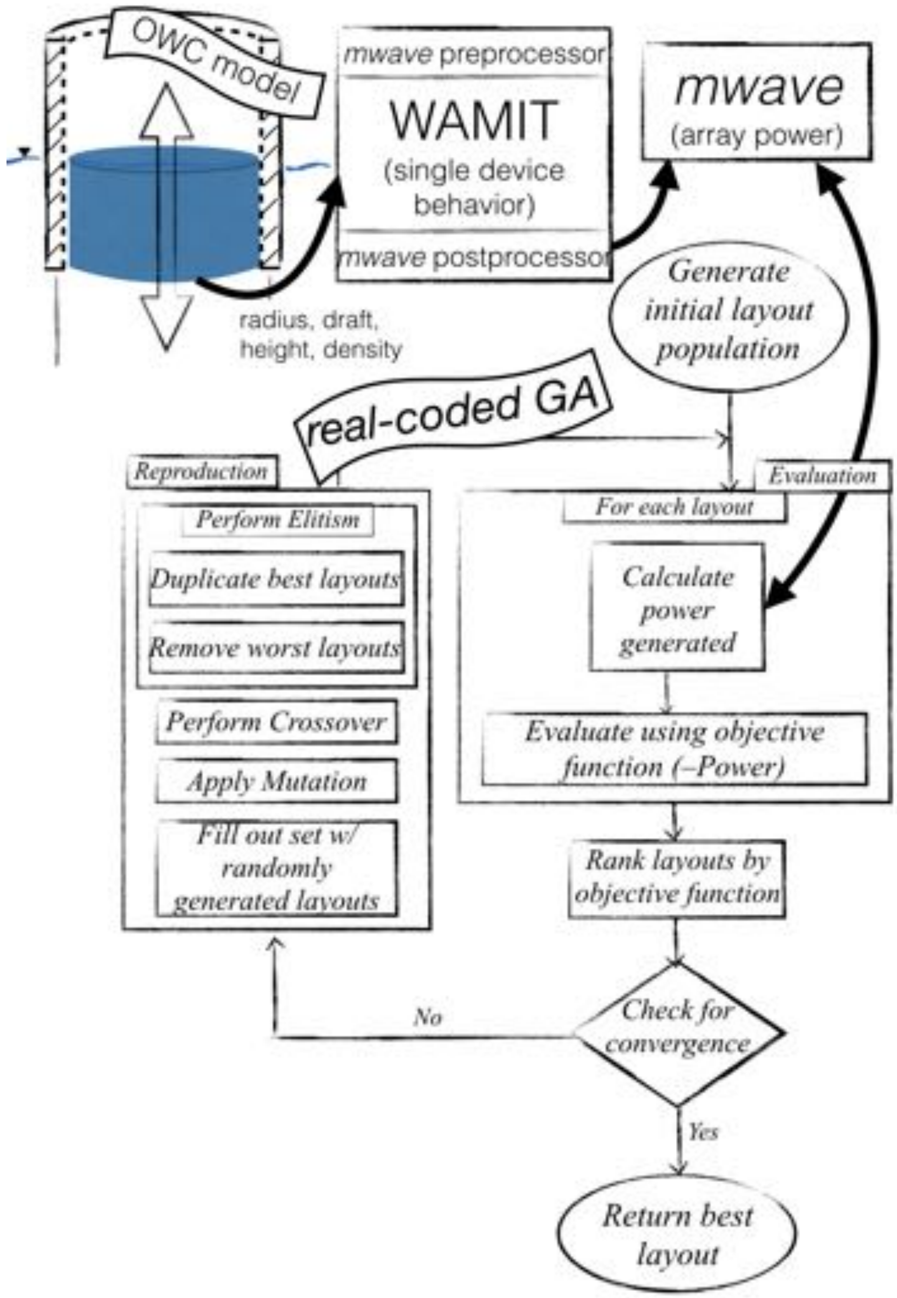

Figure 6.1: Optimization process overview

(a) Photo of OWCs being built

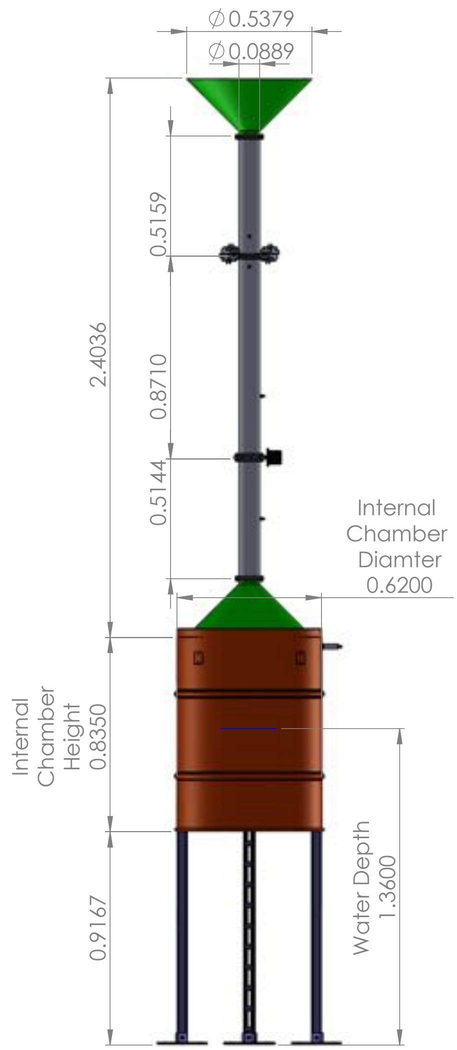

(b) Schematic of OWC

Figure 6.2: OWC Prototype

bine due to its measurability and controllability. This valve can rotate between 0° and 90° where 0° indicates the valve completely closed and 90° indicates a completely open valve. Specific details on this can be found in the corresponding study by Bosma et al. [2].

To evaluate potential layouts of OWCs in search of an optimal solution, we model the OWC shown in Fig. 6.2 within WAMIT. Developed by Evans [60] and described in [61, 62, 63, 64], the OWC is modeled using a piston approach. This method treats the mass of water moving inside the cylinder as a point absorber. Since our OWCs are to be secured to the tank floor, the WAMIT model needs only consider the single body of the water column constrained in heave.

The water depth and desired wave periods are used as inputs into WAMIT along with the radius, draft, height and density of the representative point absorber. *Mwave* creates these necessary input files for WAMIT as a preprocessor and, once WAMIT has completed running, processes the output data to formulate an object containing the information needed to analytically determine an array's power output. The theory behind *mwave* is described in [65, 20].

WAMIT details how a converter behaves for a range of wave periods and directions at a single water depth. It is run once at the beginning of the optimization process — unless a physical WEC parameter is changed or a different sea condition is desired (i.e. differing draft or water depth). Showing the response amplitude operator (RAO) output from WAMIT and the experimentally determined RAO, Fig. 6.3 indicates the viability of our developed BEM model. The RAO indicates the behavior of a WEC in a given sea state and Fig. 6.3 shows that the behavior of our modeled converter is similar to the behavior of the actual WEC in the wave tank. H_s indicates different significant wave heights that the dominant periods are evaluated at. Full details on the initial tank test of a single OWC can be found in [2].

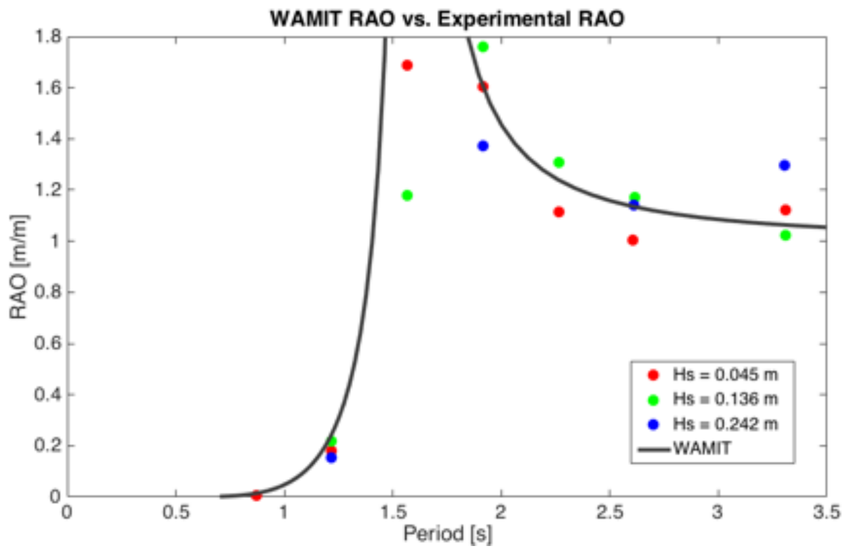

Figure 6.3: RAO comparison between WAMIT results and tank data

The output of WAMIT is needed by the power calculation within *mwave*. *Mwave*, and consequently the outputted MATLAB hydrobody, are called for every uniquely created layout within the real-coded GA.

6.6 Array Optimization

With the information derived from WAMIT, we begin the real–coded GA process. Even without guaranteeing global optimality, our GA method was, and is continually being, developed because of its ability to handle the stochasticity surrounding WEC array optimization. The real–coded GA flowchart in Fig. 6.1 shows the progression of steps. Table 6.1 contains the tunable parameters within the GA and the assigned values for the work presented in this chapter. Detailed specifics on the workings of our real-coded GA can be found in Chapter 4 and [40].

Table 6.1: Tunable GA parameters

# Of Parents	100
Elitism Rate	2%
Crossover & Mutation Rate	74%
Crossover Probability	100%
Mutation Probability	35%
Max # of WECs to Mutate	2
Convergence Requirement (generations without improvement)	100

Since every generation of children becomes a parent generation and continues the reproduction cycle, a convergence criteria is defined to conclude the algorithm. As indicated in Table 6.1, 100 generations must occur without finding a new best overall solution before the GA will stop and return the best layout. Because the search space is infinite and stochastic, the GA repeats several times for each scenario and we are presenting the overall best of the resultant layouts.

For this work, we focus on 18 different wave scenarios. A water depth of 1.36 meters and wave height of 0.136 meters is consistent across these cases while the wave period, valve angle, and wave type (regular or irregular) are varied. The selected water depth is the max depth capable in the tank and the selected wave height was chosen because it was used by Bosma et al. in [2] to generate damping values based on sea state and valve angle. For all cases, the damping values come from tank testing this OWC prototype in regular waves with the significant wave height and periods shown in Fig. 6.3. The WECs are required to be at least 3 times their diameter away from neighboring converters, this distance is measured from center–to–center, to mimic real sea constraints. Table 6.2 shows the considered scenarios and the water density is 1000 kg/m^3. The valve angles and associate damping values shown in the table were chosen based on information presented in Bosma et al. [2]. We are specifically looking to observe the potential impact of three variables — wave period, wave type (regular versus irregular), and damping (valve angle).

Table 6.2: Wave scenarios

Regular Wave Cases			
Valve Angle	Wave Height [m]	Period [s]	Damping [N/(m/s)]
80°			107.1
44°	0.136	1.22	363.9
0°			3316.2
44°		1.57	640.6
44°	0.136	1.91	774.7
44°		2.26	891.0
44°		2.61	892.4
80°			293.0
44°	0.136	3.31	775.2
0°			10032.5
Irregular Wave Cases			
Valve Angle	Significant Wave Height [m]	Peak Period [s]	Damping [N/(m/s)]
80°			107.1
44°	0.136	1.22	363.9
0°			3316.2
44°	0.136	1.91	774.7
44°		2.61	892.4
80°			293.0
44°	0.136	3.31	775.2
0°			10032.5

6.7 Results

For all cases, waves are unidirectional. The physical space is tunable within the real–coded GA so each scenario is run through several different sized spaces to ensure that the defined physical space does not become a constraint. The dimensions of the axes in the resulting layouts (shown in Fig. 6.4– 6.9) indicate the dimensions at which the best layout is found. The colorscale in these figures shows the disturbance coefficient which is the change in signifiant wave height, due to the presence of an array, when compared to the incident significant wave height.

6.7.1 Fixed Valve Angle - 44°

We first generate optimal layouts while considering a consistent valve angle of 44°. Six cases of regular waves and four cases of irregular waves are run. These cases are shown in Table 6.2. With the valve angle constant, the damping fluctuates between each run as a result of a changing wave period.

6.7.1.1 Regular Waves

The wave periods, T, for the regular wave cases range from 1.22s to 3.31s with a consistent wave height of 0.136 meters. Each scenario is run multiple times and the layouts found yielding the best interaction factors are shown in Fig. 6.4.

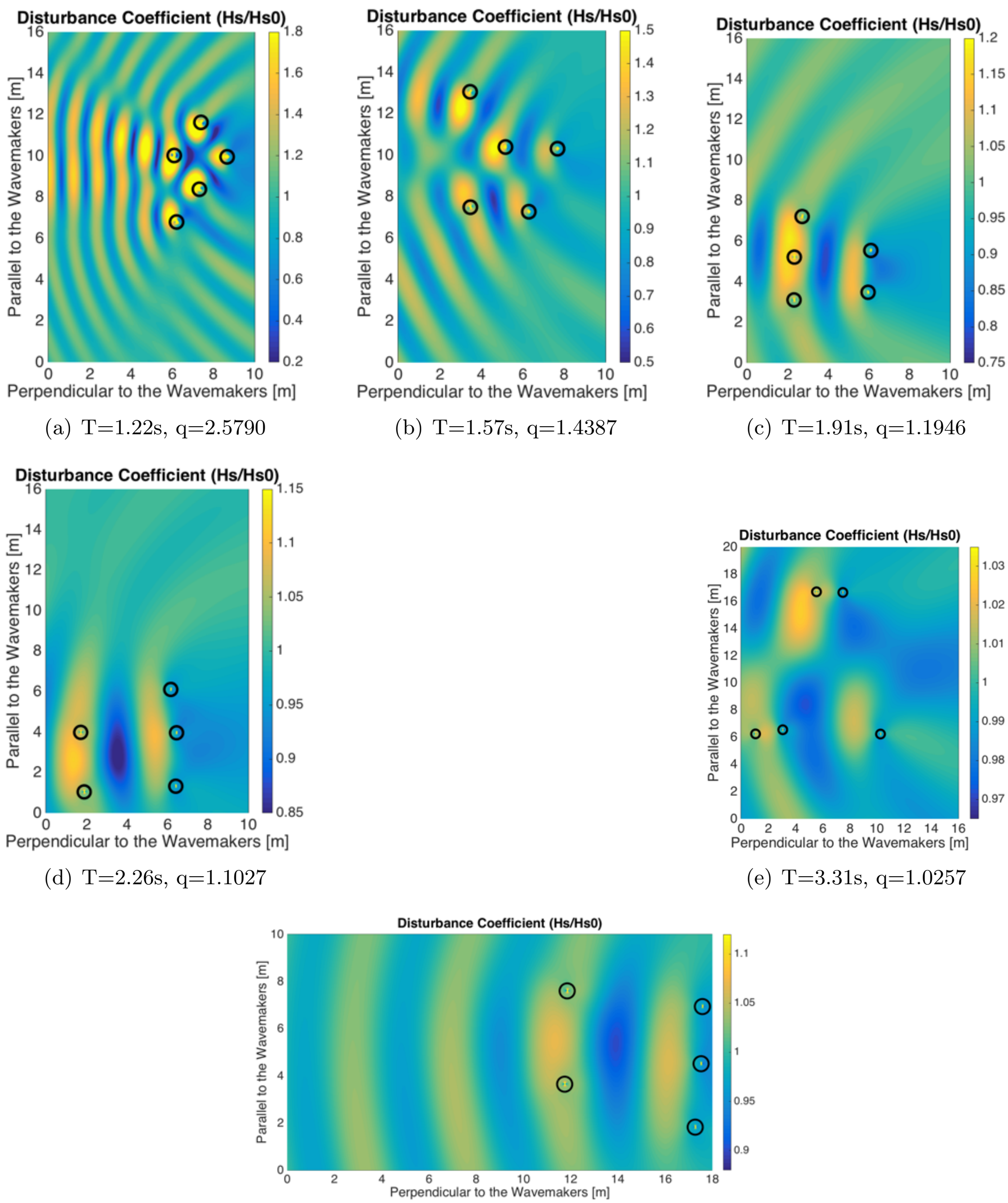

(a) T=1.22s, q=2.5790

(b) T=1.57s, q=1.4387

(c) T=1.91s, q=1.1946

(d) T=2.26s, q=1.1027

(e) T=3.31s, q=1.0257

(f) T=2.61s, q=1.0568

Figure 6.4: Optimal layouts with regular waves, a valve angle of 44° and H=0.136m

Observing the layouts obtained with regular waves, we note that in all scenarios the GA is able to generate a configuration with an interaction factor greater than one. These interaction factors greatly depend on the incident wave period and behave much better with the shorter wave periods tested. For a period of 1.22s a layout is found that yields an interaction factor of 2.579 (Fig. 6.4(a)). For the longest tested period, 3.31s, an interaction factor of 1.0257 (Fig. 6.4(e)) is obtained. This behavior is expected since a shorter period means that the converter will undergo more oscillations in a set amount of time when compared to longer periods. The results from the shorter periods (Figs. 6.4(a) & 6.4(b)) indicate WECs taking advantage of individual neighbor's diffracted waves. The increased periods (Figs. 6.4(c), 6.4(d) & 6.4(f)) show WECs acting in groups that place themselves in semi-parallel lines perpendicular to the incident waves. Figure 6.4(e) shows WECs pairing up and benefiting from another paired converter's diffracted waves.

6.7.1.2 Irregular Waves

We next obtained layouts for irregular wave conditions with a valve angle of 44°. The experienced sea states come from a Bretschneider spectrum and have a significant wave height of 0.136 meters. We considered two different wave periods, T_p, and the results are shown in Fig. 6.5.

As with the layouts obtained using regular waves, the layouts obtained with the 44° valve angle in irregular waves obtain interaction factors consistently greater than one and follow a similar trend to the regular waves. The shorter period in Fig. 6.5(a) shows WECs acting individually and the rest show WECs acting in groups. The longer waver periods (shown in Figs. 6.5(c) & 6.5(d)) indicate the converters grouping and then

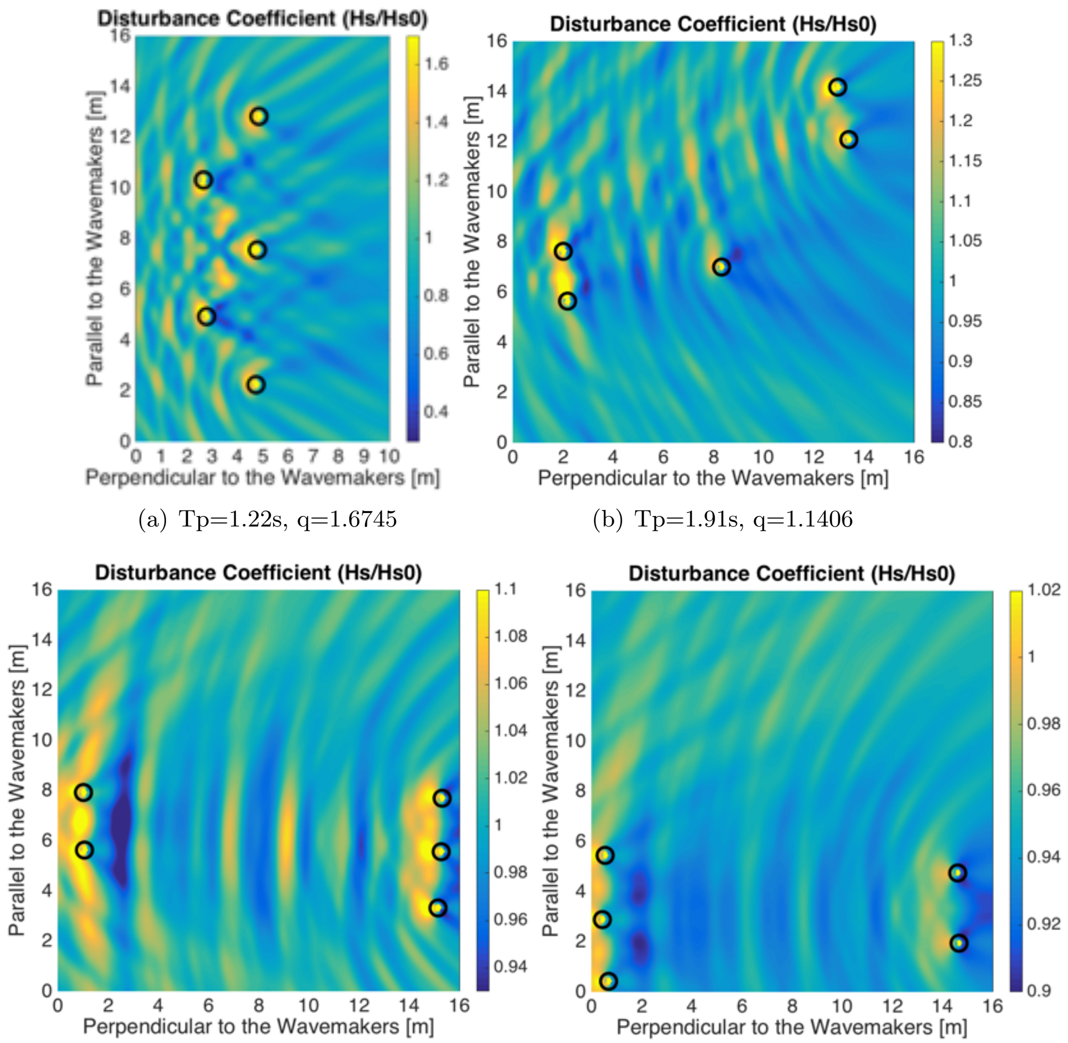

(a) Tp=1.22s, q=1.6745

(b) Tp=1.91s, q=1.1406

(c) Tp=2.61s, q=1.0646

(d) Tp=3.31s, q=1.0392

Figure 6.5: Optimal layouts with irregular waves, a valve angle of 44°, and H_{mo}=0.136m

creating space between the groups. This is likely in order to allow the diffracted waves of the first group to begin filling in before reaching the second group. The increase in interaction factor from these scenarios is likely due to the subgroups of converters more so than the entire group of WECs.

We also note that while the overall trend is similar to that of the regular waves for the same valve angle, the range of observed interaction factors is less extreme. Also, the interaction factors of the longer irregular periods are greater than those from regular waves, but less for the shorter periods.

6.7.2 Varied Valve Angles

To further understand how WEC control might affect the power production we examine two different simulated valve angles in both regular and irregular wave conditions (experienced through changes in the damping value). The damping values come from regular wave tests of an OWC in the wave tank and are listed in Table 6.2. They range from 107.1 N/(m/s) with the shortest wave period and 80° to 100032.5 N/(m/s) with the longest wave period and 0°. We select the damping values from the extreme valve positions to gain understanding into the effect on power over the full range of valve angles. We can compare these results with the damping values from the valve angle of 44° that is between these extremes. As with the 44° results, the irregular sea states come from a Bretschneider spectrum which is chosen for consistency with our previous work [11, 40].

6.7.2.1 Regular Waves

Having already shown the results found for a 44° valve angle, Fig. 6.6 shows the best layouts obtained when optimizing the array with a valve angle almost completely open at 80°. Based on the data from a tank test of a single OWC, a fixed valve angle will cause damping changes dependent on the incident wave. The 80° scenarios simulate converters allowing close to the maximum amount of air flow in and out of the interior chamber of the OWC.

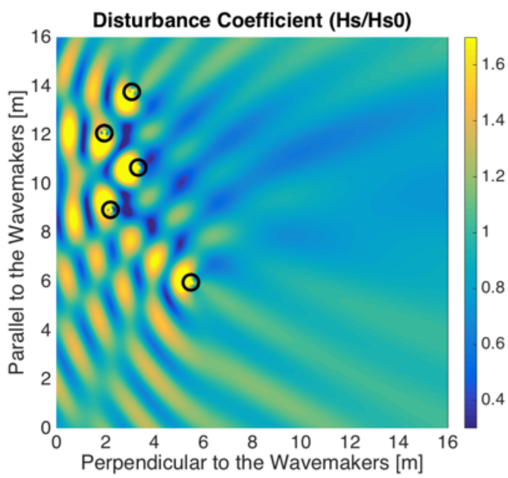

(a) T=1.22s, q=2.8095

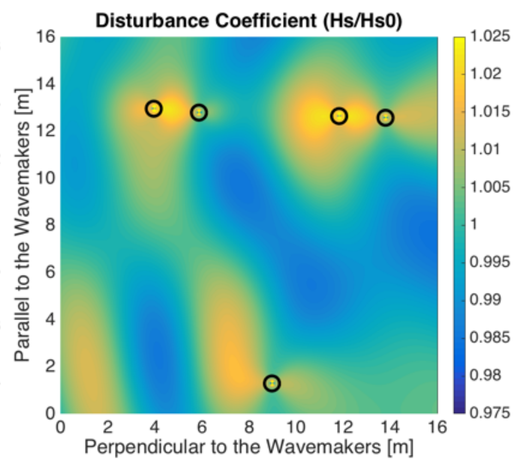

(b) T=3.31s, q=1.0243

Figure 6.6: Optimal layouts with regular waves, a valve angle of 80° and H=0.136m

The next valve angle we consider with regular waves is 0° — to mimic when the valve is completely shut. Though an OWC would be unable to generate power without air flow, we use this scenario to compare what interaction could be obtained with the maximum damping created by this valve position. The resulting layouts and corresponding interaction factors are displayed in Fig. 6.7.

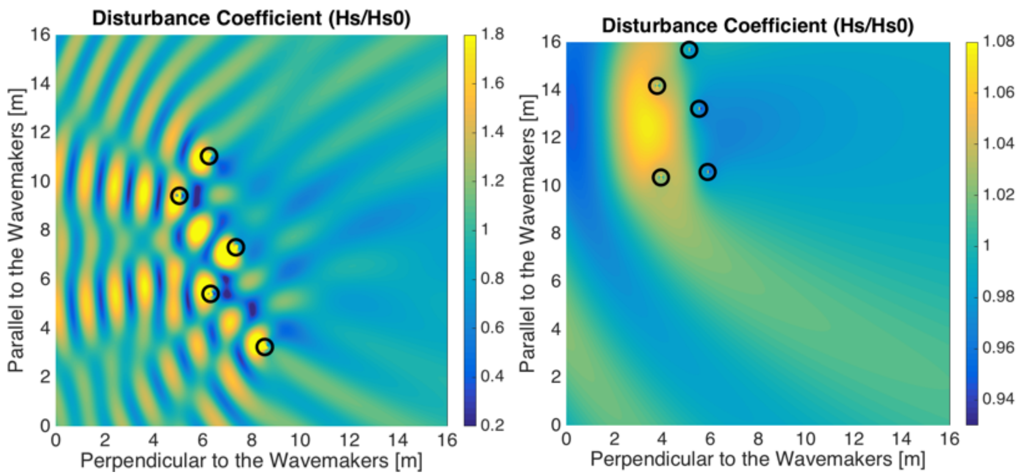

(a) T=1.22s, q=2.5561 (b) T=3.31s, q=1.0645

Figure 6.7: Optimal layouts with regular waves, a valve angle of 0°, and H=0.136m

For regular waves, the 80° scenarios follow a configuration trend similar to the previous results seen in the layouts generated for the shorter and longer wave periods. Shorter periods yield individual behavior and longer periods yield grouping behavior. However, the result in Fig. 6.7(b) for the 0° scenario has a layout that is difficult to determine if the WECs are acting individually or are grouped. We also observe that with the 1.22s period the greatest interaction factor occurs at 80° and the lowest interaction factor at 0°. Alternatively, the inverse is true for the period of 3.31s.

6.7.2.2 Irregular Waves

We now look at the behavior observed for different valve positions under irregular wave conditions. The same valve positions are evaluated as in the regular wave scenarios and a Bretschneider spectrum is used. (The scenarios are shown in Table 6.2.) Based on the results of the fixed valve angle we expect to see tendencies similar to those from the regular wave scenarios.

The best layouts found when the valve is almost completely open are shown in Fig. 6.8. The resulting layouts again show WECs taking individual advantage of neighboring converters for the shorter period and separating into two distinct groups for the longer period.

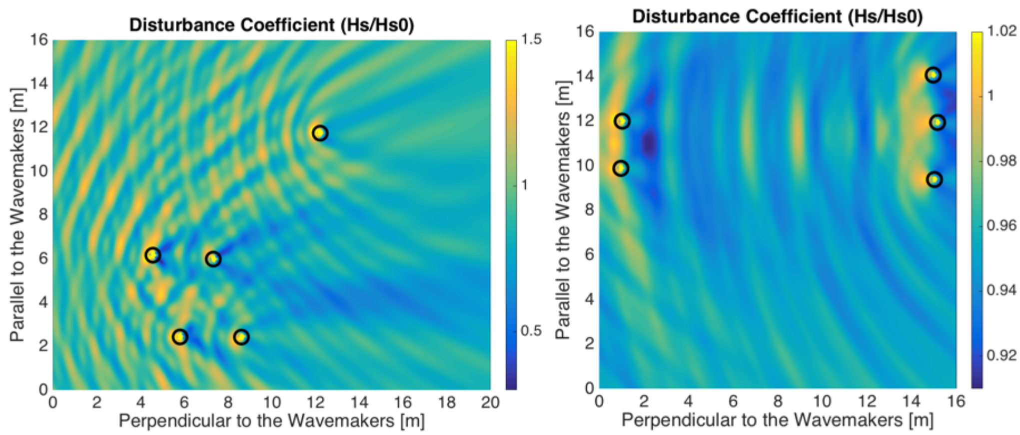

(a) Tp=1.22s, q=1.4559 (b) Tp=3.31s, q=1.0465

Figure 6.8: Optimal layouts with irregular waves, a valve angle of 80° and H_{mo}=0.136m

The last valve angle we consider with irregular waves is 0°. The layouts determined are shown in Fig. 6.9 and are similar to the regular wave results with the same valve angle. In this case, results from both periods seem to indicate converters acting individually.

Considering the interaction factors for the scenarios with 1.22s periods and irregular waves, the highest interaction factor is found at 0° and the lowest interaction factor is at 80°. This is an inverse pattern to what is seen from the regular wave results; however, the

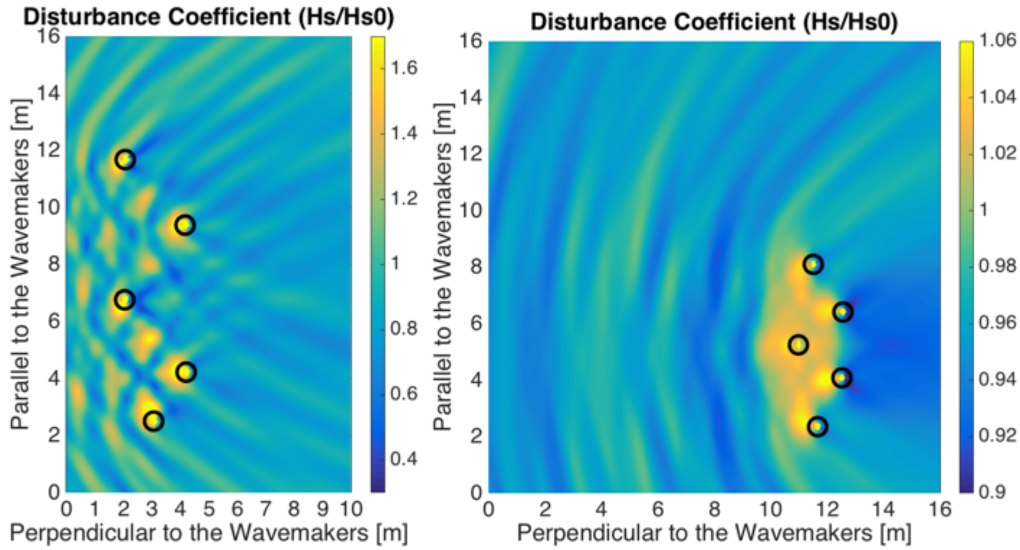

(a) Tp=1.22s, q=1.7597

(b) Tp=3.31s, q=1.0723

Figure 6.9: Optimal layouts with irregular waves, a valve angle of 0° and H_{mo}=0.136m

interaction factors' trend for scenarios with 3.31s periods and irregular waves is unique with the highest interaction factor found at 0° and the lowest interaction factor at 44°. These trends point to the importance of matching a damping value to the sea state being experienced. One valve angle does not work best for all sea states. Rather, the optimal valve angle will depend on what damping is needed which is dependent on the sea state.

6.8 Discussion

From the 18 different scenarios detailed previously, we gain understanding into the potential for including active WEC control in a WEC array optimization method. The results from the runs are compiled in Table 6.3. The number of generations refers to how many cycles the real-coded GA went through before converging. We note behaviors dependent on wave period, wave type (regular or irregular), and valve angle (damping).

Table 6.3: Interaction factors from different wave scenarios

Regular Waves ($H_s = 0.136m$)

Valve Angle	Period [s]	Interaction Factor	# of Generations
80°		**2.8095**	561
44°	1.22	**2.5790**	318
0°		**2.5561**	463
44°	1.57	**1.4387**	634
44°	1.91	**1.1946**	192
44°	2.26	**1.1027**	278
44°	2.61	**1.0554**	475
80°		**1.0243**	260
44°	3.31	**1.0257**	257
0°		**1.0645**	485

Irregular Waves ($H_s = 0.136m$)

Valve Angle	Peak Period [s]	Interaction Factor	# of Generations
80°		**1.4559**	306
44°	1.22	**1.6745**	316
0°		**1.7597**	483
44°	1.91	**1.1406**	445
44°	2.61	**1.0646**	520
80°		**1.0465**	208
44°	3.31	**1.0392**	500
0°		**1.0723**	453

6.8.1 Wave Period

Both regular and irregular wave conditions indicate a relationship of the interaction factor with the wave period. For our model's geometry and dimensions, the shorter periods are found to yield higher interaction factors and the longer periods lower interaction factors. However, all periods we tested resulted in power production greater than what would be obtained by five WECs acting in isolation. With a valve angle of 44° and regular waves, a period of 3.31s results in an increase in power of 2.57% and a period of 1.22s results in a 158% power increase. Similarly the same valve angle but with irregular waves results in power increases of 3.69% and 67.5% respectively. For the WEC we have chosen, and its dimensions, the shorter periods yield better interaction results. This is best observed in the interaction factors from the 44° results for both regular and irregular waves; however, the trend can also be seen for the 0° and 80° scenarios.

The behavior of the interaction factor resulting from an experienced wave period reinforces the need to consider WEC design based on expected sea state as well as the importance of introducing WEC control. With the observed variation in interaction factors across the periods, it is important to consider, during the initial design process, the environment in which converters will be deployed. Additionally, these results indicate the ability of our optimization framework to determine layouts which can provide great improvements over the summed power of isolated WECs.

6.8.2 Wave Type (Regular and Irregular Behavior)

Considering a 1.22s wave period with corresponding valve angles of 80°, 44° and 0°, the regular wave scenarios perform much better than the irregular wave scenarios; however, for the same valve angles and a 3.31s wave period, the regular wave scenarios perform slightly worse. This could be that for short-period, regular waves, the algorithm positions converters to best take advantage of neighboring converters' diffracted waves due to the wave period consistency. As we noted previously, the WECs do not perform as well with longer periods and therefore the interaction factors are lower for both regular and irregular waves. Consequently, the WECs are not able to capitalize well on neighboring converters' diffracted waves.

While some waves in an irregular wave climate will not have the energy efficiently captured by up–wave WECs, there is still the possibility of developing a slightly enhanced wave condition behind those front WECs. Comparatively, the wave consistency in regular wave conditions likely aids in improving the energy capture efficiency. The overall best power improvement of 181% occurs when the valve angle is 80° with short period regular waves. While the ocean does not contain regular waves, the introduction of WEC control could effectively reap similar power increases as the PTO responds to each wave individually. Alternatively, the smallest amount of power improvement is 2.43% and is also found with a valve angle of 80° and in regular waves, but with a long wave period. Once again, the consistent interaction factors that are greater than one show the capability of the array optimization framework and the necessity of utilizing optimization methods for maximizing power by incorporating the experienced sea states and WEC interactions.

6.8.3 Valve Angle (Damping)

While the optimal layouts and corresponding interaction factors are dependent on the incident wave's period, there is also an observed dependency on the damping associated with the input valve angle (Table 6.2). Keeping a fixed wave period, we examine the interaction factors obtained by scenarios with valve angles of 80°, 44° and 0°. This is done for our evaluated wave period's upper and lower limits of 1.22s and 3.31s. For the former period, the interaction factor increases with a decreased valve angle. For the period of 1.22s, an interaction factor is found yielding a power increase of 45.4% when the valve angle is 80°. This increases to 67.5% and 76.0% for valve angles of 44° and 0° respectively. It is important to note that generating power with a valve angle of 0° is not physically possible for our OWC since no airflow would be possible. However, since we modeled our OWC as a heaving point absorber, scenarios where the 0° performs best indicate the desire of the model to utilize the damping associated with that valve angle. When the period is 3.31s, somewhat similar behavior is found with valve angles of 80° and 0°; however, the value found for 44° is slightly less than that of the 0°. This difference is potentially due to a GA not guaranteeing global optimality and also because of lacking converter efficiency at the period of 3.31s.

To further evaluate the sensitivity of the power output when considering array optimization and variable damping values (based on valve angle and wave period), we determined optimal layouts for 42 more irregular sea states with wave height, $H_s = 0.136$m, and wave periods, $T_p = 1.22$s, 1.57, 1.91s, 2.26s, 2.61s, and 3.31s. The additional values are in between the extreme periods utilized for the 18 results shown earlier. For each wave period, we consider the damping values associated with 10 different valve angles ranging from 0° to 80° and record the maximum interaction factor. These damping values are acquired from Bosma et al. [2]

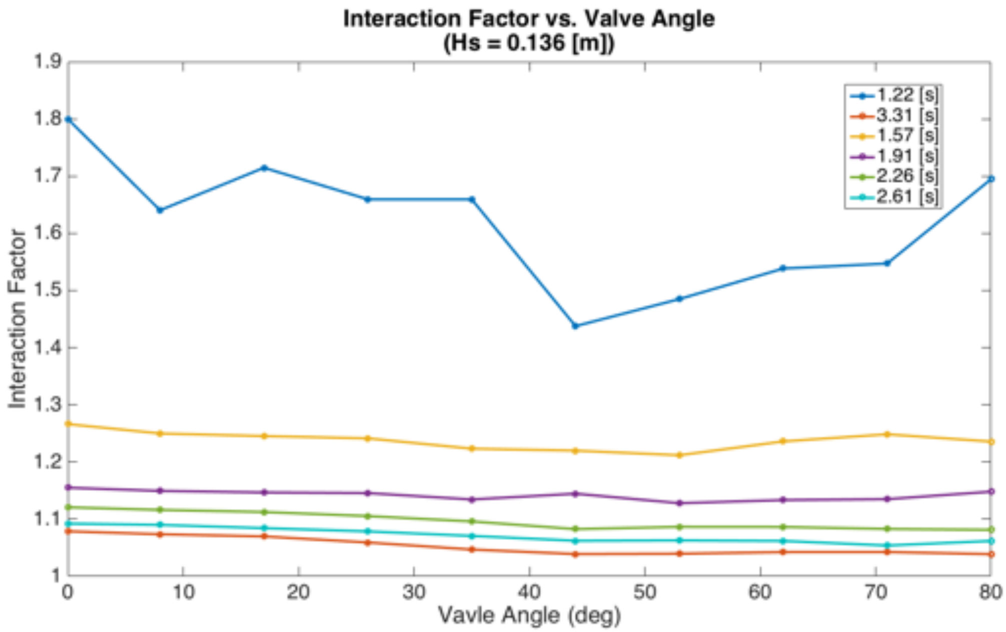

Figure 6.10: Interaction factor sensitivity based on valve angle and wave period

Observing Fig. 6.10 we see that the largest improvement in interaction factor is primarily dependent on the experienced wave conditions and then on the valve angle (damping). This reiterates the importance of including and considering both layout optimization and WEC control in array design. This figure also indicates the need to consider the sea state a WEC will experience when designing the physical WEC itself. Since converters will likely be placed in locations which have variability in the sea states to be experienced, it will be necessary to incorporate active WEC control to take advantage of each individual wave. And for layout optimization, there is a need to consider real sea states within the optimization process. Research has primarily considered a unidirectional and irregular (but constant) wave state. Consequently, research forward should include probabilistic sea states based on real conditions. In Chapter 8, we will introduce probabilistic wave conditions from buoy data.

6.9 Conclusion

To ensure that WECs operate as efficiently as possible, two methods have been promoted as future means of increasing the power development of grid connected WEC arrays. These are the creation of automated schemes for array optimization and the development of advanced WEC controls. To date, we have acquired optimized configurations for five OWCs based on a validated BEM model of our WEC (see Fig. 6.3) and have determined how the results differ based on varied wave type (regular and irregular), incident wave period, and valve angle (damping).

We observe that — while always greater than one — the interaction factor varies greatly depending on the incident wave period and, in our case, increases with shorter periods. Considering irregular waves, the lowest found power improvement is 3.92% (valve angle of 80° and period of 3.31s) and the largest found power improvement is 76.0% (valve angle of 0° and period of 1.22s). As mentioned previously, the 0° valve angle is not realistic for an OWC, but points to the damping that the model would like to utilize. The valve angle's connection with the interaction factor is less clear, but does indicate the ability to obtain greater power based on the position of the valve and its consequence damping. This information reveals the importance of concurrently implementing control in array optimization methods.

While the interaction factor is shown to be influenced more by the incident period than the damping, both are necessary for achieving maximum power. We also show that maximizing power requires considering converter design given expected wave conditions. Thus far, the results of this project have provided useful information for better understanding what influences power development of a WEC array and prepares for future integration of active WEC control with array optimization. Continuing forward, we will be optimizing layouts such that optimal damping is determined for individual WECs within an array.

Chapter 7: Array Design and WEC Damping Assignment of Fixed Oscillating Water Columns

As a component of the DOE's Advanced Laboratory and Field Arrays (ALFA) project, discussed in Chapter 6, we are performing an initial study regarding how to best jointly consider array optimization and active WEC control. Both array optimization and active WEC control have theoretically shown substantial power increases [42, 40, 41, 26]. What has yet to be seen is the power that can be developed when WEC control and array optimization are combined.

We propose that a valuable first consideration is to consider this initial study in several stages — specifically considering different combinations of fixed and optimized array designs with fixed and optimized WEC damping values. Only seen preliminary in the literature [21], this research lays further groundwork for future integration of active control scenarios into an array optimization scheme.

To best understand the impact of array optimization with optimal, WEC–specific damping, we consider three case studies. These include fixed layouts with a fixed array damping (Case 1), fixed layouts with optimized WEC–specific damping (Case 2), and optimized layouts with a fixed array damping (Case 3). We opted not to consider optimized layouts with optimized WEC–specific damping due to minuscule improvements in power and computational expense. For the cases with fixed layouts, the layouts are informed by existing research. For the cases with fixed damping, these values are obtained by determining the optimal damping value of a single converter in isolation. Figure 7.1 shows the relationship between these case studies. In this chapter we will describe our WEC damping value optimization method and the results we have obtained for the different cases.

		Device Specific Damping	
		Optimized	*Not Optimized*
Layout	*Optimized*	——	Case 3
	Not Optimized	Case 2	Case 1

Figure 7.1: Overview of cases being considered.

7.1 Methodology

We are using the same OWCs from Chapter 6 for this study, but before the three cases can be considered, our chosen WEC is modeled in WAMIT [45] using a model with higher fidelity due to a broader range of input periods. Another addition to Chapter 6 is the inclusion of damping optimization based on experienced sea state.

7.1.1 OWC Damping Assignment

After modeling our converter in WAMIT, we then determine an optimized damping value for a single WEC. This value will be used throughout Cases 1 and 3 and as an initial starting value for Case 2. The optimized damping values are highly dependent on the sea state experienced by the WEC. In this work, we are considering the four sea states shown in Table 7.1.

Table 7.1: Evaluated Sea States and Associated Single WEC Optimal Damping.

Sea State	Hs [m]	Tp [s]	damping [kg/s]
A	0.136	1.91	**174.82**
B	0.136	2.26	**318.93**
C	0.139	2.48	**428.01**
D	0.242	3.30	**818.46**

In the *mwave* power development code, the damping value of the wave energy converter is a tunable parameter. Our previous work treated this value as a constant, utilizing the value given by Child & Venugopal [33]. In order to obtain an optimal damping value for our WEC, we implemented a Golden Section search to determine the optimal damping value that results in the highest power development. We observed that for a single OWC, in a set wave field, there is one distinct maximum. The optimal values for damping are shown in Table 7.1.

7.1.2 Array Design

Depending on the case being evaluated, the array's layout may be either predefined (Cases 1 & 2) or found using our problem–specific optimization scheme (Case 3).

7.1.2.1 Predefined Layouts

To choose the predefined layouts for evaluation, we selected a set of 11 potential layouts from existing literature [12, 66, 67]. From these 11 layouts, four were ultimately selected for in-depth evaluation in Cases 1 and 2. These four layouts are shown in Fig. 7.2 and were selected based on their performance and their prevalence in existing research. The separation distance scaling factor is denoted by n and Dia is the diameter of the OWCs (0.62 meters). This separation distance is measured from center to center of the WECs. All the OWCs in Fig. 7.2 are the same size, but may look different based on the axes scale.

7.1.2.2 Optimized Layouts

To find the optimal layouts for Case 3, we utilized the problem–specific GA we have developed and discussed in Chapter 4 and 6 [40, 41]. The methodology for Case 3 is presented in depth in Sharp et al. [41]. The GA explores many different potential layouts of OWCs in the space as well as exploiting potential solutions in order to converge on a layout that optimizes the developed power. This algorithm has been developed further to include WEC-specific damping optimization within the objective evaluation; however the small improvement in power and interaction factor was not worth the computation time needed — primarily because of the need to generate results promptly for tank testing.

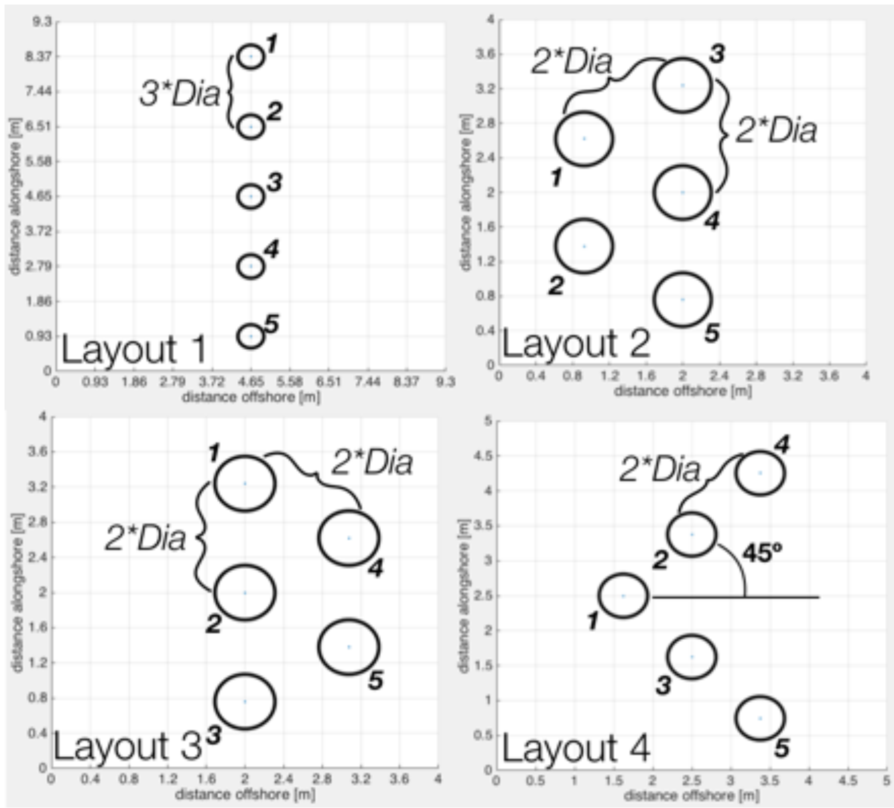

Figure 7.2: Predetermined Layouts for Cases 1/2

7.2 Results

In this section, we show the results we have obtained thus far from our work investigating the three cases. As with Chapter 7, we are not concerned with the cost in this work since the number of WECs is static and because our OWC is only intended for tank testing (without intention of being scaled up for use in the ocean). That said, the results will provide useful information for future ocean deployment by developers.

7.2.1 Case 1: Fixed Layouts with Fixed Damping

In Case 1, the four fixed layouts from Fig. 7.2 are evaluated with one fixed damping value for all OWCs (shown in Table 7.1). Examining Table 7.2, we see that the converter exhibits the most power development with the more extreme sea state, sea state D. However, while this sea state might exhibit the most power also has the potential to overwhelm the WEC due to the increased signifiant wave height. We also observe that Layout 1 (vertical line orthogonal to the incident wave) performs the best across all the sea states. Given that we did not evaluate every possible layout of our five OWCs, we cannot be very confident that this is the best layout.

7.2.2 Case 2: Fixed Layouts with Optimized Damping

Case 2 uses the same predetermined layouts as Case 1; however, instead of a single damping value used for all WECs, optimized damping values are found for each individual WEC. To determine these values, a Golden Section search is again used. For the search, the damping values from Table 7.1 are used as initial values and the search intervals used when determining these initial values are used as initial search intervals for the WEC–specific search.

The optimal damping for each OWC is sought so that all the damping values except for one are fixed. Searching iteratively through all the OWCs in the array, the WEC–specific optimums are selected when the overall objective function no longer changes. To ensure that the global optimal damping values are found, the OWCs are iteratively searched through in a random order to ensure that the global optimal is found. Table 7.3

Table 7.2: Case 1 Results

Layout 1	(from Fig. 7.2)			
Sea State	A	B	C	D
Power [W]	14.114	13.913	14.310	40.339
q-factor	1.1030	1.0643	1.0505	1.0231
Layout 2	(from Fig. 7.2)			
Sea State	A	B	C	D
Power [W]	13.053	13.640	14.184	39.682
q-factor	1.0200	1.0434	1.0413	1.0065
Layout 3	(from Fig. 7.2)			
Sea State	A	B	C	D
Power [W]	12.804	13.526	14.122	39.697
q-factor	1.0006	1.0347	1.0368	1.0069
Layout 4	(from Fig. 7.2)			
Sea State	A	B	C	D
Power [W]	12.505	13.125	13.778	39.691
q-factor	0.9773	1.0039	1.0115	1.0067

shows the WEC specific damping for each fixed layout in each sea state. As expected, the damping values are symmetrical about the incident wave direction. Also, the higher damping values are associated with the WECs that will be experiencing higher significant wave heights from neighboring WECs. Since the increase in power was small, the overall trends are the same as in Case 1.

7.2.3 Case 3: Optimized Layouts with Fixed Damping

This case is similar, and based on, Chapter 6 [41]. Utilizing a fixed damping value for all the WECs within the array, this informed value is dependent on a single WEC's behavior in a given sea state and is shown in Table 7.1. Each sea state yields a unique layout and power output as shown in Fig. 7.3. These layouts, while similar in appearance to Layout 1 of the fixed layouts, these optimal configurations do differ slightly in the spacing between WECs. The layout for sea state D differs drastically from the other three showing the influence of sea state on optimal layout configuration. The power and interaction factors associated with each of these layouts can be found in Table 7.5.

Table 7.3: Case 2 WEC Damping

Layout 1	(from Fig. 7.2)				
Sea State	WECs				
	1	2	3	4	5
A	167.26	153.87	170.50	153.87	167.26
B	317.20	308.93	327.56	308.93	317.20
C	429.31	426.86	443.11	426.86	429.31
D	828.96	829.18	833.72	829.18	828.96
Layout 2	(from Fig. 7.2)				
Sea State	WECs				
	1	2	3	4	5
A	225.68	225.68	167.83	259.21	167.83
B	326.62	326.62	346.77	423.12	346.77
C	402.18	402.18	469.81	529.88	469.81
D	720.92	720.92	872.12	989.33	872.12
Layout 3	(from Fig. 7.2)				
Sea State	WECs				
	1	2	3	4	5
A	220.43	200.07	220.43	215.90	215.90
B	354.11	292.97	354.11	401.60	401.60
C	441.76	369.23	441.76	522.55	522.55
D	775.30	706.24	775.30	913.93	913.93
Layout 4	(from Fig. 7.2)				
Sea State	WECs				
	1	2	3	4	5
A	186.33	209.50	209.50	195.54	195.54
B	297.99	363.98	363.98	357.13	357.13
C	393.69	465.50	465.50	474.48	474.48
D	747.24	822.43	822.43	880.06	880.06

Table 7.4: Case 2 Results

Layout 1	(from Fig. 7.2)			
Sea State	A	B	C	D
Power [W]	14.129	13.915	14.310	40.3410
q-factor	1.1042	1.0644	1.0506	1.0232
Layout 2	(from Fig. 7.2)			
Sea State	A	B	C	D
Power [W]	13.181	13.686	14.225	39.797
q-factor	1.0300	1.0469	1.0443	1.0094
Layout 3	(from Fig. 7.2)			
Sea State	A	B	C	D
Power [W]	12.895	13.529	14.183	39.814
q-factor	1.0078	1.0397	1.0412	1.0098
Layout 4	(from Fig. 7.2)			
Sea State	A	B	C	D
Power [W]	12.546	13.157	13.803	39.736
q-factor	0.9805	1.0064	1.0133	1.0079

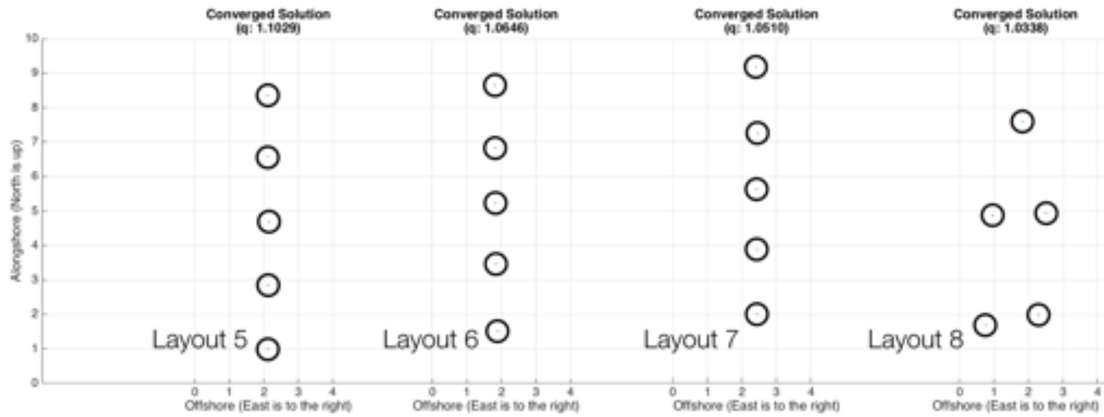

Figure 7.3: Optimized Layouts for Case 3

Table 7.5: Case 3 Results

Sea State	A	B	C	D
Layout	5	6	7	8
Power [W]	14.113	13.917	14.316	40.7570
q-factor	1.1029	1.0646	1.0510	1.0338

7.3 Observations

We made several observations from these results - primarily how the interaction factors, damping values and layout designs are effected across the different cases.

7.3.1 Interaction Factor

We observe that, when comparing across sea states, an increase in power does not necessarily correspond to an increase in interaction factor. For instance, the greatest power was achieved from sea state D, but this sea state always yielded the lowest interaction factors. The ability to achieve larger interaction factors in sea states which may be less conducive to power development is an indicator of the importance of layout optimization. Meaning that even if a layout experiences a sea state for which the individual converters are not well–designed, a layout can be found with can yield relative increases in power.

7.3.2 Damping

We also note that generating WEC specific damping values does produce improvements in power development and interaction factor. This is shown when examining Cases 1 and 2 (Tables 7.2 and 7.4). However, the improvements are relatively minor. These changes are likely small because the values are tuned to a sea state and a layout and do not consider the individual waves that are experienced. This indicates a further need to include active control scenarios in future array optimization development. The results in Table 7.3 do show that converters do perform better with individual damping. These damping values are based on an entire sea state, but if they were able to be tuned individual to real–time waves the power improvements would likely be substantial – thus indicating a need for future implementation of active WEC control.

7.3.3 Layout Design

Lastly, when we compare the behavior of predetermined layouts with optimized layouts, we see that incorporating layout optimization yields better power production across all the considered sea states (Table 7.5). Furthermore, the power produced across the sea states are more consistent (seen in Case 3) when the layouts are optimized than when they are fixed (Cases 1 and 2).

7.4 Conclusions

The goal of this work is to better understand the connection between layout design and WEC damping adjustment. Eventually, layout optimization methods should include active control in order to provide better informed layout options. To explore the potential influence of active control in array optimization, we have examined three distinct cases that include fixed/optimized layouts and fixed/optimized WEC–specific damping. These results provide a strong foundation from which to further explore active control in conjunction with layout optimization.

Chapter 8: WEC Arrays for Blackout Risk Mitigation: Influence of WEC Size and Location

8.1 Introduction

This chapter is being written in partial fulfillment of the National Science Foundation Research Traineeship (NRT) program at Oregon State University. As a part of the NRT program, I worked with a transdisciplinary group investigating the potential of wave energy being utilized in emergency blackout scenarios.

Energy security is an important yet often overlooked vulnerability to coastal communities. Electricity availability is necessary for the functioning of our current society and coastal towns in Oregon have a unique vulnerability due to limited transmission lines connecting the coast with primary power sources on the East side of the Coastal Range. If enough lines fail, as occurred during a major winter storm in 2007, the coast would be electrically stranded from the primary electrical grid. Consequently, there is development potential for renewable power generation that takes advantage of the ocean's energy in times of emergency.

As part of a multi–disciplinary team of graduate researchers, we assessed key technical, natural system, socio–economic, and regulatory considerations surrounding the validity and value of wave energy as an emergency power source for the example community of

Newport, Oregon. The team was comprised of two Mechanical Engineering students, one Electrical Engineering student, and one student in Marine Resource Management. This project involved considering coupled natural human systems, quantification and communication of risk a uncertainty and big data. Our project focused heavily on the first two areas mentioned, but did include some inclusion of big data.

In addition to our trandisciplinary research [68], we also conducted individual research tangential to the topic. As my work is in the realm of WEC array design, I investigated how power production (Eq. 2.1) and interaction factor (Eq. 1.1) would be affected by variations in sea state and WEC size. This chapter will begin the process of characterizing the array design solution space in an effort to better understand what is most important to account for in wave energy implementation.

8.2 Motivation

We determined that wave energy may be a valid emergency generation alternative from a technical and regulatory standpoint. Based on our findings, it appears that temporary WEC systems would be economically infeasible given the estimated power demand of critical services and the generation capabilities of current converters. However, our research shows that there are significant gaps in knowledge regarding how we value critical services in a long emergency, and advancements in this field may change the value proposition of an emergency WEC use case. Additionally, advancements in wave energy technology or emergency power demand management may reduce the total size requirements for an emergency WEC array, or the logistical ability to deploy the WEC system, changing the feasibility and cost of the system in the future. Moreover, there is additional uncertainty regarding the recurrence interval of an outage of sufficient scale to warrant investment.

Several such gaps in knowledge include: how to efficiently extract power from ocean waves, what should be prioritized when designing an array, and possible use–cases for WECs. For example, the creation of microgrid–capable, wave energy "resilience zones" could potentially improve coastal energy infrastructure for use as a nominal energy provider under normal circumstances and as a primary energy supply for emergency situations. However, since the sea state will vary depending on location and the industry has yet to converge on a common geometry, this potential scenario requires further investigation. With limited understanding of the nuances that influence array design, it is necessary to determine what most affects the behavior of a WEC array. From our previous work, we have observed that facets which may impact the power development include WEC geometry and experienced sea state.

8.3 Problem Formation

Since the solution space for WEC array design has yet to be well characterized, we chose to fix the number of converters in the array and focus this initial characterization study on the experienced sea state and the WEC geometry.

8.3.1 Geometries

The geometries for all the cases is that of a truncated cylinder similar to the WEC modeled in our previous work. Given the wide range of WEC types under development, our simple structure serves as a place holder. One key difference between the model used for the work presented in this chapter and the model used in previous chapters is that three degrees of freedom are allowed (pitch, surge, and heave). We looked at three different versions of the truncated cylinder. These models were based on our work done on the ALFA project (discussed in Chapter 7), Ocean Power Technology's PB3 [69], and Child and Venugopal's research [34]. The specific dimensions can be found in Table. 8.2. The ALFA WEC was physically an OWC, but was modeled as a heaving point absorber. The intention of using these representative dimensions is not to represent the converters exactly, but to have a basis for the dimensions being used for potential comparison.

Table 8.1: WEC geometry dimensions

	ALFA	**OPT–PB3**	**Child & Venugopal**
Diameter [m]	0.62	2.7	10
Height [m]	0.4392	14.3	10
Draft [m]	0.4392	10.8	5

8.3.2 Sea State

To understand what impact the sea state would have on an array's configuration and power production, we chose four locations around the United States to gather historical wave date from in order to better note differences. We also utilized wave data from a buoy off the northwest coast of Ireland for an international perspective. The names of the buoys used to acquire data and clustered views of that data can be found in Table 8.2. The water depth is h; the significant wave height is H_s; and the dominant wave period is T_p. The approximate location of the buoys in the world can been seen in

Fig. 8.1. In our previous work we had only been able to use single values for the input sea state, but for better accuracy this algorithm was updated to utilize a probabilistic cluster of sea conditions. To achieve these clusters, we acquired and cleaned the data for a ten year period (2008–2017) and then applied MATLAB's k–means clustering method to group this data into a more manageable size. Cleaning the data meant removing any values which indicated that the data point was corrupted. The Irish buoy only had data from 2012 through 2018. Incorporating this new sea state input resulted in slightly slower run times due to a small increase in objective function evaluations. The objective function now must determine the power generated by each significant wave height and wave period pairing in the cluster and then multiplying and summing the resulting power results together.

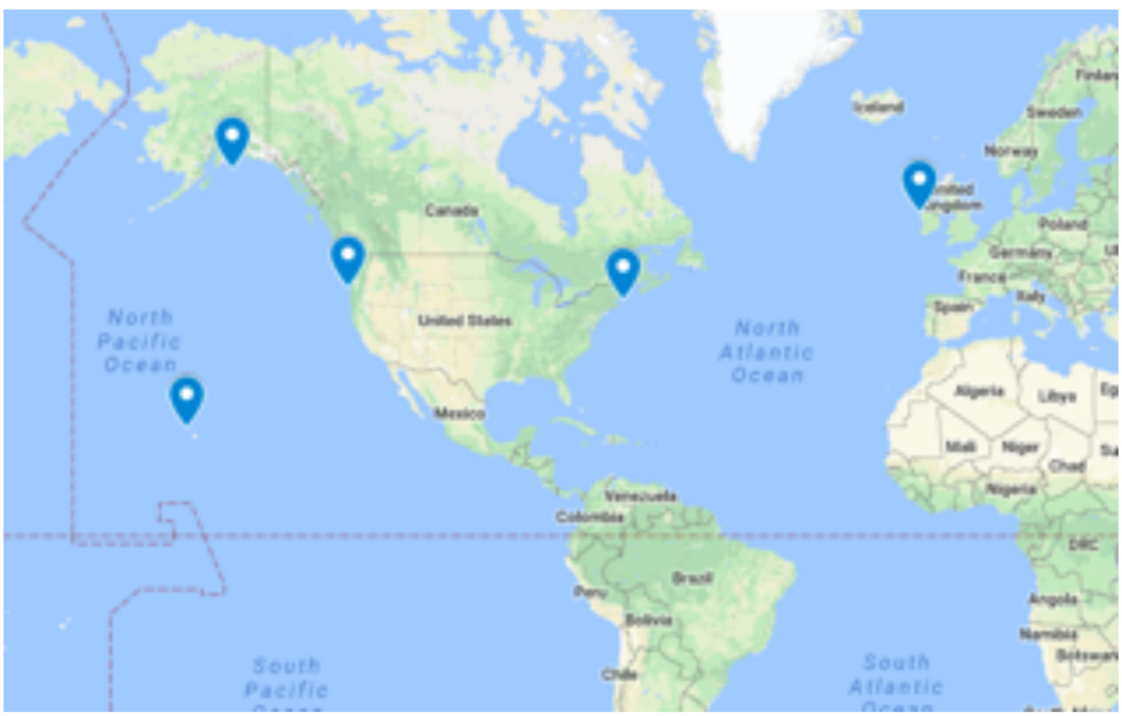

Figure 8.1: Buoy Locations

Table 8.2: Representative Sea States by Location

NOAA 46050 – Oregon (h = 140 m)			**NOAA 44098 – New Hampshire** (h = 76.5 m)		
H_s [m]	T_p [s]	Probability	H_s [m]	T_p [s]	Probability
2.09	10.15	0.33	0.94	8.22	0.21
2.20	12.91	0.17	1.55	6.05	0.25
2.60	15.31	0.10	1.14	10.61	0.18
4.46	12.19	0.11	3.71	9.71	0.05
1.71	7.24	0.27	0.99	4.33	0.25
2.71	18.14	0.03	1.20	13.55	0.06
NOAA 51202 – Hawaii (h = 89 m)			**NOAA 46076 – Alaska** (h = 195.1 m)		
H_s [m]	T_p [s]	Probability	H_s [m]	T_p [s]	Probability
1.97	10.63	0.24	1.85	8.38	0.33
1.99	13.27	0.12	2.03	10.62	0.23
2.00	18.59	0.01	1.03	13.89	0.08
8.08	15.86	0.03	4.43	11.66	0.11
1.83	7.76	0.60	1.37	6.06	0.23
1.60	22.44	0.00	1.06	16.41	0.02
Belmullet A – Ireland (h = 100 m)					
H_s [m]	T_p [s]	Probability			
3.98	11.40	0.22			
5.88	13.45	0.11			
2.15	10.79	0.28			
8.08	16.14	0.04			
1.18	7.99	0.26			
3.32	14.34	0.10			

8.4 Results

We will observe four primary things about the results - the obtained layouts across the different sea states, the layouts across the different sizes, the generated power and the observed interaction factors. Figure 8.2 shows the different layouts found when the smallest converter is used. Figures 8.3 and 8.4 show the generated WEC configurations for WECs of increasing size. As a note, none of the layouts are definitively the global optimum. Due to computational time constraints, we were only able to run a single iteration of each geometry and sea state combination. So it is possible that the algorithm only obtained a local optima. That said, there are trends across the layouts.

Looking through the resulting configurations, we note similarity in layouts when the geometry is held constant. The layouts in Fig. 8.2 from Hawaii, Alaska and Ireland are in the form of a W with the points of the W pointing in the up–wave direction while the sea states of Oregon and New Hampshire resulted in layouts that tended more towards two groupings of WECs. Figure 8.3 shows definite off–camber lines that appear throughout all of the configurations. Within that similarity though, there is unique spacing depending on the sea state. Figure 8.3(e) appears to have been potentially space constrained based on the position of the fifth WEC in the bottom right. The results for the 10–meter WEC shows groupings of the WECs across all the sea states except for that of Fig. 8.4(e). (This specific result may have converged too quickly to a less optimal solution – more evaluations would need to be run to observe if similar arrangements are seen consistently.)

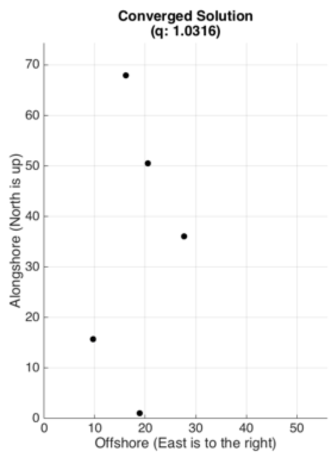

(a) NOAA 46050, OR

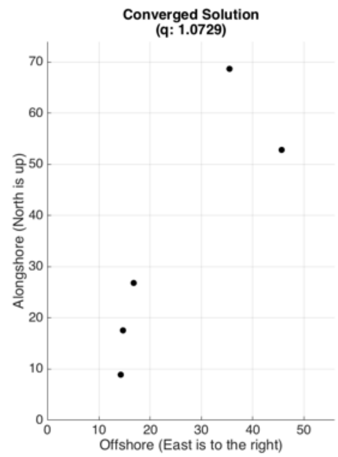

(b) NOAA 44098, NH

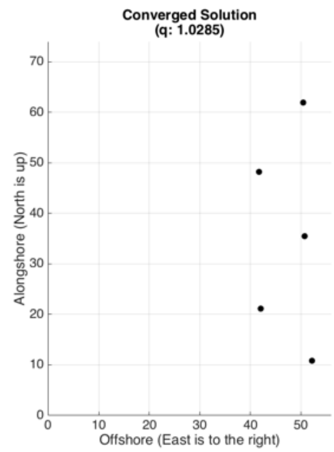

(c) NOAA 51202, HI

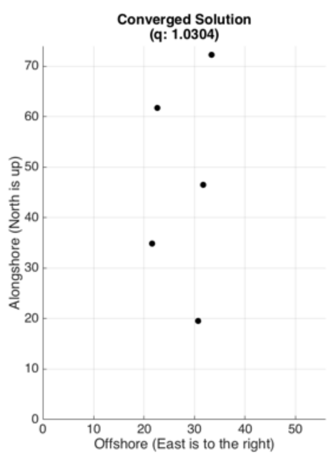

(d) NOAA 46076, AK

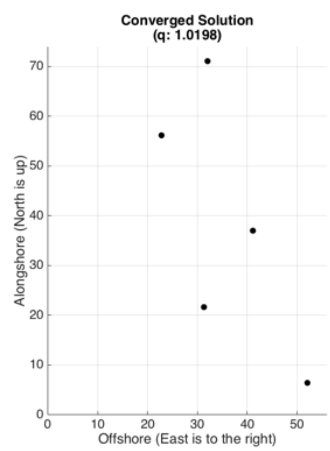

(e) Belmullet A

Figure 8.2: Optimal layouts for OWCs from ALFA Project (Dia = 0.62m)

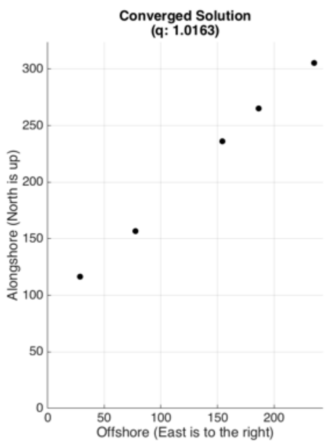

(a) NOAA 46050, OR, USA

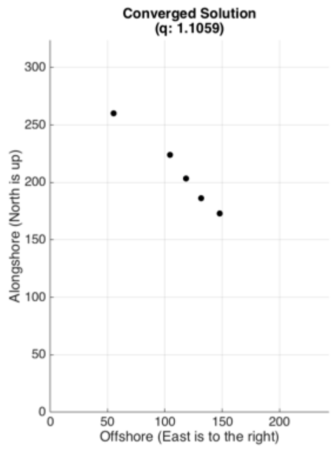

(b) NOAA 44098, NH, USA

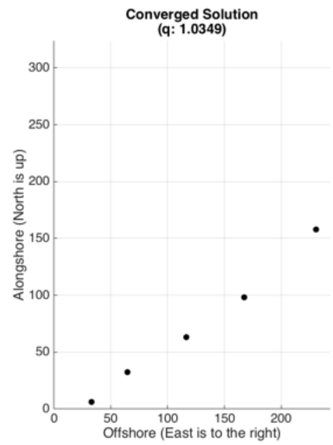

(c) NOAA 51202, HI, USA

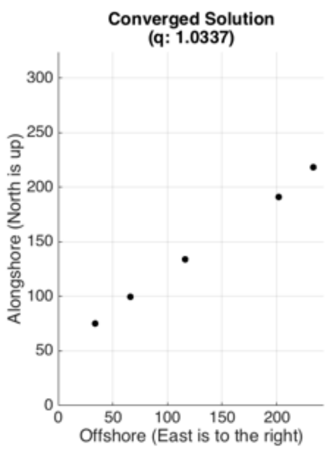

(d) NOAA 46076, AK, USA

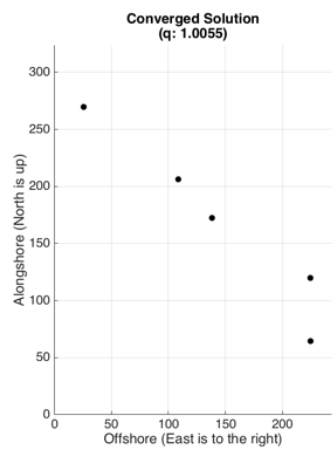

(e) Belmullet A

Figure 8.3: Optimal layouts for OPT WEC (Dia = 2.7m)

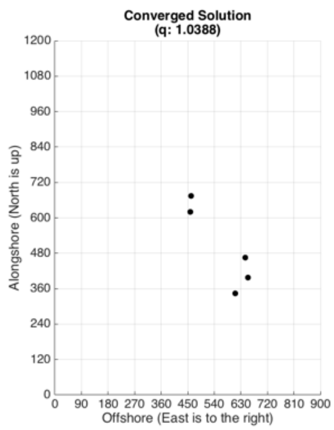

(a) NOAA 46050, OR

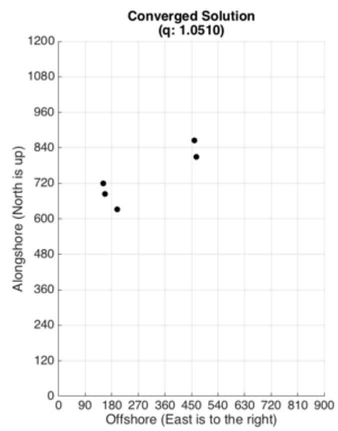

(b) NOAA 44098, NH

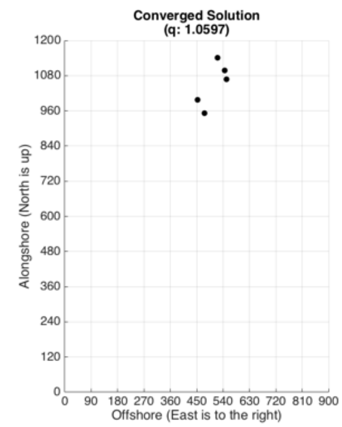

(c) NOAA 51202, HI

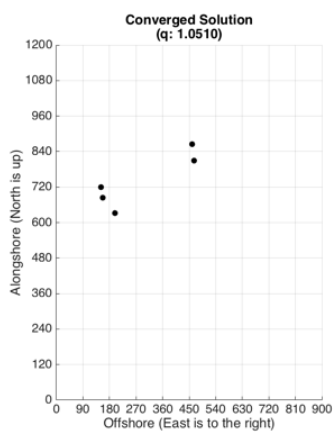

(d) NOAA 46076, AK

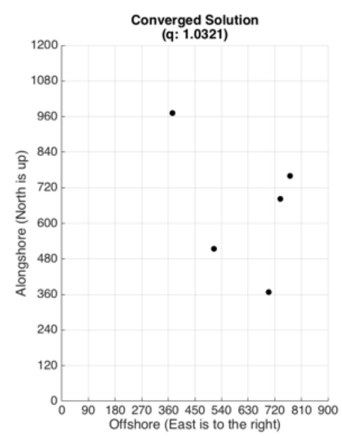

(e) Belmullet A

Figure 8.4: Optimal layouts for WEC from Child and Venugopal's research (Dia = 10m)

In addition to visually inspecting the layouts we can also examine the amount of power created by each layout and the associated interaction factors. Figure 8.5(a) shows the power generated in watts based on each location and geometry (note the legend) and Fig. 8.5(b) shows the same comparison, but with the interaction factor instead of the power.

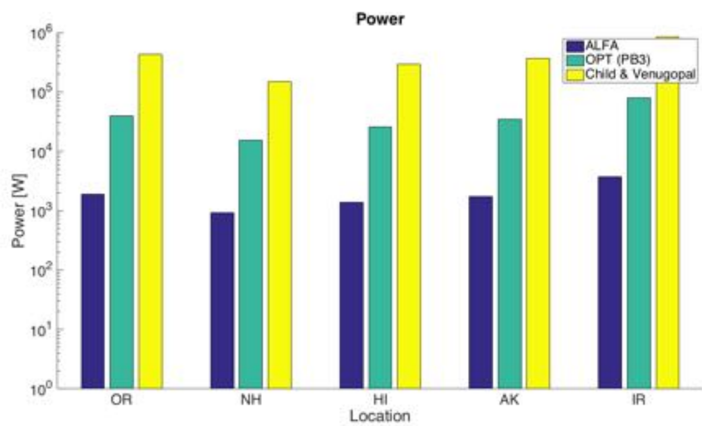

(a) Power

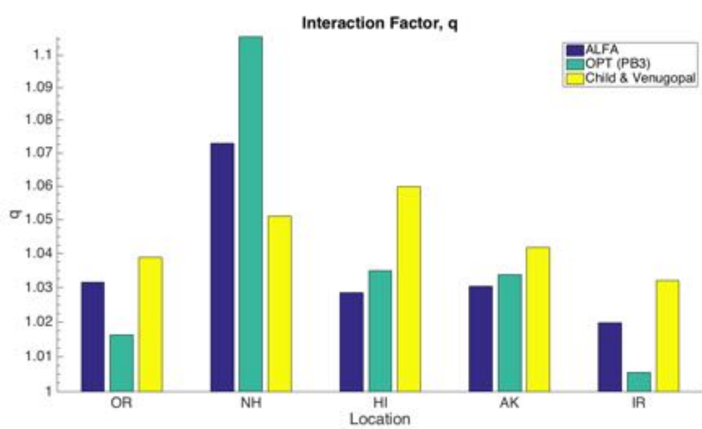

(b) Interaction factor, q

Figure 8.5: Comparing the WEC geometry against location specific sea states

8.5 Discussion

Examining the layouts across the converter geometries we note that the overarching layouts are dependent on the geometry, and that in general the layouts take advantage of diffracted waves generated by neighboring WECs or groups of WECs. Specific examples of WECs being placed in the parabolic wake of up–wave converters can be seen in Fig. 8.2(c) for single converters and Fig. 8.4(a) for grouped converters. The off-camber results of Fig. 8.3 demonstrate the converters being placed to take advantage of the cascading, diffracted waves generated by up–wave WECs.

Additionally, power increases are seen as our WECs increase in size. This is likely due to the energy in the experienced sea states and may seem to suggest that larger converters should be predominately considered. However, that would not account for the desired use of WECs or WEC economics. Examining Fig. 8.5(a), we see that the most power is generated in Oregon and Ireland (shown most clearly for the 10–meter WEC). As these locations are the most energetic - experiencing larger significant wave heights and longer dominant periods — relatively larger WECs could make more sense, especially if the intention was to generate power for the grid. In this work we considered three geometries as a preliminary investigation and future work should further study the impact of converter diameter, draft and height to find what geometry is best suitable for a specific location.

Another consideration is that a WEC should potentially not be designed for the most energetic sea states if those sea states will dramatically shorten the life span of the WEC (even if those conditions are most prevalent). Alternatively, if the intention is for the

WECs to provide power for only a short amount of time and maximization of power generation is most important, then the converters would be designed differently.

Considering the economics of the system, there is also the need to vary the number of WECs being considered. In this work we considered five WECs as as been utilized previously in literature. Once available cost models become more accurate the economic trade off between more smaller converters generating a comparable amount of power to fewer larger converters should be considered. If smaller converters are utilized there could be less of an impact if a WEC were to malfunction or need maintenance; however, if a larger WEC that was part of a smaller array experienced the same malfunction, the loss of power would have a much greater impact. Additionally, smaller WECs could allow for the size of an array to fluctuate depending on locationally dependent energy needs and would make deployment and extraction of converters much less expensive.

Specifically examining the off–camber layouts in Fig. 8.3, we notice a similar overarching design, with different spacings between the WECs. This could indicate the need to consider adjustable mooring within an array to account for variable sea conditions by adjusting device spacing. Additionally, adjustable mooring could account for locations, such as Oregon, which have multiple dominant directions. Our work shows the initial potential of an array to maximize WEC array power given a variable sea state and future work will continue to realistically vary that sea state through incorporating wave directionality.

The final note we saw when examining the data is that the interaction factor improvement was relative to a converter's ability to generate power in the sea state. Locations where converters performed better saw smaller improvements in the interaction factor and locations where the converters performed more poorly saw greater increases in the interaction factor. This is promising for array optimization and for the potential utilization of more smaller devices in an array because WECs will not always be experiencing their most optimal sea conditions and developer can now prepare for that through array design.

8.6 Conclusion

In conclusion, this preliminary characterization study points to the need to further develop and investigate the many factors that will influence the power generation and cost of a layout. WECs have the potential to be used to generate power on a large scale to the national grid or on smaller scales to communities removed from primary power sources. The results presented here provide an initial understanding of the impact that location and device geometry might have on power development and discuss the other factors that should be considered in conjunction.

For the specific potential of wave energy to be used for coastal communities in the occurrence of a blackout, there are many stakeholders who would need to be included and questions that would need to be answered. Stakeholders would include residents, tourists, associate industries (such as electric utilities or insurance agencies), ocean users, scientists, and elected officials. Each of these groups would provide useful knowledge to aid in determining the feasibility of utilizing WECs as emergency power generators from when a device could be deployed after a storm to what regulatory processes would need to be completed.

Additionally, the economics would need to be fully considered as most of these communities currently have backup diesel generators. Deployment of WECs would be much more appealing in the occurrence of a blackout where fuel supplies run low and can not be replenished. Alternatively, if devices are already in place providing nominal power, then their economic viability in the event of a blackout would increase greatly. Resiliency zones could be created, in areas subject to blackouts, that have WECs in place or have the cables in place ready for connection. An example is the Pacific Marine Energy Center's test facility being constructed off the coast of Newport, Oregon. If this area were to experience a blackout, the existing infrastructure could potentially be used to generate power for emergency services.

Given the observed relationship between power generation and interaction factor, further investigation is required to better understand the trade off of deploying a single device or an array of smaller devices to meet an energy need. While at this point the feasibility of wave energy as an emergency power source is not definitively known, our work lays the groundwork for better understanding the questions involved specifically regarding location and geometry.

Part III

Concluding Discussion

Chapter 9: Conclusion

As the industry moves closer to widespread ocean deployment of WECs, we have been considering the deployment of multiple WECs acting together in array scenarios. As has been observed with the research and implementation of wind farms [47], the configuration of individual converters in relation to each other influences the power production and the economics of a WEC array. Over the course of the work presented in this dissertation, we have been intentional about progressing our optimization algorithm towards becoming a useful tool that will minimize cost, increase power, and increase confidence through better incorporation of influencing factors such as spacing, damping, location, and geometry. Deploying WECs in the ocean to generate usable power over an economic lifespan requires the consideration of many aspects by the industry.

9.1 Contributions of the Work

- Focused attention on optimization algorithm development for WEC array design.
- Showed that a binary GA performs better than an EA or SA algorithm as the complexity of the solution space increases.
- Created a real–coded GA that improved the power production when compared to the binary GA.
- Demonstrated the importance of layout configuration for power improvement.

- Indicated the potential value of considering both active WEC control and array optimization.
- Integrated WEC specific damping optimization within the array optimization algorithm.
- Noted that designing a WEC for a sea state influences the power more than passive damping control.
- Showed that the experienced sea state affects the resulting layout.
- Incorporated probabilistic sea states into the optimization algorithm in order to better utilize buoy data as an input.

With the current state of the wave industry and an initial limited focus on array design and development, we have been methodical in our approach to WEC array optimization. We have found that array layout design either increases or decreases power production, that experienced sea state changes the design, and that device geometry has a major influence on power production. Given that all our studies consider unidirectional waves, it is doubtful that similar arrays will be utilized in ocean deployment or even that similar interaction factors will be attained (without the incorporation of active WEC control), but the increased knowledge of the system we have gained will provide better context for future research that should include multi-directional waves and realtime sea states. Even if the results shown are not realistic when compared to ocean deployment they provide us a broader understanding regarding the behavior of WEC arrays — specifically that devices should be designed with array behavior in mind, that spacing constraints can drastically change an array configuration, and that location will change an array's design.

If we consider the Oregon ocean as an example with its two dominant directions we might see a layout that minimizes negative interactions through wave interaction or a layout that takes greater advantage of the direction seen in the winter due to more energetic sea conditions. We also might see fewer larger devices with an relatively small overall footprint or more smaller devices generating the same total power but designed to be less expensive. Beyond power production, the economics of a WEC array will likely drive an array's design since the cost to lay cable, the cost to service the WECs, and the available ocean space will probably have a greater impact on an array's efficiency. However, even if not a driving influence, it is important to include all factors as part of the design process and maximizing power production (or minimizing power losses) is important given the the many challenges facing the survival of the industry.

9.2 Avenues for Continued Research

There are many avenues of research that could continue from this work, but the most apparent would be the incorporation of active control into the GA's process. Additionally, greater incorporation of computation optimization techniques of a WEC's geometry when considering array performance should be considered. Both of these research options would prove challenging given the complicated nature of the wave energy industry and the number of unknowns, but are necessary for future development. As the industry advances and further models describing the space are developed, such as environmental and social impact models, this information should also be included in the array optimization process.

9.3 Final Thoughts

In order to meet growing energy demands, and to utilize energy sources that are renewable, research and development is being conducted to determine efficient and cost–effective methods of extracting energy from the ocean's waves, tides, and currents. The estimated 16,000 – 18,500 TWh of global energy in the ocean waves makes extraction of this energy for use by the large portion of the population living near a coastline highly promising [6, 9].

In this research, we sought to find a cost–effective means of capturing the energy of ocean waves. Developers are at the point of planning and preparing for array deployment and it is vital that they are as well-informed as possible. Given that WECs deployed in arrays have the capability of producing more power than the same number of WECs acting in isolation and this ability will influence array efficiency, an understanding of optimal configuration is important. Research into array optimization is currently limited, and very little has been done about the best way of determining an optimal arrangement. In light of this, we developed a problem specific GA which generates potential optimal WEC arrays that takes into account many influencing factors such as device geometry, sea state, device damping, power and cost. Results from our research provide insight regarding the challenge of WEC array optimization that can inform the wave energy industry concerning WEC and WEC–array design as movement is made towards ocean deployment.

Bibliography

[1] 2014 Water Power Program Peer Review: Marine and Hydrokinetic Technologies. Technical report, United States Deptment of Energy, 2014.

[2] B. Bosma, T. Brekken, P. Lomonaco, A. McKee, B. Paasch, and B. Batten. Physical Model Testing and System Identification of a Cylindrical OWC Device. In *12th European Wave and Tidal Energy Conference*, pages 1–9, Cork, Ireland, 2017.

[3] B.G. Reguero, I.J. Losada, and F.J. Méndez. A Global Wave Power Resource and its Seasonal, Interannual and Long-Term Variability. *Applied Energy*, 148:366–380, 2015.

[4] Quadrennial Technology Review: An Assessment of Energy Technologies and Research Opportunities. Technical report, United States Deptartment of Energy, 2015.

[5] Mapping and Assessment of the United States Ocean Wave Energy Resource. Technical report, Electric Power Research Institute, 2011.

[6] Water Power Program - Water Power for a Clean Energy Future. Technical Report April, United States Deptartment of Energy, 2013.

[7] C.M. Linton and D.V. Evans. The Interaction of Waves with Arrays of Vertical Circular Cylinders. *Journal of Fluid Mechanics*, 215(-1):549, 1990.

[8] S. Mavrakos and P. McIver. Comparison of Methods for Computing Hydrodynamic Characteristics of Arrays of Wave Power Devices. *Applied Ocean Research*, 1187(97):283–291, 1998.

[9] B. Borgarino, A. Babarit, and P. Ferrant. Impact of Wave Interactions Effects on Energy Absorption in Large Arrays of Wave Energy Converters. *Ocean Engineering*, 41:79–88, 2011.

[10] A. Babarit. On the Park Effect in Arrays of Oscillating Wave Energy Converters. *Renewable Energy*, 58:68–78, 2013.

[11] C. Sharp and B. DuPont. Wave Energy Converter Array Optimization A Review of Current Work and Preliminary Results of a Genetic Algorithm Approach Introducing Cost Factors. In *ASME 2015 International Design Engineering Technical Conference & Computers and Information in Engineering Conference*, pages 1–10, Boston, MA, USA, 2015. ASME.

[12] A.D. De Andrés, R. Guanche, L. Meneses, C. Vidal, and I.J. Losada. Factors that Influence Array Layout on Wave Energy Farms. *Ocean Engineering*, 82:32–41, 2014.

[13] R.I. Rawlinson-Smith, I. Bryden, M. Folley, V. Martin, T.J. Stallard, and R.H.J. Willden. The PerAWaT project : Performance Assessment of Wave and Tidal Array Systems. In *3rd International Conference on Ocean Energy*, pages 1–7, Bilbao, Spain, 2010.

[14] J. Cruz, R. Sykes, P. Siddorn, and R. Eatock Taylor. Wave Farm Design: Preliminary Studies on the Influences of Wave Climate , Array Layout and Farm Control. In *8th European Wave and Tidal Energy Conference*, pages 1–10, Uppsala, Sweden.

[15] A. Nambiar, A. Collin, S. Karatzounis, J. Rea, B. Whitby, and A. Kiprakis. Optimising Network Design Options for Marine Energy Converter Farms. In *11th European Wave and Tidal Energy Conference*, pages 1–10, Nantes, France, 2015.

[16] P.M. Ruiz, F. Ferri, and J.P. Kofoed. Sensitivity Analysis of WEC Array Layout Parameters Effect on the Power Performance. In *11th European Wave and Tidal Energy Conference*, number 1, pages 1–8, Nantes, France, 2015.

[17] M. Vicente, M. Alves, and A. Sarmento. Layout Optimization of Wave Energy Point Absorbers Arrays. In *10th European Wave and Tidal Energy Conference*, pages 1–8, Aalborg, Denmark, 2013.

[18] H.A. Wolgamot, P.H. Taylor, and R. Eatock Taylor. The interaction factor and directionality in wave energy arrays. *Ocean Engineering*, 47:65–73, 2012.

[19] W. Chen, F. Gao, X. Meng, and J. Fu. Design of the Wave Energy Converter Array to Achieve Constructive Effects. *Ocean Engineering*, 124:13–20, 2016.

[20] C.J. McNatt, V. Venugopal, and D. Forehand. A Novel Method for Deriving the Diffraction Transfer Matrix and its Application to Multi-Body Interactions in Water Waves. *Ocean Engineering*, 94:173–185, 2014.

[21] P. Balitsky, G. Bacelli, and J.V. Ringwood. Control-Influenced Layout Optimization of Arrays of Wave Energy Converters. In *ASME 2014 International Conference on Ocean, Offshore and Arctic Engineering*, pages 1–10, San Francisco, California, 2014.

[22] S. Bellew, T. Stallard, and P.K. Stansby. Optimisation of a Heterogeneous Array of Heaving Bodies. In *8th European Wave and Tidal Energy Conference Conference*, pages 1–9, Uppsala, Sweden, 2009.

[23] B.F.M. Child, J. Cruz, M. Livingstone, and A. Motivation. The Development of a Tool for Optimising Arrays of Wave Energy Converters. Technical report, Garrad Hassan and Partners Ltd., Southampton, United Kindom, 2011.

[24] P. Ricci, J. Saulnier, and A.F. de O. Falcão. Point-Absorber Arrays: A Configuration Study off the Portuguese West-Coast. In *7th European Wave and Tidal Energy Conference*, pages 1–10, Porto, Portugal, 2007.

[25] C. Sharp and B. DuPont. Wave Energy Converter Array Design: A Preliminary Study on the Effect of Minimum Separation Distance Between Converters. In *3rd Marine Energy Technology Symposium*, pages 1–5, Washington D.C., U.S.A., 2015.

[26] D.G. Wilson, G. Bacelli, R.G. Coe, D.L. Bull, O. Abdelkhalik, U.A. Korde, and R.D. Robinett. A Comparison of WEC Control Strategies. Technical report, Sandia National Laboratory, 2016.

[27] C. Fitzgerald and G. Thomas. A Preliminary Study on the Optimal Formation of an Array of Wave Power Devices. In *7th European Wave and Tidal Energy Conference*, pages 1–9, Porto, Portugal, 2007.

[28] L. Mao. *Optimizing Wave Farm Layouts Under Uncertainty*. Masters thesis, Lehigh University, 2013.

[29] L.V. Snyder and M.M. Moarefdoost. Layouts for Ocean Wave Energy Farms: Models, Properties, and Heuristic. In *2nd Marine Energy Technology Symposium*, pages 1–8, Washington D.C., U.S.A., 2014.

[30] M.M. Moarefdoost, L.V. Snyder, and B. Alnajjab. Layouts for Ocean Wave Energy Farms: Models, Properties, and Optimization. *Omega*, 66:185–194, 2017.

[31] L.V. Snyder and M.M. Moarefdoost. Optimizing Wave Farm Layouts Under Uncertainty. In *3rd Marine Energy Technology Symposium*, number 1, pages 1–6, Washington D.C., U.S.A., 2013.

[32] J.P.L. McGuinness and G. Thomas. Optimal Arrangements of Elementary Arrays of Wave-Power Devices. In *11th European Wave and Tidal Energy Conference*, pages 1–10, Nantes, France, 2015.

[33] B.F.M. Child and V Venugopal. Modification of Power Characteristics in an Array of Floating Wave Energy Devices. In *8th European Wave and Tidal Energy Conference*, pages 1–10, Uppsala, Sweden, 2009.

[34] B.F.M. Child and V. Venugopal. Optimal Configurations of Wave Energy Device Arrays. *Ocean Engineering*, 37(16):1402–1417, 2010.

[35] B. Child. *On the Configuration of Arrays of Floating Wave Energy Converters*. Doctoral dissertation, University of Edinburgh, 2011.

[36] DNV GL. WaveFarmer. https://www.dnvgl.com/services/wavefarmer-3772, 2015.

[37] D. Sarkar, E. Contal, N. Vayatis, and F. Dias. Prediction and Optimization of Wave Energy Converter Arrays Using a Machine Learning Approach. *Renewable Energy*, 97:504–517, 2016.

[38] J. Wu, S. Shekh, N.Y. Sergiienko, B.S. Cazzolato, B. Ding, F. Neumann, and M. Wagner. Fast and Effective Optimisation of Arrays of Submerged Wave Energy Converters. In *Genetic and Evolutionary Computation Conference*, pages 1–8, Denver, CO, U.S.A., 2016.

[39] F. Ferri. Computationally Efficient Optimisation Algorithms for WECs Arrays. In Anthony Lewis, editor, *12th European Wave and Tidal Energy Conference*, pages 1–7, Cork, Ireland, 2017.

[40] C. Sharp and B. DuPont. A Multi-Objective, Real-Coded Genetic Algorithm Method for Wave Energy Converter Array Optimization. In *ASME 2016 35th International Conference on Ocean, Offshore and Arctic Engineering*, pages 1–10, Busan, Korea, 2016.

[41] C. Sharp, B. Dupont, B. Bosma, P. Lomonaco, and B. Batten. Array Optimization of Fixed Oscillating Water Columns for Active Device Control. In *12th European Wave and Tidal Energy Conference*, pages 1–10, Cork, Ireland, 2017.

[42] M. Giassi, M. Göteman, S. Thomas, J. Engström, M. Eriksson, and J. Isberg. Multi-Parameter Optimization of Hybrid Arrays of Point Absorber Wave Energy Converters. In Anthony Lewis, editor, *12th European Wave and Tidal Energy Conference*, pages 1–6, Cork, Ireland, 2017.

[43] C. Sharp and B. DuPont. Analysis of WEC Array Economics: Current State-of-the-Art and Future Needs. In *11th European Wave and Tidal Energy Conference*, pages 1–10, Nantes, France, 2015.

[44] M. Previsic. Cost Breakdown Structure for WEC. Sandia National Laboratory. 2012. http://energy.sandia.gov/download/23667/.

[45] WAMIT V7.2 User Manual. WAMIT Inc., 2016.

[46] J. Cruz, editor. *Ocean Wave Energy: Current Status and Future Perspectives*. Springer, Berlin, 2008.

[47] G. Mosetti, C. Poloni, and B. Diviacco. Optimization of Wind Turbine Positioning in Large Windfarms by Means of a Genetic Algorithm. *Journal of Wind Engineering and Industrial Aerodynamics*, 51(1):105–116, 1994.

[48] S. Droste, T. Jansen, and I. Wegener. On the Analysis of the (1+1) Evolutionary Algorithm. *Theoretical Computer Science*, 276:51–81, 2002.

[49] G. Zhang, M. Gheorghe, and C. Wu. A Quantum-Inspired Evolutionary Algorithm Based on P systems for a Class of Combinatorial Optimization. *IEEE Transactions on Evolutionary Computation*, 6(6):580 – 593, 2002.

[50] T. Baumert, T. Brixner, V. Seyfried, M. Strehle, and G. Gerber. Rapid Communication Femtosecond Pulse Shaping by an Evolutionary Algorithm with Feedback. *Applied Physics B: Lasers and Optics*, 782:779–782, 1997.

[51] David E. Goldberg. *Genetic Algorithms in Search, Optimization, and Machine Learning*. Addison-Wesley Longman Publishing Co., Inc., Boston, MA, USA, 1st edition, 1989.

[52] H.P. Schwefel. *Evolution and Optimum Seeking: The Sixth Generation*. John Wiley & Sons, Inc., New York, NY, USA, 1993.

[53] Q. Zhang, J. Sun, and E. Tsang. An Evolutionary Algorithm With Guided Mutation for the Maximum Clique Problem. *IEEE Transactions on Evolutionary Computation*, 9(2):192–200, 2005.

[54] S. Kirkpatrick, C.D. Gelatt, and M.P. Vecchi. Optimization by Simulated Annealing. *American Association for the Advancement of Science*, 220(4598):671–680, 2007.

[55] D.N. Simopoulos, S.D. Kavatza, and C.D. Vournas. Reliability Constrained Unit Commitment Using Simulated Annealing. *IEEE Transactions on Power Systems*, 21(4):1699–1706, 2006.

[56] P.J.M. Laarhoven and E.H.L. Aarts. *Simulated Annealing: Theory and Applications*. Kluwer Academic Publishers, Norwell, MA, USA, 1987.

[57] D.N. Simopoulos, S.D. Kavatza, and C.D. Vournas. Unit Commitment by an Enhanced Simulated Annealing Algorithm. *IEEE Transactions on Power Systems*, 21(1):68–76, 2006.

[58] B. Metropolis, A.W. Rosenbluth, M.N. Rosenbluth, A.H. Teller, and E. Teller. Equation of State Calculations by Fast Computing Machines, 1953.

[59] N.M. Razali and J Geraghty. Genetic Algorithm Performance with Different Selection Strategies in Solving TSP. In *World Congress on Engineering*, volume II, pages 4–9, London, U.K., 2011.

[60] D.V. Evans. The Oscillating Water Column Wave Energy Device. *IMA Journal of Applied Mathematics*, 22(4):423–433, 1978.

[61] T. Kelly, T. Dooley, J. Campbell, and J. Ringwood. Modelling and Results for an Array of 32 Oscillating Water Columns. In *10th European Wave and Tidal Energy Conference*, pages 1–10, Aalborg, Denmark, 2013.

[62] M. Penalba and J.V. Ringwood. A Review of Wave-to-Wire Models for Wave Energy Converters. *Energies*, 9(7), 2016.

[63] W. Sheng, A. Lewis, and R. Alcorn. Numerical Studies on Hydrodynamics of a Floating Oscillating Water Column. In *30th International Conference on Ocean, Offshore and Arctic Engineering*, pages 1–8, Rotterdam, The Netherlands, 2011.

[64] I. Simonetti, L. Cappietti, H. El Safti, and H. Oumeraci. Numerical Modelling of Fixed Oscillating Water Column Wave Energy Conversion Devices: Toward Geometry Hydraulic Optimization. In *34th International Conference on Ocean, Offshore and Arctic Engineering*, volume 9, page V009T09A031, St. John's, Newfoundland, Canada, 2015.

[65] C.J. McNatt, V. Venugopal, and D. Forehand. The Cylindrical Wave Field of Wave Energy Converters. *International Journal of Marine Energy*, 3-4:26–39, dec 2013.

[66] B. de Miguel, P. Ricci, I. Touzón, and M. Ojanguren. New Perspectives on the Long Term Feasibility of Wave Energy Conversion: a Techno-Economical Approach. In *4th International Conference on Ocean Energy*, pages 1–7, Dublin, Ireland, 2012.

[67] L. Myers, A.S. Bahaj, C. Retzler, P. Ricci, and J-F. Dhedin. Inter-Device Spacing Issues within Wave and Tidal Energy Converter Arrays. In *3rd International Conference on Ocean Energy*, pages 1–6, Bilbao, Spain, 2010.

[68] J. Burright, C. Clark, B. Johnson, and C. Sharp. Validity and Value of Wave Energy Generation as Blackout Risk Mitigation for the Central Oregon Coast Marine Renewable Energy NRT Group Transdisciplinary Report. Technical report, Oregon State University, 2017.

[69] Ocean Power Technologies. Products PB3, 2018.